

Functional roles of transient receptor potential
canonical channels and myristoylated alanine-rich
protein kinase C substrate as novel interaction
partners of the neural cell adhesion molecule
NCAM and polysialic acid in *Mus musculus*
(Linnaeus, 1758)

Dissertation

von

Thomas Theis

aus

Georgsmarienhütte, Deutschland

zur Erlangung des akademischen Grades
Doktor der Naturwissenschaften
(*doctor rerum naturalium*)
am Fachbereich Biologie der Fakultät für
Mathematik, Informatik und Naturwissenschaften
der Universität Hamburg

Hamburg, März 2013

Genehmigt vom Fachbereich Biologie
der Fakultät für Mathematik, Informatik und Naturwissenschaften
an der Universität Hamburg
auf Antrag von Professor Dr. M. SCHACHNER
Weiterer Gutachter der Dissertation:
Priv.-Doz. E. KRAMER
Tag der Disputation: 17. Mai 2013

Hamburg, den 02. Mai 2013



Professor Dr. C. Lohr
Vorsitzender des
Fach-Promotionsausschusses Biologie

Table of Contents

Table of Contents

1.1 Abstract	6
1.2 Zusammenfassung	8
2. Introduction	10
2.1 Cell adhesion.....	10
2.2 Neural cell adhesion molecule (NCAM)	10
2.3. Posttranslational modifications of NCAM.....	12
2.4 Polysialic acid.....	14
2.5 NCAM in the nervous system	15
2.6 Homo- and heterophilic NCAM interactions.....	16
2.7 Myristoylated alanine-rich C-kinase substrate.....	18
2.8 Transient receptor potential canonical or classical family	20
2.9 Structure of the TRPC proteins.....	22
2.10 Aims of the study	24
3. Materials	25
3.1 Antibodies	25
3.1.1 Primary antibodies.....	25
3.1.2 Secondary antibodies	28
3.2 Bacterial strains.....	29
3.3 Chemicals	29
3.4 Synthesized peptides	29
3.5 Molecular weight standards.....	30
3.5.1 1 kb DNA ladder	30
3.5.2 Precision plus protein™ all blue standards (BioRad).....	30
3.6 Plasmids.....	30
3.7 Mice.....	33

Table of Contents

3.8 Solutions and buffers.....	33
4 Methods	39
4.1 Biochemistry	39
4.1.1 Bind assay	39
4.1.2 Cell surface biotinylation.....	40
4.1.3 Chloroform/methanol protein precipitation.....	41
4.1.4 Co-immunoprecipitation.....	41
4.1.5 Coupling of hydrazide dyes to colominic acid and chondroitin sulfate	42
4.1.6 Coupling of hydrazide dyes to PSA-NCAM	42
4.1.7 Protein cross-linking using photo-L-leucine.....	42
4.1.8 Determination of protein concentration	43
4.1.9 Ethanol precipitation of carbohydrates.....	43
4.1.10 Isolation of nuclear fractions from cultured cells using the Qproteome™ Nuclear Protein kit (Qiagen)	44
4.1.11 Measurements of the capacitance of an artificial lipid bilayer	44
4.1.12 Measurements of DNA methylation and hydroxymethylation	45
4.1.13 Pull-down experiments	46
4.1.14 Recombinant expression of proteins in <i>Escherichia coli</i> using the pQE-system or pGEX-system	46
4.1.15 Sodium dodecyl sulfate-polyacrylamide gel electrophoresis (SDS-PAGE)	47
4.1.16 Coomassie blue staining of SDS polyacrylamide gels	48
4.1.17 Western blot analysis.....	48
4.1.18 Stripping of a nitrocellulose membrane.....	49
4.2 Cell biology	49
4.2.1 Cell lines.....	49
4.2.2 Primary cell culture.....	50
4.2.2.1 Cell culture of primary cerebellar granule cells.....	50

Table of Contents

4.2.2.2 Explants of the cerebellum	50
4.2.2.3 Cell culture of primary hippocampal cells.....	51
4.2.3 Calcium imaging experiments	51
4.2.4 Immunocytochemistry	52
4.2.5 Live staining.....	52
4.2.6 Fluorescence resonance energy transfer	53
4.2.7 Neurite outgrowth	53
4.2.8 Migration assay.....	54
4.2.9 Coating of glass cover slips with poly-L-lysine.....	54
4.2.10 Transfection of cells with Fugene 6™	54
4.2.11 Transfection of cells with calcium phosphate.....	55
4.3.1 Polymerase chain reaction (PCR).....	55
4.3.2 Horizontal agarose gel electrophoresis.....	57
4.3.3 Linearization of the pGEX-3X vector	57
4.3.4 Dephosphorylation of the pGEX-3X vector.....	58
4.3.5 Ligation of the insert into the pGEX-3X vector.....	58
4.3.6 Extraction of DNA from agarose gel	59
4.3.7 Transformation of <i>Escherichia coli</i>	59
4.3.8 Plasmid isolation from <i>Escherichia coli</i> culture.....	59
4.3.9 Determination of DNA concentration.....	60
4.3.10 DNA sequencing.....	60
4.3.11 Site directed mutagenesis.....	60
5. Results.....	61
5.1 NCAM interacts with TRPC1, 4 and 5	61
5.2 NCAM co-localizes with TRPC1, 4 and/or 5 at the cell surface of hippocampal neurons	63
5.3 TRPC1, TRPC4/5 and TRPC3/6/7 interact with Kir3.3 and PrP, but not with TrkB	64

Table of Contents

5.4 TRPC proteins play an important role in NCAM-mediated neurite outgrowth from hippocampal neurons.....	65
5.5 Treatment of hippocampal neurons with antibodies against the extracellular domain of NCAM or L1 triggers different calcium responses.....	67
5.6 TRPC4 and 5 are localized at the cell surface of cultured primary hippocampal neurons	69
5.7 NCAM and TrkB regulate the localization of Kir3.1/3.3 heteromers at the cell surface	70
5.8 The intracellular domains of NCAM140/180 interact with the N- terminus of TRPC1 ..	71
5.9 The interaction between the intracellular domain of NCAM180 and the N-terminus of TRPC5 is calmodulin-dependent	74
5.10 Inhibition of TRPC by SKF96365 reduces the nuclear import of the 50 kDa NCAM fragment.....	75
5.11 PSA and HNK-1 are found in the nucleus upon NCAM stimulation	76
5.12 A 50 kDa NCAM fragment is present in the nuclear fraction after PSA digestion and NCAM stimulation.....	80
5.13. Nuclear PSA-NCAM levels are increased after NCAM stimulation and decrease rapidly after 30 min.....	81
5.14. NCAM stimulation leads to changes in DNA methylation and hydroxymethylation ...	84
5.15 NCAM-mediated neuritogenesis, but not neuronal cell migration, is PSA-dependent	86
5.16 PSA expression and levels of methylated DNA are significantly reduced during maturation of neurons	88
5.17 NCAM stimulation leads to the appearance of a high molecular weight complex containing histone H1 in the nucleoplasmic protein fraction.....	89
5.18 PSA and MARCKS co-localize in primary hippocampal neurons	91
5.19 PSA interacts with the effector domain of MARCKS within the plasma membrane....	93
5.20 The interaction between PSA and the ED of MARCKS through an artificial lipid bilayer influences its electrical properties.....	102
5.21 The interaction between PSA and MARCKS is necessary for the PSA-mediated neurite outgrowth.....	105
5.22 Phosphorylation of the ED of MARCKS is prevented by the interaction between PSA and MARCKS	107

Table of Contents

6. Discussion	109
6.1 The interaction between NCAM140/180 and TRPC1, 4 and 5.....	109
6.2 Functional interplay between NCAM, TRPC1, 4 and 5 with PrP and Kir3.3	112
6.3 NCAM-stimulated import of PSA into the nucleus	113
6.4 Interaction between MARCKS and PSA	115
7. Literature	119
8. Abbreviations	137
9. Publications.....	141
10. Acknowledgements	142

1.1 Abstract

The neural cell adhesion molecule (NCAM) is a member of the immunoglobulin superfamily which plays important roles in fundamental events during development of the nervous system such as neuritogenesis, synaptic plasticity and long-term potentiation. In the nervous system three major NCAM isoforms are expressed: NCAM120, NCAM140 and NCAM180. NCAM120 is attached to the cell membrane via a glycosylphosphatidylinositol (GPI)-anchor, whereas NCAM140 and NCAM180 are single pass transmembrane proteins. NCAM140 differs from NCAM180 by an additional sequence stretch in the intracellular domain (ICD). All NCAM isoforms are glycosylated and carry the functionally important human natural killer cell glycan (HNK-1) and polysialic acid (PSA). Numerous intra- and extracellular binding partners of NCAM have been identified, among them are the fibroblast growth factor receptor (FGFR), the tyrosine kinase TrkB and the inwardly-rectifying potassium channel Kir3.3. The aim of my thesis was to identify novel direct interaction partners of NCAM and PSA and to investigate their functional roles in the nervous system.

I could identify the transient receptor potential canonical channel (TRPC) 1, 4 and 5 as novel intracellular interaction partners of NCAM140 and NCAM180. Furthermore, a direct calmodulin-dependent binding of the N-termini of these TRPCs to the ICD of NCAM180, but not to the ICD of NCAM140 could be shown by a label free binding assay. Cell surface biotinylation and immunostainings of cultured murine hippocampal neurons confirmed that TRPC4 and 5 were present at the cell surface and that they co-localized with NCAM, respectively. NCAM-mediated neurite outgrowth of hippocampal neurons was blocked with the TRPC channel inhibitor SKF96365 and a function-blocking antibody against TRPC1. Calcium imaging revealed that stimulation of hippocampal neurons with an antibody against NCAM led to opening of SKF96365-sensitive calcium channels in the plasma membrane, suggesting that TRPC channels mediate NCAM-induced calcium influx at the plasma membrane. The TRPC inhibitor SKF96365 also reduced the generation and nuclear import of a transmembrane 50 kDa NCAM fragment upon stimulation of cerebellar neurons with NCAM antibodies directed against the extracellular domain (ECD).

Abstract

Interestingly, increased levels of PSA and HNK-1 have been found in the nucleus after NCAM stimulation.

Numerous binding partners of NCAM have been identified, whereas only a few binding partners for PSA have been identified. Here, I characterize the interaction between PSA and its novel binding partner myristoylated alanine-rich C-kinase substrate (MARCKS). MARCKS is an intracellular protein which can be inserted into the plasma membrane via its effector domain (ED). I could show that the interaction of PSA and MARCKS takes place in the plane of the plasma membrane. PSA inserts into the plasma membrane from the extracellular side of the membrane, while MARCKS inserts from the cytoplasmic side of the membrane. Co-localization of MARCKS and PSA at the plasma membrane of transfected CHO cells and cerebellar neurons could be demonstrated by immunostaining and fluorescence resonance energy transfer (FRET) analysis using fluorescence-labelled PSA. The distance between the green fluorescent protein (GFP) labelled MARCKS and fluorescently labelled PSA was 20-40 nm. Furthermore, when cells were transfected with a MARCKS-GFP mutant containing five alanine residues in the ED instead of five phenylalanine residues a drastically reduced FRET signal was observed indicating that mutation of the ED disrupts the interaction between MARCKS and PSA within the membrane. Treatment or transfection of hippocampal neurons with a peptide containing the ED of MARCKS blocked PSA-triggered neurite outgrowth of wild-type and NCAM-deficient mice. Capacitance measurements using artificial lipid bilayers provide supportive evidence that PSA interacts with the ED of MARCKS from opposite sides of the membrane. In addition, the interaction between PSA and MARCKS leads to changes in the electrical properties of the artificial membrane, suggesting that PSA-MARCKS interactions can modulate electrical properties of neuronal membranes.

1.2 Zusammenfassung

NCAM (*neural cell adhesion molecule*) ist ein Zelladhäsionsmolekül der Immunoglobulin-Superfamilie, welches eine wichtige Rolle in der Entwicklung und der Plastizität des Nervensystems spielt. Im Nervensystem werden überwiegend die drei Isoformen NCAM120, NCAM140 und NCAM180 exprimiert. NCAM120 ist mit einem Glykosylphosphatidylinositol (GPI)-Anker mit der Zellmembran verbunden. NCAM140 und NCAM180 enthalten eine transmembrane und eine intrazelluläre Domäne. Die intrazelluläre Domäne von NCAM180 enthält einen zusätzlichen Sequenzabschnitt. NCAM ist glykolisiert und kann das HNK-1 (*human natural killer cell*) Glykan und/oder PSA (*polysialic acid*) tragen. Eine wachsende Anzahl von intra- und extrazellulären Bindungspartnern von NCAM, wie der Fibroblasten-Wachstumsfaktorrezeptor, die Tyrosinkinase TrkB und der einwärts gerichtete Kaliumkanal Kir3.3, wurden identifiziert, wohingegen nur wenige Rezeptoren für PSA bekannt sind. Das Ziel meiner Arbeit war neue Interaktionspartner von NCAM und PSA zu identifizieren und deren funktionelle Rolle im Nervensystem zu untersuchen.

In der vorliegenden Arbeit konnte ich TRPC (*transient receptor potential canonical*)-1, -4 und -5 als neue Interaktionspartner von NCAM identifizieren. Immunfärbungen und Oberflächenbiotinylierung von hippokampalen Neuronen zeigten dass TRPC4/5 mit NCAM kolokalisiert und an der Oberfläche lokalisiert ist. Mit einer markierungsfreien Bindungsstudie wurde eine Calmodulin-abhängige Interaktion zwischen dem N-Terminus von TRPC1, -4 und -5 und der intrazellulären Domäne von NCAM180 nachgewiesen. Um die funktionellen Konsequenzen der TRPC-NCAM Interaktion zu untersuchen, wurden Neuritenwachstumsexperimente mit primären hippokampalen Neuronen durchgeführt. NCAM-vermitteltes Neuritenwachstum konnte durch den TRPC Kanal Inhibitor SKF96365 und einen inhibitorischen Antikörper gegen TRPC1 blockiert werden. *Calcium imaging* Experimente zeigten ein Öffnen von SKF96365-sensitiven Kalziumkanälen in der Zellmembran nachdem die Neurone mit einem Antikörper gegen NCAM stimuliert wurden. Dies deutet darauf hin, dass TRPC Kanäle notwendig für den NCAM-induzierten Kalziumeinstrom sind. Darüber hinaus

Abstract

reduzierte der TRPC Inhibitor SKF96365 die Erzeugung und den nuklearen Import eines transmembranen 50 kDa NCAM Fragments nach der Stimulation von Körnerzellen aus dem Kleinhirn mit NCAM Antikörpern gegen die extrazelluläre Domäne. Interessanter Weise wurden die Gykane HNK-1 und PSA nach NCAM Stimulation vermehrt im Zellkern gefunden.

Eine Vielzahl an Bindungspartnern wurde für NCAM identifiziert, wohingegen für PSA nur wenige Bindungspartner bekannt sind. In der vorliegenden Arbeit habe ich die Interaktion zwischen PSA und MARCKS (*myristoylated alanine-rich C-kinase substrate*) charakterisiert. MARCKS ist ein intrazelluläres Protein, welches mit seiner ED (*effector domain*) in die Plasmamembran eindringen kann. Es konnte gezeigt werden, dass diese Interaktion in der Plasmamembran stattfindet. PSA dringt von der extrazellulären Seite und MARCKS von der cytoplasmatische Seite in die Membran ein.

Durch immunozytochemische und FRET (*fluorescence resonanz energie transfer*) Versuche mit transfizierten CHO Zellen und Körnerzellen aus dem Kleinhirn konnte eine Kolokalisation von PSA und MARCKS gezeigt werden. Die ermittelte Entfernung zwischen dem GFP (*green fluorescent protein*) markierten MARCKS und dem fluoreszenz-markierten PSA betrug 20 bis 40 nm. Darüber hinaus wurde eine drastische Reduzierung des FRET Signals beobachtet, wenn die Zellen mit einer MARCKS Mutante transfiziert wurden, in der die fünf Phenylalanine in der ED durch Alanine ausgetauscht wurden. Dieses Ergebnis weist darauf hin, dass die Mutation der ED die Interaktion zwischen MARCKS und PSA stört. Nach Behandlung oder Transfektion von hippokampalen Neuronen aus Wildtyp oder NCAM-defizienten Mäusen mit einem Peptid, welches die Aminosäuresequenz der ED von MARCKS enthält, wurde das PSA-induzierte Neuritenwachstum blockiert. Messungen der elektrischen Kapazität einer künstlichen Lipiddoppelschicht unterstützten die These, dass PSA mit der ED von MARCKS von unterschiedlichen Seiten der Membran interagieren. Zusätzlich wurden Änderungen in den elektrischen Eigenschaften der Membran bei der PSA-MARCKS Interaktion gezeigt, was die Vermutung nahe legt, dass die PSA-MARCKS Interaktion die elektrischen Eigenschaften von Neuronen moduliert.

2. Introduction

2.1 Cell adhesion

Without controlled adhesion, it would not be possible for higher organisms to form three-dimensional multicellular structures and, thus, organize the correct architecture of organs. Adhesion between cells takes place at the plasma membrane and is mediated by proteins and glycans. There are three major classes of proteins which play a role in adhesion: the extracellular matrix (ECM) molecules, the cell adhesion molecules (CAMs) and the cytoplasmic plaque proteins (Gumbiner, 1996). The ECM proteins are glycoproteins, such as collagens, fibronectins or laminins. They form an extracellular protein network which is connected to adhesion molecules at the surfaces of the cells. The cytoplasmic plaque proteins are the linkage between the adhesion system and the cytoskeleton. The vast majority of CAMs are glycoproteins with a transmembrane domain or GPI-anchor. CAMs can be divided into four main groups: integrins, cadherins, selectins and the immunoglobulin-like proteins (Aplin *et al.*, 1998). The CAMs of the immunoglobulin superfamily play an essential role in morphogenesis (Krog and Bock, 1992; Williams and Barclay, 1988). They all contain at least one extracellular immunoglobulin (Ig) domain and most of them have at least one fibronectin type 3 (Fn3) domain. These proteins mediate adhesion between cells and the ECM through homo- and heterophilic interactions. Homo- and heterophilic interactions lead for instance to phosphorylation of protein substrates, opening of ion channels (Klinz *et al.*, 1995) and activation of different signal cascades (Ditlevsen *et al.*, 2010; Loers and Schachner, 2007) which are involved in dynamic adhesive mechanisms such as neurite outgrowth, cell migration and synaptogenesis.

2.2 Neural cell adhesion molecule (NCAM)

NCAM was the first CAM discovered in the nervous system (Rutishauser *et al.*, 1976; Jørgensen *et al.*, 1974) and it belongs to the immunoglobulin superfamily. NCAM is not only present in the nervous system but is also expressed in the lung, stomach,

Introduction

kidney (Filiz *et al.*, 2002), heart (Burroughs *et al.*, 1991; Reyes *et al.*, 1991) and muscle (Fidziańska *et al.*, 1995). Moreover, a subpopulation of natural killer (NK) cells expresses NCAM (CD56) (Farag *et al.*, 2006; Carson *et al.*, 1996).

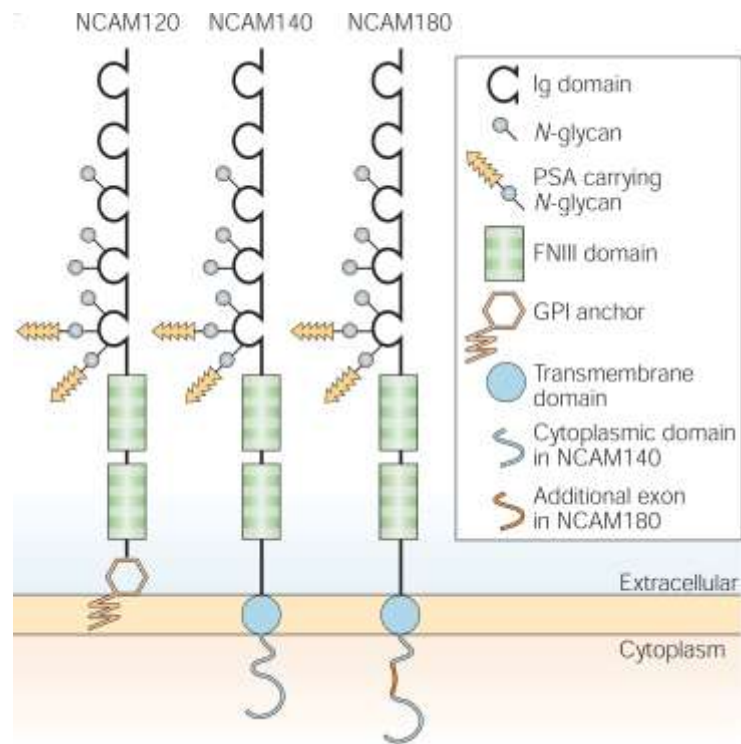


Figure 2.1: Schematic drawing of the three major splice variants of NCAM. The structures of the three major splice variants of NCAM are shown. NCAM120 is attached to the cell surface via a GPI anchor and lacks an ICD. NCAM140 and NCAM180 are transmembrane proteins and the ICD of NCAM180 contains additional sequence encoded by exon18. The ECDs of the three splice variant are identical, they contain two Fn3 and five Ig domains. Six N-glycosylation sites are present the Ig domains, but only the fifth and/or sixth glycosylation sites in the fifth Ig domain can be modified with PSA. **(Representation was taken from Kleene and Schachner, 2004)**

Three major isoforms of NCAM are known: NCAM120, NCAM140 and NCAM180 (Fig.2.1). They are named according to their apparent molecular weight observed in the sodium dodecyl sulfate polyacrylamide gel electrophoresis (SDS-PAGE) (Barthels *et al.*, 1988; Owens *et al.*, 1987). NCAM protein is encoded by a single gene, which has been mapped to chromosome 9 in mice (D'Eustachio *et al.*, 1985)

Introduction

and to band q23 on chromosome 11 in human (Nguyen *et al.*, 1986). At least 27 different splice variants of NCAM are known (Reyes *et al.*, 1991) which are emerging from the NCAM gene containing 24 exons. In brain and in muscle, an NCAM splice variant which contains the SEC exon located between exon 12 and 13 was found. This splice variant encodes a secreted form of NCAM (Gower *et al.*, 1988). Furthermore, soluble NCAM can be generated by enzymatic cleavage of the GPI-anchor by a phosphatidylinositol-specific phospholipase C (PI-PLC) (Sadoul *et al.*, 1986) or by proteolytic cleavage within the ECD by metalloproteases or serine proteases (Kleene *et al.*, 2010; Kalus *et al.*, 2007).

All three major isoforms are composed of five amino terminal Ig domains, followed by two Fn3 domains (Cunningham *et al.*, 1987). NCAM120 is attached via a GPI anchor to the cell surface, whereas NCAM140 and NCAM180 contain a transmembrane domain and an ICD. The only difference between NCAM140 and NCAM180 is that NCAM180 contains an additional sequence stretch encoded by exon18 (Fig. 2.2). In the nervous system, NCAM120 is predominantly expressed in glial cells; NCAM140 is expressed in glial cells and neurons and NCAM 180 is predominantly expressed in neurons (Schachner *et al.*, 1997). It has been suggested that NCAM180 stabilizes cell-cell contacts in differentiated cells by interacting with the cytoskeleton. This interaction reduces lateral mobility of NCAM180 within the plasma membrane (Pollerberg *et al.*, 1987; 1986). Furthermore, it was shown that NCAM180 is not only localized at sites of cell-cell contacts, but also in growth cones contacting other cells (Pollerberg *et al.*, 1987; 1986) and in postsynaptic regions (Leshchyns'ka *et al.*, 2011; Schuster *et al.*, 2001).

2.3. Posttranslational modifications of NCAM

NCAM is synthesized in the endoplasmic reticulum with a high mannose core and is transferred to the cell surface within 35 minutes after translation (Alcaraz *et al.*, 1991). The biosynthesis of NCAM is regulated by growth factors and by the intracellular calcium concentration (Lyles *et al.*, 1993).

Introduction

Different posttranslational modifications of NCAM are known: ubiquitinylation (Diestel *et al.*, 2007), phosphorylation (Sorkin *et al.*, 1984), sulfation (Lyles *et al.*, 1984), palmitoylation (Niethammer *et al.*, 2002; Little *et al.*, 1998) and glycosylation (Albach *et al.*, 2004). NCAM140 and NCAM180 contain up to 49 serine and threonine residues in the ICD, which can be phosphorylated (Lyles *et al.*, 1984; Sorkin *et al.*, 1984). In addition, the only tyrosine residue in the ICD of NCAM140 and NCAM180 can be phosphorylated by the tyrosine kinase TrkB (Cassens *et al.*, 2010). It has been suggested that the tyrosine phosphorylation stabilizes cell-cell adhesion (Diestel *et al.*, 2004).

NCAM can be modified by N- and O-linked glycosylation. Glycans are N-linked, when the oligosaccharides are linked via N-acetylglucosamine to the amide group on asparagines, and O-linked, when oligosaccharides are linked via N-acetylgalactosamine to the hydroxyl group on the side chain of serine or threonine residues (Kolkova *et al.*, 2010). O-linked glycans have only been detected on NCAM120 expressed in myotubes (Walsh *et al.*, 1989) whereas N-linked glycans could be detected on NCAM proteins from different organs and cells. The ECD of NCAM contains six putative N-glycosylation sites (Fig. 2.2) (Albach *et al.*, 2004). NCAM140 and NCAM180 expressed in the nervous system were shown to carry the HNK-1 glycan on N-glycans (Kruse *et al.*, 1984), while it was not found on NCAM isoforms isolated from muscle (Sanes *et al.*, 1986). The HNK-1 was found at NCAM glycosylation sites 2, 4, 5 and 6 (Wuhrer *et al.*, 2003). Another N-linked glycan attached to NCAM is PSA. NCAM contains an unusually high proportion of PSA which decreases during maturation of the nervous system (Finne *et al.*, 1983). Two polysialyltransferases, ST8Sia II (STX) and ST8Sia IV (PST), synthesize the PSA moiety on NCAM (Nakayama *et al.*, 1998). STX is active during the development of the nervous system, while PST plays an important role in the mature brain (Hildebrandt *et al.*, 1998; Angata *et al.*, 1997). NCAM is decorated with PSA only at the fifth and sixth N-glycosylation sites in the fifth Ig domain (Fig. 2.1) (Wuhrer *et al.*, 2003; von der Ohe *et al.*, 2002; Nelson *et al.*, 1995). The correct position of the N-glycans on the fifth Ig domain depends on an interaction of the fifth Ig domain with the first Fn3 domain (Mendiratta *et al.*, 2006). NCAM carries no PSA at the time of its first appearance at embryonic day 8.0–8.5 in the mouse. Shortly after this time the

Introduction

expression of PSA-NCAM becomes predominant and reaches its maximum in the postnatal phase (Probstmeier *et al.*, 1994). After reaching its peak expression the PSA-NCAM level decreases rapidly by approximately 70% within one week (Oltmann-Norden *et al.*, 2008).

2.4 Polysialic acid

PSA is a linear polymer of neuraminic acids, namely 5-N-acetylneuraminic acid (Neu5Ac), 5-N-glycolylneuraminic acid (Neu5Gc) or 5-deamino-3,5-dideoxyneuraminic acid (2-keto-3-deoxynononic acid, KDan) (Mühlenhoff *et al.* 1998). In mammals, PSA moieties are exclusively homopolymeric structures composed of only one neuraminic acid linked by α 2,8-glycosidic bonds (Finne *et al.*, 1983). The major building units in mammalian PSA are Neu5Ac and KDan (Mühlenhoff *et al.* 1998). PSA carrying NCAM was first discovered as “embryonic” NCAM (Finne *et al.*, 1983) and PSA on NCAM is composed of α 2,8-linked Neu5Ac (Mühlenhoff *et al.* 1998).

PSA is a large, negatively charged and highly hydrated glycan chain (Mühlenhoff *et al.* 1998). When NCAM is decorated with PSA, the ECD of NCAM doubles its hydrodynamic radius because of the chemical properties of PSA. This leads to an increase of the intermembrane space and a disruption of the adhesive properties of NCAM and other CAMs (Johnson *et al.*, 2005a, 2005b; Fujimoto *et al.*, 2001). PSA on NCAM was found on di, tri, and tetra antennary glycans (Wuhrer *et al.*, 2003). PSA chains containing 4 or more neuraminic acids form a helical structure (Battistel *et al.*, 2012; Evans *et al.*, 1995). It was shown that these PSA chains penetrate the inner membrane of certain *Escherichia coli* strains and thereby change the membrane potential (Janas *et al.*, 2001; 2000).

NCAM is the most common PSA carrier. Only a few other glycoproteins are known to carry PSA, such as the α -subunit of the voltage-gated sodium channel in rat brain (Zuber *et al.*, 1992), the scavenger receptor CD36 in human milk (Yabe *et al.*, 2003), neuropilin-2 on human dendritic cells (Curreli *et al.*, 2007), the polysialyltransferases

Introduction

STX and PST (Close *et al.*, 1998) and the synaptic cell adhesion molecule 1 in mouse brain (Galuska *et al.*, 2010). Although PSA seems to be required for many functions of NCAM, it has been shown that it regulates functions in a NCAM-independent manner and vice versa NCAM functions in PSA-independent manner (Kleene and Schachner, 2004). While binding partners are known for NCAM, fewer binding partners are known for PSA. These include histone H1 (Mishra *et al.*, 2010), brain-derived neurotrophic factor (BDNF) and fibroblast growth factor 2 (Ono *et al.*, 2012) (Fig. 2.3).

2.5 NCAM in the nervous system

In mice, NCAM plays a role in several behaviors, including anxiety (Stork *et al.*, 1999; Cremer *et al.*, 1994), post-intruder hormonal stress response (Stork *et al.*, 1997) and depression (Aonurm-Helm *et al.*, 2008). In addition NCAM plays an important role in avoidance conditioning (Plappert *et al.*, 2006; Stork *et al.*, 2000) and spatial learning (Bukalo *et al.*, 2004; Cremer *et al.*, 1994). In humans, NCAM is linked to several neuronal disorders. It is associated with mood disorders such as bipolar disorder (Arai *et al.*, 2006; 2004) and schizophrenia (Vawter, 2000) and with degenerative diseases such as Alzheimer's disease (Todaro *et al.*, 2004) and multiple sclerosis (Zabel *et al.*, 2006). The expression of NCAM and PSA is enhanced in different brain tumors, such as astroglomas (Sasaki *et al.*, 1998) and neuroblastomas (Lantuejoul *et al.*, 1998; Komminoth *et al.*, 1994). Moreover, the concentration of soluble NCAM in the cerebrospinal fluid is increased in patients with brain tumors (Todaro *et al.*, 2007; Glüer *et al.*, 1998) or Alzheimer's disease (Strekalova *et al.*, 2006; Todaro *et al.*, 2004).

In the nervous system, NCAM and its glycan PSA are involved in many cellular functions which are essential for development, regeneration and plasticity (Loers and Schachner, 2007; Kleene and Schachner, 2004; Durbec and Cremer, 2001). NCAM plays an important role in neuritogenesis (Euteneuer *et al.*, 2012 Seidenfaden *et al.*, 2012; Rønn *et al.*, 2000), synaptic plasticity (Kochlamazashvili *et al.*, 2012; 2010; Schachner *et al.*, 1997; Durbec and Cremer, 2001), synaptic morphogenesis

Introduction

(Dityatev *et al.*, 2004) myelination and re-myelination after injury (Koutsoudaki *et al.*, 2010; Papastefanaki *et al.*, 2007), cell migration (Ono *et al.*, 1994) and stability of reinnervated neuromuscular junctions (Chipman *et al.*, 2010). PSA-NCAM is present in the adult brain mainly in regions which are undergoing structural plasticity (Bonfanti *et al.*, 1992), such as the hypothalamo-neurohypophyseal system (Theodosis *et al.*, 1994), the olfactory bulbs (Miragall *et al.*, 1988), the piriform and the entorhinal cortices (Seki *et al.*, 1991), the amygdala (Varea *et al.*, 2005), the hippocampus (Seki *et al.*, 1991) and the prefrontal cortex (Varea *et al.*, 2005).

2.6 Homo- and heterophilic NCAM interactions

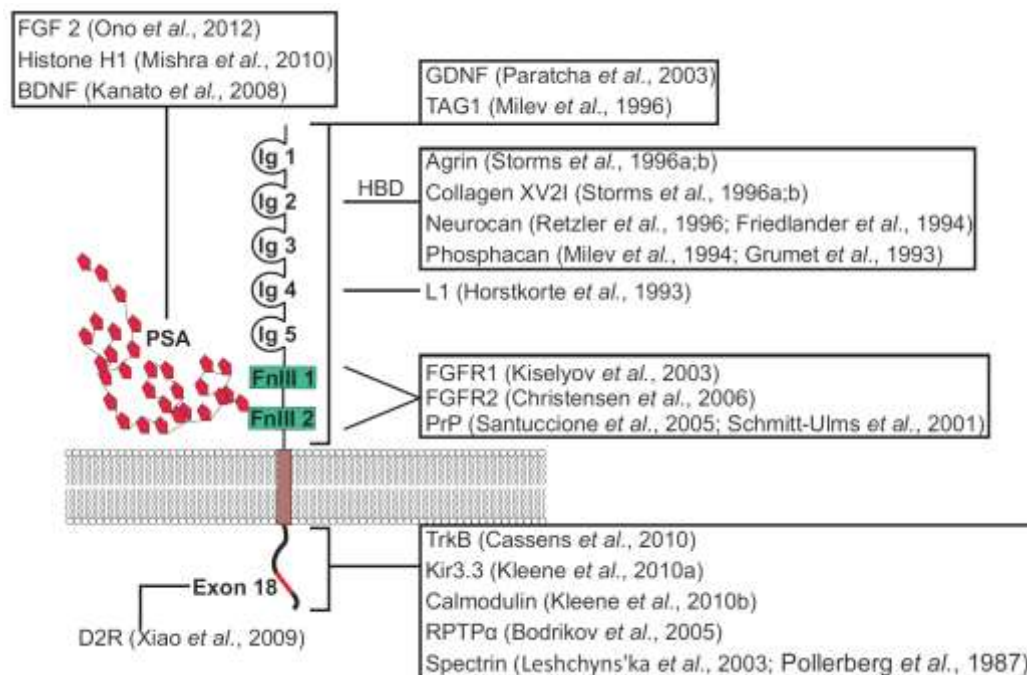


Figure 2.2: Direct interaction partners of NCAM and PSA. This schematic drawing illustrates the interaction between PSA-NCAM and its binding partners. The acronyms are: BDNF, brain-derived neurotrophic factor; CaM, calmodulin; D2R, dopamine receptor D2; FGF2, fibroblast growth factor 2; FGFR, fibroblast growth factor receptor; GDNF, glial cell line-derived neurotrophic factor; HBD, heparin binding domain; L1, cell adhesion molecule L1; PrP, prion protein; RPTPα, receptor protein tyrosine phosphatase α.

Introduction

NCAM-mediated functions are triggered via homophilic NCAM interactions or heterophilic interaction of NCAM with interaction partners. These interactions can be either between molecules on the same cell ('cis') or on opposite cells ('trans').

A variety of intra- and extracellular interaction partners of NCAM are known (Fig. 2.2). The ICD of NCAM interacts with cytoplasmic proteins depending on its posttranslational modification and the presence of proteins already bound to it. The hetero- and homophilic interactions can trigger signaling cascades which regulate cellular events, such as NCAM-mediated neurite outgrowth and cell migration. The extracellular signal regulated kinase 1/2 (ERK1/2) pathway is one of the central pathways in NCAM signaling (Ditlevsen and Kolkoya., 2010; Schmid *et al.*, 1999). This pathway is activated by homophilic NCAM interaction or by heterophilic interaction of NCAM with the FGFR, and thus, leads to the induction of the ERK pathway (Hinsby *et al.*, 2004; Downward, 1996). The binding of RPTP α to NCAM is essential for triggering of this pathway by the homophilic NCAM interaction. RPTP α links the Fyn/FAK complex to NCAM (Bodrikov *et al.*, 2005).

The heterophilic interaction of NCAM with the FGFR (Sanchez-Heras *et al.*, 2006) activates phospholipase C (PLC) and protein kinase A (PKA) (Jessen *et al.*, 2001). This activation leads to an increase in the cytoplasmic calcium concentration. A functional triggering polyclonal antibody against the ECD of NCAM (Klinz *et al.*, 1995; Schuch *et al.*, 1989) mimics the homo and/or heterophilic interactions of NCAM and increases also the intracellular calcium concentration (Schuch *et al.*, 1989). This increase in the calcium concentration was later shown to depend on PLC activation and activates the calcium-calmodulin-dependent protein kinase II (Williams *et al.*, 1995; 1994). It has been proposed that non-selective cation channels, such as TRPCs, and T-type voltage-gated calcium channels are required for NCAM-mediated calcium entry (Kiryushko *et al.*, 2006). It was reported, that this increased intracellular calcium concentration leads to proteolytic cleavage of NCAM by tumor necrosis factor- α -converting enzyme (TACE) (Kalus *et al.*, 2007) and generation of a 50 kDa NCAM fragment by a serine protease activity (Kleene *et al.*, 2010b). This fragment contains a part of the ECD, the transmembrane domain and a part of the ICD of

Introduction

NCAM. Furthermore, nuclear import of this 50 kDa NCAM fragment has been described (Kleene *et al.*, 2010b). Proteolytic cleavage of NCAM is essential for NCAM-mediated neurite outgrowth and cell migration (Kleene *et al.*, 2010b; Kalus *et al.*, 2007; Diestel *et al.*, 2005).

2.7 Myristoylated alanine-rich C-kinase substrate

Immunoaffinity chromatography using a PSA mimicking anti-idiotypic single chain variable fragment (scFv) antibody led to the identification of MARCKS as a novel binding partner for PSA (Maren von der Ohe, PhD thesis, Hamburg). MARCKS was identified as phosphorylation target for the protein kinase C (PKC) in brain synaptosomes. The phosphorylation of MARCKS by PKC is inhibited by binding of calmodulin to MARCKS (Wu *et al.*, 1982). PKC is the major mediator of G-protein-coupled receptor signaling and involved in regulating growth control, differentiation, secretion and metabolism (Newton *et al.*, 1998). Calmodulin is a highly conserved, soluble calcium binding and calcium regulatory protein. It plays an important role in many cellular functions such as channel modulation (Saimi *et al.*, 2002), control of gene expression, cell growth, cell cycle progression and muscle contraction (Plattner *et al.*, 2005).

MARCKS is a ubiquitously expressed cytoplasmic, rod-shaped acidic protein and it accounts for 0.2% of all soluble proteins in the brain (Albert *et al.*, 1987). It is important for development of the brain, postnatal survival, endo-, exo- and phagocytosis, cellular migration, cell adhesion and neurosecretion (Blackshear, 1993; Aderem, 1992). MARCKS and the MARCKS-related protein belong to the group of natively unfolded proteins (Weinreb *et al.*, 1996).

MARCKS contains three highly conserved domains: 1. an MH2 domain of unknown function that is similar to the cytoplasmic tail of the cation-independent mannose-6-phosphate receptor, 2. an N-terminal consensus sequence for myristoylation and 3. the phosphorylation site domain, in which all four serine residues are phosphorylatable by PKC (Arbuzova *et al.*, 2002). Myristoylation is a co-translational

Introduction

modification, in which myristic acid is attached via an amide bond to the amino group of an N-terminal glycine residue (Boutin, 1997). The phosphorylation site domain is also called effector domain (ED) (Arbuzova *et al.*, 2002) and is essential for the function of MARCKS.

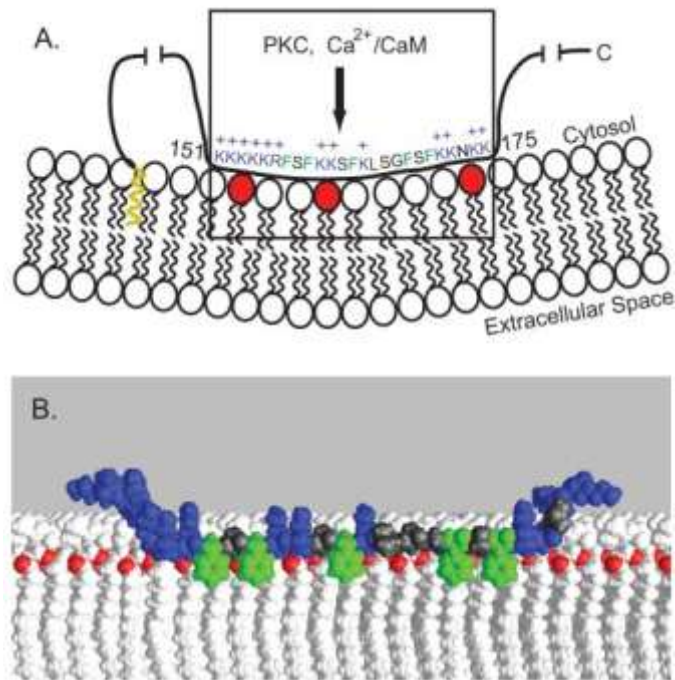


Figure 2.3: Molecular model of the attachment of MARCKS to the plasma membrane. (A) The figure schematically shows the attachment of MARCKS protein to the plasma membrane. The hydrophobic myristoylated N-terminus is shown in yellow and the ED (residues 151-175 from bovine MARCKS) which interacts electrostatically with acidic lipids (red) is depicted by the box. Phosphorylation of MARCKS by PKC or binding of calmodulin to MARCKS neutralizes the electrostatic interaction of MARCKS with the membrane and leads to detachment of MARCKS from the membrane. A molecular model of the ED at the membrane is depicted in (B). The five phenylalanine residues of the ED-domain penetrating into the lipid head group region of the membrane are shown in green and the basic residues of the ED are colored blue. **(Presentation was taken from Gambhir *et al.*, 2004)**

MARCKS binds via its highly basic ED to the acidic lipids of the plasma membrane of macrophages (Allen *et al.*, 1995a, b; Rosen *et al.*, 1990), neurons (Ouimet *et al.*,

Introduction

1990) and fibroblasts (Allen *et al.*, 1995a, b; Swierczynski *et al.*, 1995). The association of MARCKS with the membrane is stabilized by myristoylation of MARCKS, which anchors MARCKS in the plasma membrane (Fig. 2.3). Furthermore, the five phenylalanine residues within the ED insert into the lipid head group region of the membrane (Fig. 2.3) and stabilize the association of the ED with the membrane (Gambhir *et al.*, 2004).

The interaction of the myristoyl moiety and ED with lipids allow binding of MARCKS to the cell membrane (Bhatnagar *et al.*, 1997; Murray *et al.*, 1997). Calmodulin binds to the ED of MARCKS in a calcium-dependent manner. When the ED is phosphorylated by PKC, or when calmodulin binds to the ED, MARCKS detaches from the membrane and is released to the cytoplasm (Ohmori *et al.*, 2000; Arbusova *et al.*, 1998). The binding affinity of calmodulin to the ED of MARCKS is decreased significantly, when the ED is phosphorylated by PKC (Porumb *et al.*, 1997). MARCKS also binds to actin and phosphorylation by PKC and binding of calmodulin can inhibit binding of MARCKS to actin (Hartwig *et al.*, 1992).

MARCKS-deficient mice show brain malformations and perinatal death (Stumpo *et al.*, 1995). MARCKS heterozygous mice appear normal but have deficits in spatial learning (McNamara *et al.*, 1998). Obviously MARCKS plays an important role in the development of the central nervous system.

2.8 Transient receptor potential canonical or classical family

In hippocampal neurons, treatment with an NCAM-function triggering peptide leads to calcium entry into the cells (Kiryushko *et al.*, 2006). Application of an inhibitor of voltage-dependent calcium channels could not completely block this calcium entry, suggesting that part of this NCAM-induced calcium entry is not mediated by voltage-dependent calcium channels but could depend on ligand-gated calcium channels. Treatment of cells with a TRPC inhibitor could completely abolish calcium entry into the neurons (Kiryushko *et al.*, 2006). This finding shows that NCAM-mediated

Introduction

calcium entry in hippocampal neurons depends on voltage-gated calcium channels as well as TRPC calcium channels. NCAM and TRPC1/4/5 channels share the dopamine receptor D2 (Xiao *et al.*, 2009) and the FGFR (Kiselyov *et al.*, 2003) as common interaction partners. It has been shown that TRPC1, 4 and 5 channels play important roles in different physiological functions in the nervous system (Abramowitz *et al.*, 2009).

TRPC1 plays a role in proliferation of neural stem cells (Fiorio *et al.*, 2005), differentiation of cultured H19-7 hippocampal cells (Wu *et al.*, 2004), neurotrophic factor-induced growth cone turning and axon guidance (Shim *et al.*, 2005; Wang *et al.*, 2005), glutamate secretion from astrocytes (Malarkey *et al.*, 2008) and neuroprotection (Bollimuntha *et al.*, 2006; 2005). TRPC4 is involved in the response to neural injury (Wu *et al.*, 2007), the regulation of neurite outgrowth (Wu *et al.*, 2008; 2007) and the secretion of GABA (Munsch *et al.*, 2003). TRPC5 is linked to the inhibition of neurite outgrowth in hippocampal neurons (Greka *et al.*, 2003) and the response of the glutamate receptors to glutamate in lateral amygdala pyramidal neurons (Faber *et al.*, 2006). A heteromer of TRPC4/5 seems to be responsible for different electrical properties of neurons (Zhang *et al.*, 2011; Fowler *et al.*, 2007; Wang *et al.*, 2007).

TRPC proteins are nonselective cation channels permeable for calcium, sodium and potassium and they are expressed in all tissues. They can play a role in receptor-operated calcium entry or store-operated calcium entry (SOCE) (Selvaraj *et al.*, 2007) which is triggered by the activation of the phospholipase C β (PLC β) pathway. Upon activation, PLC hydrolyzes phosphatidylinositol (4,5) bisphosphate (PIP₂) to inositol-1,4,5-trisphosphate (IP₃) and diacylglycerol (DAG). In the case of receptor operated calcium entry (Hofmann *et al.*, 1999), DAG directly activates calcium channels in the plasma membrane. SOCE is triggered by binding of IP₃ to the IP₃ receptor (Salido *et al.*, 2009). The IP₃ receptor is an ionotropic receptor in the membrane of the endoplasmic reticulum, and it releases calcium from the intracellular stores into the cytoplasm after binding of IP₃ to its receptor. This increased calcium concentration in the cytoplasm activates store operated calcium channels in the plasma membrane.

2.9 Structure of the TRPC proteins

The TRPC channels are transmembrane proteins with six transmembrane segments and a cytoplasmic N- and C-terminus. The N-terminus of the TRPC channels contains three to four ankyrin repeats and a putative coiled-coil region (Fig. 2.4). The ankyrin repeats in the N-terminus of the TRPC channels are the most common repeat motifs in many different classes of proteins (Mosavi *et al.*, 2004) and are involved in cell-cell signaling, regulation of the cell cycle, transcription, transport and development.

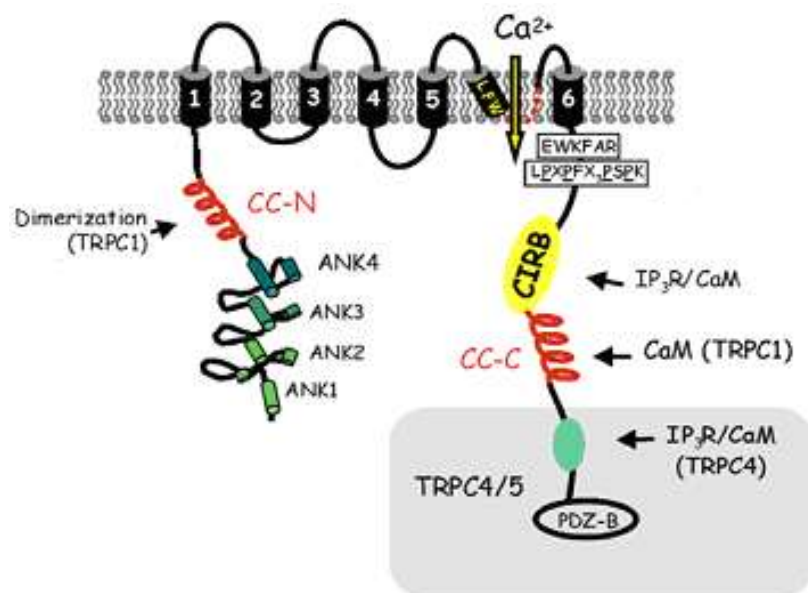


Figure 2.4: Structure of TRPC channels. The gray shaded region at the end of the C-terminus is unique in TRPC4/5. EWKFAR is the TRP box. LPXPF(X)₃PSPK is the conserved proline-rich sequence. Y(X)₄F(X)₁₃W is the caveolin-1 binding site. The acronyms are: ANK 1-4, ankyrin repeats 1-4; CC-N, N-terminal coiled-coil region; CC-C, C-terminal coiled-coil regions; PDZ-B, PDZ binding domain; CIRB, IP₃ receptor and calmodulin binding site; IP₃R, IP₃ receptor; CaM, calmodulin; LFW, amino acid motif conserved in all TRPC channels in the putative pore region. **(Presentation was taken from Vazquez *et al.*, 2004 and modified)**

The coiled-coil domain is an abundant protein motif; which consists of several heptad repeats folded into an alpha-helix. Two or more of these alpha-helices are curled into

Introduction

each other to form the coiled-coil domain. The coiled-coil region in the N-terminus, but not in the C-terminus, of TRPC1 is able to homodimerize (Engelke *et al.*, 2002).

The C-terminus of the TRPC channels is composed of a transient receptor potential (TRP) domain containing the TRP-box (Zhu *et al.*, 1995) and a proline-rich sequence (Latorre *et al.*, 2009), a calmodulin and IP₃ receptor-binding site (CIRB) region and a coiled-coil region (Fig. 2.4). The TRP box (Fig. 2.4) is a highly conserved 'EWKFAR motif and its function is still unclear. The CIRB motive was first identified in the C-terminus of TRPC3 and later also in other TRPC proteins (Tang *et al.*, 2001). Calmodulin and the IP₃ receptor compete for this binding site and the binding of calmodulin has an inhibitory effect on the channel (Zhang *et al.*, 2001). A calmodulin binding motif is present in the coiled-coil domain of the C-terminus of TRPC1. Deletion of this motif leads to a decrease of calcium-dependent inactivation of store-operated calcium entry (Singh *et al.*, 2002). Although the C-termini of TRPC4 and TRPC5 both contain an extended end terminating in a PDZ binding motive, their overall homology is rather low. In the extended end of TRPC4 an additional binding site for the IP₃ receptor and calmodulin was identified (Mery *et al.*, 2001; Trost *et al.*, 2001). Deletion of the PDZ binding motif in TRPC4 leads to a reduction of the surface localization (Mery *et al.*, 2002).

The TRPC channels form mainly homotetramers (Mio *et al.*, 2005), but they also form heterotetramers (Strübing *et al.*, 2001; Lintschinger *et al.*, 2000). An active tetramer is formed by interactions between the N-terminal ankyrin repeats and the C-terminal coiled-coil region (Lepage *et al.*, 2006). It has been proposed that TRPC proteins form heteromers with their closest phylogenetic relatives: TRPC1, TRPC4 and TRPC5 or TRPC3, TRPC6 and TRPC7 (Liman *et al.*, 2003; Hofmann *et al.*, 2002). However, recent studies could also identify heteromers containing TRPC1 and TRPC3 (Liu *et al.*, 2005; Lintschinger *et al.*, 2000) or TRPC3 and TRPC4 (Poteser *et al.*, 2006).

The ion pore of the TRPC channels is formed by the fifth and the sixth transmembrane domain. The conserved LWF motive as well as E576 and D581 have been proposed to form a helix in the pore region (Fig. 2.4) and are essential for pore formation. A change of one of these amino acids leads accordingly to a conversion of

Introduction

a non-selective ion channel to a channel selective for monovalent ions (Liu *et al.*, 2003). In addition, these mutations abolished or decreased store-mediated calcium currents and/or sodium currents (Liu *et al.*, 2003; Strübing *et al.*, 2003; Hofmann *et al.*, 2002).

2.10 Aims of the study

Previous experiments provide indications for an interaction of NCAM with TRPC channels, direct binding of PSA to MARCKS, and nuclear import of a glycosylated NCAM fragment. Based on these observations, my study has three major aims:

1. Verification of the functional interaction of TRPC channels with NCAM and investigation of the functional roles of this interaction.
2. Verification of NCAM-mediated import of PSA and HNK-1 into the nucleus.
3. Characterization of the binding between MARCKS and PSA and physiological consequences of this interaction.

3. Materials

3.1 Antibodies

3.1.1 Primary antibodies

<u>Name</u>	<u>Source</u>	<u>Species</u>	<u>Epitopes and application</u>
HNK-1 (412)	Kruse <i>et al.</i> , 1984	rat	raised against HNK-1; monoclonal; WB: 1:400 IF: 1:40
Histone H1 (FL-219)	Santa Cruz; sc-10806	rabbit	raised against amino acids 1-219 of Histone H1; polyclonal; WB: 1:200
Kir3.3 (C-18)	Santa Cruz; sc-19572	goat	raised against a peptide mapping near the C- terminus of Kir3.3; polyclonal; WB: 1:200 IP: 1:100
L1 (rabbit)	Pineda	rabbit	raised against the ECD of L1; polyclonal; WB: 1:1,000 St: 1:200
MARCKS (rb)	Lobaugh <i>et al.</i> , 1990 Kind gift from Prof. Dr. Perry J. Blackshear, Durham, USA	rabbit	raised against MARCKS; WB: 1:1,000 IF: 1:100
p-MARCKS	Santa Cruz; sc-12971	goat	Raised against amino acid sequence containing phosphorylated Ser 159

Materials

			and Ser 163 of MARCKS IF: 1:50
NCAM (1 β 2)	Niethammer <i>et al.</i> , 2002	rabbit	raised against the ECD of NCAM120/140/180; polyclonal; WB: 1:1,000 IP: 1:250 St: 1:200
NCAM 5B8	Gennarini <i>et al.</i> , 1984 (Hybridoma bank, Iowa, USA)	mouse	raised against the ICD of NCAM140/180; monoclonal; WB: 1:400
NCAM (chicken)	Pineda	chicken	raised against the ECD of NCAM; polyclonal; WB: 1:2,000 St: 1:200
NCAM D3	Schlosshauer <i>et al.</i> , 1989	mouse	raised against the ICD of NCAM180 (Exon 18); monoclonal; WB: 1:2,000
NCAM H28	Niethammer <i>et al.</i> , 2002	rat	raised against the ECD of NCAM120/140/180; monoclonal; WB: 1:100 IF: 1:50 IP: 1:25
NCAM P61	Gennarini <i>et al.</i> , 1984	rat	raised against the ICD of NCAM140/180; monoclonal; WB: 1:100 IF: 1:50
PSA (735)	Frosch <i>et al.</i> , 1985	mouse	raised against polysialic

Materials

	Kind gift of Prof. Dr. Rita Gerardy-Schahn, Hannover, Germany		acid; monoclonal; WB: 1:2,000 IF: 1:200
PrP (M-20)	Santa Cruz; sc-7694	goat	raised against a peptide mapping near the C-terminus; polyclonal; IP: 1:100
TRPC1 (H-105)	Santa Cruz; sc-20110	rabbit	raised against amino acids 689-793 (C- terminus); polyclonal; WB: 1:200 IF: 1:50 IP: 1:100
TRPC1 (E-6)	Santa Cruz; sc-133076	mouse	raised against amino acids 689-793 (C- terminus); monoclonal; WB: 1:200
TRPC1 (A-14)	Santa Cruz; sc-23011	goat	raised against amino acids 101-150 (N- terminus); polyclonal; WB: 1:200
TRPC1 (T1E3)	Kwan <i>et al.</i> , 2009; Xu <i>et al.</i> , 2005 Kind gift of Prof. Dr. Yao Xiaoqiang, Hong Kong, China	rabbit	raised against amino acids 586-606 (extracellular loop 3); polyclonal; I: 1:100
TRPC4 (N77/15)	NeuroMab; 75-119	mouse	raised against amino acids 930-947 (C- terminus); monoclonal; WB: 1:1,000
TRPC5 (N67/15)	NeuroMab; 75-104	mouse	raised against amino acids 827-845 (C-

Materials

			terminus); monoclonal; WB: 1:1,000
TRPC4/5 (H-80)	Santa Cruz; sc-28760	rabbit	raised against amino acids 1-80 (N-terminus of TRPC5); polyclonal; WB: 1:200 IF: 1:50 IP: 1:100
TRPC3/6/7 (H-100)	Santa Cruz; sc-20111	rabbit	raised against amino acids 1-100 (N-terminus of TRPC3); polyclonal; WB: 1:200 IF: 1:50 IP: 1:100
TRPC3/6/7 (A-15)	Santa Cruz; sc-20111	goat	raised against the C- terminus of TRPC3); polyclonal; WB: 1:200

Table 3.1: Table shows the antibodies used. The acronyms are: WB, Western blot; I, inhibition; St, stimulation; IF, immunofluorescence; IP, immunoprecipitations.

3.1.2 Secondary antibodies

All horseradish peroxidase (HRP)-, Cy2- Cy3- and Cy5-coupled secondary antibodies were purchased from the Jackson Laboratory (Dianova. Hamburg. Germany). HRP-coupled antibodies were used in a dilution of 1:10,000 to 1:20,000 in 4% skim milk powder in phosphate buffered saline solution pH 7.4 (PBS) containing 0.01% Triton X-100 (PBST) for immunoblotting and Cy2-, Cy3- and Cy5-coupled antibodies were used in a dilution of 1:200 to 1:400 in PBS for immunocytochemistry.

3.2 Bacterial strains

Escherichia coli DH5 α (Life Technologies, Karlsruhe, Germany)

Escherichia coli BL21 (DE3) (Novagen, Merck, Darmstadt, Germany)

3.3 Chemicals

All chemicals were obtained from following companies in p.a. quality: Bio-Rad (Hercules, CA, USA), Carl Roth (Karlsruhe, Germany), Enzo Life Sciences (Lörrach, Germany), Th. Geyer (Hamburg, Germany), Life Technologies (Karlsruhe, Germany), Macherey-Nagel (Düren, Germany), Merck (Darmstadt, Germany), Perbio Science (Bonn, Germany), Roche Diagnostics (Mannheim, Germany), Serva (Heidelberg, Germany) and Sigma-Aldrich (Deisenhofen, Germany).

3.4 Synthesized peptides

All peptides were synthesized by Dr. Christian Schafer-Nielsen (Schafer-N, Copenhagen, Denmark) with a purity of more than 95%.

MARCKS ED peptide:

H-KKKKKRFSFKKSFKLSGFSFKKNKK-OH

MARCKS control peptide:

H-KKKKKR**ASAKKSAK**LSG**ASAK**KNKK-OH

The alanine residues in the control peptide which replace the phenylalanine residues are shown in bold.

Materials

3.5 Molecular weight standards

3.5.1 1 kb DNA ladder

14 bands within a range of 100 to 12,000 bp (Life Technologies)

3.5.2 Precision plus protein™ all blue standards (BioRad)

Band No.	apparent molecular weight (kDa)
1	250
2	150
3	100
4	75
5	50
6	37
7	25
8	20
9	15
10	10

3.6 Plasmids

<u>Plasmid</u>	<u>Informations</u>
pcDNA (Life Technologies)	mammalian expression vector, ampicillin resistance
pcDNA-NCAM140 (Claas Cassens, PhD thesis, Hamburg)	mammalian expression vector of full length NCAM140
pcDNA-Kir3.1/Kir3.3 (Claas Cassens, PhD thesis, Hamburg)	mammalian expression vector of concatameric Kir3.1/3.3
pcDNA-TrkB	mammalian expression vector of full

Materials

(Claas Cassens, PhD thesis, Hamburg)	length TrkB
pcDNA-TRPC1 Kind gift from Dr. Markus Delling, Boston, USA	mammalian expression vector of full length TRPC1
pcDNA-TRPC4 Kind gift from Dr. Markus Delling, Boston, USA	mammalian expression vector of full length TRPC4
pcDNA-TRPC5 Kind gift from Dr. Markus Delling, Boston, USA	mammalian expression vector of full length TRPC5
pGEX-4T-2 (Amersham Pharmacia Biotech)	prokaryotic expression vector for recombinant expression of proteins carrying glutathione sulfotransferase (GST) tag at the 5' end, ampicillin resistance
pGEX-4T-2 TRPC1 N-terminus	prokaryotic expression vector for GST- tagged N-terminus of TRPC1
pGEX-4T-2 TRPC1 C-terminus	prokaryotic expression vector for GST- tagged C-terminus of TRPC1
pGEX-4T-2 TRPC4 N-terminus	prokaryotic expression vector for GST- tagged N-terminus of TRPC4
pGEX-4T-2 TRPC4 C-terminus	prokaryotic expression vector for GST- tagged C-terminus of TRPC4
pGEX-4T-2 TRPC5 N-terminus	prokaryotic expression vector for GST- tagged N-terminus of TRPC5
pGEX-4T-2 TRPC5 C-terminus	prokaryotic expression vector for GST- tagged C-terminus of TRPC5
pQE30 (Qiagen)	prokaryotic expression vector for recombinant expression of proteins carrying polyhistidine tag (6xHis) at the 5' end, ampicillin resistance

Materials

pQE30 NCAM140 ICD	prokaryotic expression vector for His-tagged NCAM140 ICD
pQE30 NCAM180 ICD	prokaryotic expression vector for His-tagged NCAM180 ICD
pQE30 NCAM140 ICD Δ N (Daniel Novak, PhD thesis, Hamburg)	prokaryotic expression vector for His-tagged NCAM140 ICD missing the N-terminus
pQE30 NCAM140 ICD Δ M (Daniel Novak, PhD thesis, Hamburg)	prokaryotic expression vector for His-tagged NCAM140 ICD missing the middle part
pQE30 NCAM140 ICD Δ C (Daniel Novak, PhD thesis, Hamburg)	prokaryotic expression vector for His-tagged NCAM140 ICD missing the C-terminus
pQE30 NCAM140 ICD Δ CaM (Mounir M'Zoughi, PhD thesis, Hamburg)	prokaryotic expression vector for His-tagged NCAM140 ICD with mutated calmodulin binding motif
pQE30 NCAM180 ICD Δ CaM (Mounir M'Zoughi, PhD thesis, Hamburg)	prokaryotic expression vector for His-tagged NCAM180 ICD with mutated calmodulin binding motif
pEGFP-N1-MARCKS-GFP wt Kind gift from Prof. Dr. Perry J. Blackshear, Durham, USA	mammalian expression vector of GFP-tagged full length MARCKS wild-type
pEGFP-N1-MARCKS-GFP A2G2 Kind gift from Prof. Dr. Perry J. Blackshear, Durham, USA	mammalian expression vector of GFP-tagged full length MARCKS mutant with alanine replacement of the amino-terminal glycine
pEGFP-N1-MARCKS-GFP F/A	mammalian expression vector of GFP-tagged full length MARCKS mutant with alanine replacement of the ED containing phenylalanine

Table 3.2: Table shows the plasmids used.

Materials

3.7 Mice

NCAM-deficient mice (NCAM^{-/-}) (Cremer *et al.*, 1994) were generated by breeding heterozygous mutant mice on a C57BL/6J background. C57BL/6 mice were used as wild-type mice and obtained from the breeding colony of the University clinics Hamburg-Eppendorf. Mice were kept under standard conditions with food and water *ad libitum* and a light:dark cycle of 12:12 hrs. Animals were sacrificed in a CO₂ chamber before the removal of brains. All animal experiments were approved by the University and State of Hamburg animal care committees and conform to NIH guidelines.

3.8 Solutions and buffers

<u>Buffer or solution</u>	<u>Amount</u>	<u>Ingredients</u>
5x sample buffer orange-G	0.025% 20%	orange G glycerol in TAE buffer
Ampicillin stock	100 mg/ml	in H ₂ O
Blotting buffer	250 mM 190 mM 20%	Tris glycine methanol
Blocking solution	137 mM 2.7 mM 8 mM 1.5 mM 0.05% 4%	NaCl KCl Na ₂ HPO ₄ KH ₂ PO ₄ pH 7.4 Tween 20 skim milk powder
Cerebellum medium	1 mM 1 mM 5 U/ml	L-glutamine sodium pyruvate penicillin/streptomycin

Materials

	0.1% 10 µg/ml 4 nM 100 µg/ml 30 nM 1x	bovine serum albumin (BSA) insulin L-thyroxine bovine transferrin, holo sodium-selenite B-27 supplement in Neurobasal A (Life Technologies)
CHO cell medium	10% 1 mM 1 mM 5 U/ml	foetal calf serum (FCS) L-glutamine sodium pyruvate penicillin/streptomycin in HAM's F12/GMEM 1:1 (PAA Laboratories, Cölbe, Germany)
Digestion solution	135 mM 5 mM 7 mM 4 mM 25 mM	NaCl KCl Na ₂ HPO ₄ NaHCO ₃ HEPES, pH 7.4
Dissection solution	4 mM 10 mM 6 mg/ml 5 µg/ml 3 mg/ml 12 mM	Hanks's balanced salt solution (HBSS) NaHCO ₃ HEPES D-glucose gentamycin BSA MgSO ₄
Electrode buffer	250 mM 10 mM 10 mM	KCl Tris-HCl, pH 7.0 MOPS
Elution buffer for the pGEX –system	20 mM	reduced glutathione

Materials

	50 mM	Tris-HCl, pH 8.0
Elution buffer for the pQE-system	50 mM 300 mM 250 mM	NaH ₂ PO ₄ NaCl imidazole
Ethidiumbromide staining solution	10 µg/ml	ethidiumbromide in TAE buffer
HEPES-buffered saline (HBS) (2x)	50 mM 280 mM 12 mM 10 mM 1.5 mM	HEPES, pH 7.1 NaCl dextrose KCl NH ₂ PO ₄
HEK cell medium	1 mM 1 mM 5 U/ml 10%	L-glutamine sodium pyruvate penicillin/streptomycin foetal calf serum (FCS) in high glucose Dulbecco modified Eagle's
Hippocampus medium	2 mM 1x 12 ng/ml	L-glutamine B-27 supplement bFGF in Neurobasal A
Kanamycin stock	25 mg/ml	in H ₂ O
LB-medium	10 g/l 10 g/l 5 g/l	bacto-tryptone, pH 7.4 NaCl yeast extract
LB-ampicillin medium	100 mg/l	ampicillin in LB-medium
LB-kanamycin medium	25 mg/l	kanamycin in LB-medium
LB-ampicillin plate	20 g/l 100 mg/l	agar in LB medium ampicillin
LB- kanamycin plate	20 g/l 25 mg/l	agar in LB medium kanamycin

Materials

Lysis buffer for the pQE-system	50 mM 300 mM 10 mM	NaH ₂ PO ₄ NaCl imidazole
Lysis buffer for the pGEX-system	1x 1% 1x	PBS Triton X-100 EDTA-free protease inhibitor (Roche)
N2a cell medium	1 mM 1 mM 5 U/ml 10%	L-glutamine sodium pyruvate penicillin/streptomycin foetal calf serum (FCS) in high glucose Dulbecco modified Eagle's medium (DMEM)
PBS (phosphate buffered saline)	137 mM 2.7 mM 8 mM 1.5 mM	NaCl KCl Na ₂ HPO ₄ KH ₂ PO ₄ , pH 7.4
PBST	137 mM 2.7 mM 8 mM 1.5 mM 0.05%	NaCl KCl Na ₂ HPO ₄ KH ₂ PO ₄ pH 7.4 Tween 20
Radio immunoprecipitation assay (RIPA) buffer	50 mM 180 mM 1 mM 1%	Tris-HCl, pH 7.4 NaCl Na ₄ P ₂ O ₇ NP-40
Running gel	2.3 ml 60 µl 15 µl	1 M Tris-HCl, pH 8.8 10% sodium dodecyl sulphate (SDS) 10% ammonium persulfate (APS)

Materials

	6 µl	tetramethylethylenediamine (TEMED)
→ 6%	2.5 ml	H ₂ O
	1.2 ml	30% acrylamide / 0.8% bisacrylamide
→ 8%	2.1 ml	H ₂ O
	1.6 ml	30% acrylamide / 0.8% bisacrylamide
→ 10%	1.7 ml	H ₂ O
	2.0 ml	30% acrylamide / 0.8% bisacrylamide
→ 12%	1.3 ml	H ₂ O
	2.4 ml	30% acrylamide / 0.8% bisacrylamide
→ 14%	0.9 ml	H ₂ O
	2.8 ml	30% acrylamide / 0.8% bisacrylamide
SDS sample buffer	10 g	SDS
	40 ml	1 M Tris-HCl, pH 6.8
	50 ml	glycerine (100%)
	5 mg	bromphenol blue
→ 4x	ad 125 ml	H ₂ O
→ 5x	ad 125 ml	H ₂ O
per 20 ml	200 mg	dithiothreitol (DTT)
SDS running buffer (10x)	250 mM	Tris
	1.9 M	glycine
	1%	SDS
Stacking gel (5 %)	1.6 ml	H ₂ O
	0.4 ml	30% acrylamide / 0.8% bisacrylamide
	0.3 ml	1M Tris-HCl, pH 6.8
	30 µl	10% SDS

Materials

	15 µl 6 µl	10% APS TEMED
Staining solution	1% 1% 1%	toluidine blue methylene blue sodium-tetraborate
Stripping solution	3.125% 500 mM	acetic acid NaCl
Tris-acetate-EDTA (TAE) buffer (50x)	2 M 100 mM	Tris-acetate, pH 8.0 ethylenediaminetetraacetic acid (EDTA)
Washing buffer for the pGEX – system	1x 1%	PBS, pH 7.4 Triton X-100
Washing buffer for the pQE – system 1	50 mM 600 mM 10 mM	NaH ₂ PO ₄ NaCl imidazole
Washing buffer for the pQE – system 2	50 mM 300 mM 20 mM	NaH ₂ PO ₄ NaCl imidazole
Washing buffer for the pQE – system 3	50 mM 300 mM 40 mM	NaH ₂ PO ₄ NaCl imidazole
Washing buffer for the pQE – system 4	50 mM 300 mM 60 mM	NaH ₂ PO ₄ NaCl imidazole

Table 3.3: Table shows the solutions and buffers used.

4 Methods

4.1 Biochemistry

4.1.1 Bind assay

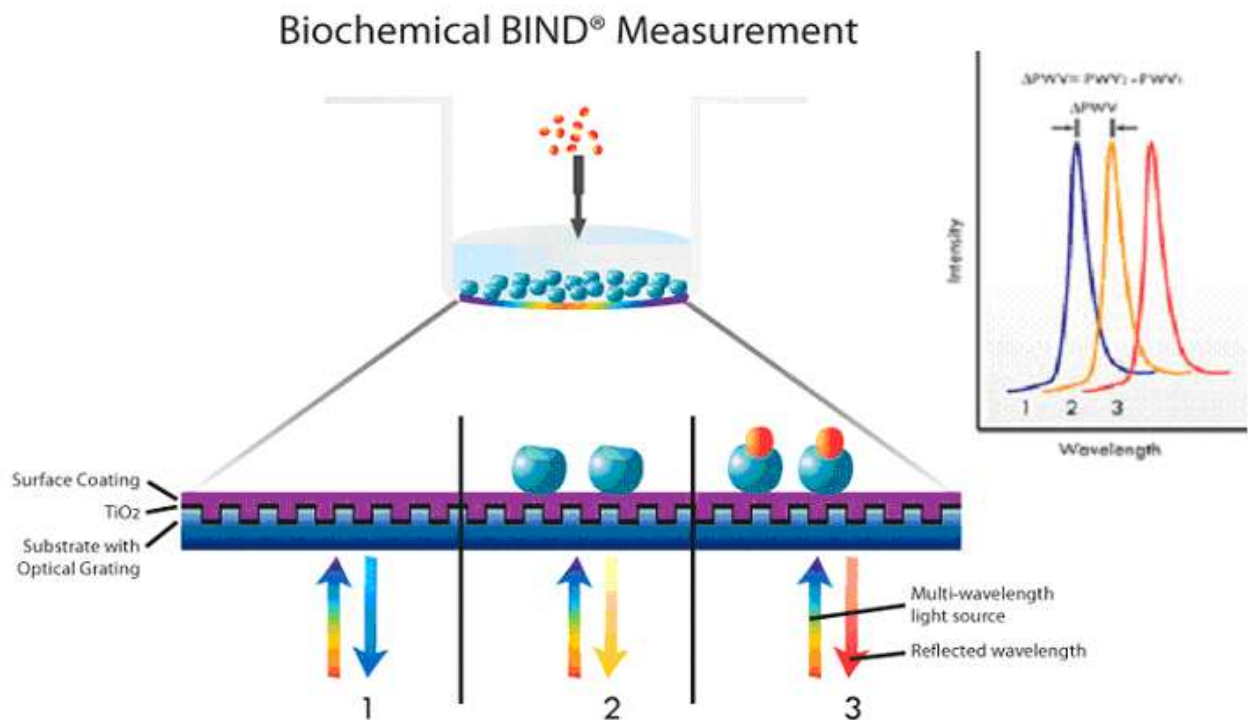


Figure 4.1: Schematic drawing of the principle of the label-free Bind assay. BIND uses a novel optical effect to provide highly sensitive measurements of changes in binding or adherence in the proximity of the biosensor surface. The bottom of the 384-well plates (SRU Biosystems, BIND®) contains layers with nanostructured optical grating. The optical grating reflects only a narrow range of wavelengths of light upon illumination with broadband light. Immobilization of a protein/receptor on the surface coating layer leads to a shift in the reflected wavelength (PWV shift). The shift in the reflected wavelength is proportional to the size and amount of protein that is bound to its surface. When a ligand is added to the wells with immobilized protein/receptor its binding/presence in close proximity of the biosensor leads to a further shift in the reflected wavelength. (Figure taken from: <http://www.srubiosystems.com/images/BiochemicalMeasurementLG.jpg>)

Methods

Bind assays were performed with the BIND[®] reader PROFILER turbo (SRU Biosystems, Woburn, MA, USA) (Fig. 4.1). As a starting point, 384-well plates with TiO₂ surface (SRU Biosystems) were washed with PBS²⁺ (PBS containing calcium and magnesium; PAA Laboratories) and the reflected wavelength was measured. Wells were coated overnight with the N- or C- termini of TRPC1, 4 or 5 at 4°C and afterwards the peak wavelength shift was measured. Then wells were blocked with 2% BSA in PBS for 3 hours at room temperature, washed and ICDs of NCAM140, NCAM180 or L1 with or without pre-treatment with calmodulin were added to the N- or C- termini of TRPC1, 4 or 5. The peak wavelength shift was monitored every 30 seconds for 1 hour. The shift of the peak wavelength is a measure of the binding affinity between the TRPC fragments and the ICDs of NCAM140, NCAM180 or L1.

4.1.2 Cell surface biotinylation

By cell surface biotinylation all primary amines in proteins, which are present outside of the cell, can be tagged. All cell surface biotinylation steps were performed on ice. Hippocampal neurons or transfected CHO cells were washed once with ice-cold phosphate buffered saline with 2 mM MgCl₂ and 0.5 mM CaCl₂ (PBS²⁺). Afterwards cells were incubated for ten minutes with 0.5 mg/ml membrane-impermeable sulfo-NHS-SS-biotin (Pierce) in PBS²⁺. Unreacted of sulfo-NHS-SS-biotin was quenched for 5 minutes with 20 mM glycine in PBS²⁺. Cells were washed twice with PBS²⁺ and lysed with RIPA buffer. The cell lysates were incubated for 30 minutes at 4°C. The lysates were centrifuged for 5 minutes with 1,000 g and the pellets were discarded. An aliquot of the supernatants was used as input control and the rest was incubated under rotation overnight at 4°C with magnetic streptavidin beads (Life Technologies). Beads were washed twice with RIPA buffer and once with PBS and afterwards incubated for 5 minutes with Laemmli buffer at 95°C. The samples were subjected to sodium dodecyl sulfate polyacrylamide gel electrophoresis (SDS-PAGE) and Western blot analysis.

Methods

4.1.3 Chloroform/methanol protein precipitation

Proteins were precipitated with chloroform/methanol according to Wessel and Flügge (1984). Methanol (4 vol.), chloroform (1 vol.) and H₂O (3 vol.) were added to protein solution (1 vol.). Afterwards the samples were vortexed thoroughly and centrifuged at 15,000 g for 2 minutes at room temperature. The organic phase was removed without disturbing the interphase, which contains the proteins. Then three volumes methanol were added and the samples were vortexed thoroughly and centrifuged at 15,000 g for 2 minutes at room temperature. The supernatant was discarded and the protein pellet dissolved in SDS sample buffer and subjected to SDS-PAGE and Western blot analysis.

4.1.4 Co-immunoprecipitation

Brains from wild-type or NCAM-deficient mice were homogenized with a glass pestle and a Elvehjem homogenizer in RIPA buffer containing protease inhibitor (Roche, Complete, EDTA free). The homogenate was cleared from tissue pieces by centrifugation (1,000 g; 5 minutes; 4°C). The supernatant was incubated for one hour at 4°C with antibodies against NCAM, TRPCs, Kir3.3, PrP or as control with unspecific IgGs from the species in which the primary antibodies were generated. Afterwards, protein A/G agarose beads (Santa Cruz) were added to the samples and they were incubated overnight at 4°C. Beads were precipitated together with the antibodies and protein complexes by centrifugation (1,000 g; 5 minutes; 4°C), washed twice with RIPA buffer and once with PBS. Proteins were eluted from the beads with 2x SDS sample buffer and subjected to SDS-PAGE and Western blot analysis.

Methods

4.1.5 Coupling of hydrazide dyes to colominic acid and chondroitin sulfate

For coupling of colominic acid (Sigma-Aldrich) and chondroitin sulfate (Sigma-Aldrich) to AMCA hydrazide (Sigma-Aldrich) or HiLyte Fluor™ 405 hydrazide (MoBiTec), the carbohydrates were activated by controlled periodate oxidation with 1 ml 100 mM sodium metaperiodate (Thermo Scientific) per 10 mg carbohydrate for 15 minutes. Afterwards 1 ml ethylene glycerol (Thermo Scientific) per 15 mg carbohydrate was added and probes were incubated for one hour at 4°C. The carbohydrates were precipitated with ethanol in a ratio of 1:1.5 (v/v), centrifuged (4,000 g, 4°C, 15 minutes) and diluted to 3 mg carbohydrate per ml water. The dyes were dissolved in dimethyl formamide (Thermo Scientific) to a concentration of 2 mM and added in a ratio of 1:10 (v/v) to the carbohydrates in water diluted. After 2 hours incubation time at 4°C the carbohydrates were precipitated with ethanol, centrifuged (4,000g, 4°C, 15 minutes) and diluted in PBS to a concentration of 30 mg/ml.

4.1.6 Coupling of hydrazide dyes to PSA-NCAM

For coupling of PSA-NCAM-Fc to HiLyte Fluor™ 405 hydrazide, the carbohydrates of the glycoprotein were activated by controlled periodate oxidation with 100 mM sodium metaperiodate. Then 200 µM HiLyte Fluor™ 405 hydrazide dissolved in dimethyl formamide (Thermo Scientific) was added to the activated PSA-NCAM-Fc and samples were incubated for 2 hours at room temperature in the dark. Finally the labeled glycoproteins were dialysed against PBS to remove unbound dye.

4.1.7 Protein cross-linking using photo-L-leucine

CHO cells were seeded in 6-well plates at a density of 1×10^6 cells per well. After 24 hours the medium was changed to DMEM without leucine (Thermo Scientific) supplemented with 1% penicillin/streptomycin (PAA Laboratories), 4 mM L-photo-

Methods

leucine (Thermo Scientific) and 2 mM methionine (Sigma-Aldrich). and the cells were transfected with MARCKS-GFP wild-type or a MARCKS-GFP mutant in which the phenylalanines were replaced by alanines (MARCKS-GFP F/A mutant) using TurboFect (Fermentas). For each construct cells from one 6-well plate were used. 24 hours after transfection cells were incubated for 10 minutes with 10 µg/ml PSA-NCAM-Fc or colominic acid and then for 5 minutes under UV-light (3x 15 W: wavelength of 365 nm). Afterwards the cells were lysed with 500 µl RIPA-buffer containing protease inhibitor mix (Roche, Complete, EDTA-free) per 6-well and incubated for half an hour at 4°C. Lysates were incubated overnight at 4°C with Protein A agarose beads (Santa Cruz) or an antibody against PSA (735) or against GFP (Rockland) and with Protein A/G agarose beads (Santa Cruz). The samples were analyzed with by SDS-PAGE and Western Blot analysis.

4.1.8 Determination of protein concentration

The protein concentration was determined with a bicinchoninic acid (BCA) assay using a BCA kit (Pierce) according the manufacturer instructions. 10 µl of the sample or 10 µl of the bovine serum albumin (BSA) standard in different concentrations (50 µg/ml; 100 µg/ml; 400 µg/ml; 500 µg/ml; 600 µg/ml; 1000 µg/ml) were placed in a 96-well plate. Reagent A and B were mixed in a ratio of 50:1 (v/v), added to the samples and incubated for 30 minutes at 37°C. Finally, the absorption was measured at 560 nm with a µQuant reader (BioTek, Bad-Friedrichshall, Germany) and the protein concentration calculated from the BSA standard curve.

4.1.9 Ethanol precipitation of carbohydrates

Carbohydrates were precipitated from carbohydrate solutions by addition of 4 volumes ethanol (-20°C) and incubation at -20°C overnight. Afterwards the carbohydrate solution was centrifuged at 15,000 g and 4°C for 20 minutes. The

Methods

supernatants were discarded, the pellets containing the precipitated carbohydrates dried at room temperature and then dissolved in H₂O.

4.1.10 Isolation of nuclear fractions from cultured cells using the Qproteome™ Nuclear Protein kit (Qiagen)

Six million N2A cells or cerebellar neurons were used for each condition. Soluble nuclear and chromatin-bound fractions were isolated using the Qproteome™ Nuclear Protein kit (Qiagen) according to the manufacturer's instructions. In brief, the medium was discarded and cells were lysed with NL-buffer, centrifuged (10,000g, 4°C, 5 min) and the supernatant was saved as the non-nuclear fraction. The cell pellet was re-suspended in NX1 buffer, incubated for 30 min at 4°C with constant agitation, centrifuged (12,000g, 4°C, 10 min) and the supernatant was saved as the soluble nuclear fraction. The pellet was re-suspended in NX2 buffer, incubated for 60 min at 4°C with constant agitation, centrifuged (12,000g, 4°C, 10 min) again and the resulting supernatant was saved as the chromatin-bound fraction. The proteins from every fraction (50 µl each fraction) were precipitated using chloroform/methanol, the pellets dissolved in SDS-sample buffer and subjected to SDS-PAGE and Western blot analysis.

4.1.11 Measurements of the capacitance of an artificial lipid bilayer

The Ionovation Compact V02 (Ionovation, Osnabrück, Germany) is an instrument which measures channel characteristics in an artificially lipid bilayer. The bilayer is formed by repetitive lowering and rising of the buffer level in the *cis*-chamber at a Teflon-septum with a 120 µm pinhole, which connects two chambers with each other. The lipid bilayer consisted of a 1:1 lipid mixture of 1-palmitoyl-2-oleoyl-*sn*-glycero-3-phosphoethanolamine (POPE) and 1-palmitoyl-2-oleoyl-*sn*-glycero-3-phosphocholine

Methods

(POPC) (Ionovation, Osnabrück, Germany). The chambers were filled with 1.4 ml electrode buffer and the formation of the lipid bilayer was monitored optically (Fig. 4.2) and by capacitance measurements. A stable membrane was built up with a capacitance between 60-80 pF.

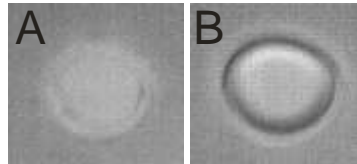


Figure 4.2: Picture of a pinhole without (A) or with (B) a lipid bilayer.

After a stable lipid bilayer was established, the capacitance of the lipid bilayer was measured and recorded every second. After 30 seconds, 3 μM colominic acid or chondroitin sulfate was added into the *trans*-chamber and the capacitance was recorded for 2 minutes. In the first setup 3 μM of the MARCKS control peptide was applied and the capacitance of the lipid bilayer was recorded for 3 minutes. Finally, 3 μM of the MARCKS-peptide was added and the capacitance of the bilayer was recorded for 6 minutes and 10 seconds. In the second setup only 3 μM of the MARCKS or control peptide was applied and the capacitance was recorded for 5 minutes and 50 seconds.

4.1.12 Measurements of DNA methylation and hydroxymethylation

For every measurement 2 million cells were used. Per condition four measurements were made, from which average values were calculated. The DNA from cerebellar granule neurons was isolated with the FitAmpTM Blood and Cultured Cell DNA Extraction Kit (Epigentek) according to the manufacturer's instructions. The DNA methylation and hydroxymethylation were measured with the MethylFlashTM

Methods

Methylated DNA Quantification Kit (Epigentek) and MethylFlash™ Hydroxymethylated DNA Quantification Kit (Epigentek).

4.1.13 Pull-down experiments

In pull-down experiments recombinant proteins were used to pull-down protein from protein extracts. Brains from wild-type mice were homogenized with a glass pestle and a Elvehjem homogenizer in RIPA buffer containing protease inhibitors (Roche; Complete, EDTA free). The homogenate was cleared from tissue debris by centrifugation (1,000 g; 5 minutes; 4°C). The supernatant was incubated for one hour at 4°C with recombinant expressed ICDs of NCAM140, NCAM180 or L1 containing a N-terminal histidine (His)-tag or with recombinantly expressed N- or C- termini of TRPC1 containing an N-terminal glutathione S-transferase (GST)-tag. To pull-down the tagged baits and proteins binding to them nickel agarose beads (Qiagen; for His-tagged proteins) or glutathione agarose beads (Sigma-Aldrich; for GST-tagged proteins) were added and the samples were incubated overnight at 4°C with constant agitation. Beads were precipitated together with bound baits and proteins binding to the bait proteins and protein complexes were precipitated by centrifugation (1,000 g; 5 minutes; 4°C), washed twice with RIPA buffer and once with PBS, eluted with 2 x sample buffer and subjected to SDS-PAGE and Western blot analysis.

4.1.14 Recombinant expression of proteins in *Escherichia coli* using the pQE-system or pGEX-system

Recombinantly expressed proteins were used for pull-down experiments or BIND assays. The cDNAs coding for the ICDs of NCAM140, NCAM180 and L1 were cloned in a pQE-vector containing a sequence coding for an N-terminal 6xHis-tag. The cDNAs coding for the N- and C- termini of TRPC1, 4 and 5 were cloned in a pGEX-vector containing a sequence coding for an N-terminal GST-tag. The *Escherichia coli* expression strain BL21 was transformed with the vectors, one clone

Methods

was grown overnight in 20 ml LB medium containing ampicillin. This 20 ml culture was added to 2 L LB medium containing ampicillin (Sigma-Aldrich) and the bacteria were grown at 37°C. Every hour the optical density (OD) was determined to monitor the growth of the bacteria. After the culture reached an OD of 0.6 the protein expression was induced by addition of 2 ml 1 M isopropyl-D-thiogalactopyranoside (ITPG; Biomol) and the culture was grown at room temperature for additional 8 hours. The protein expression was controlled by collecting small aliquots every hour after ITPG induction. Finally the cells were harvest by centrifugation (6,000 g; 10 minutes; 4°C) and the cell pellet was re-suspended in lysis buffer for the pQE-system or lysis buffer for the pGEX-system. The lysed cells were frozen at -20 C, thawed again and sonified at 4°C. To clear the protein extract from cell debris, samples were centrifuged at 10,000 g and 4°C for 20 minutes. The cleared lysates were incubated overnight at 4°C with nickel agarose (Qiagen) beads for purification of His-tagged proteins or with glutathione agarose beads (Sigma-Aldrich) for purification of GST-tagged proteins. Afterwards beads were washed with washing buffer for the pQE-system or the pGEX–system and the recombinantly expressed proteins were eluted with elution buffer for the pQE-system or elution buffer for the pGEX–system. Following dialysis against PBS, the proteins were concentrated using Vivaspin units (Vivascience; cut off 2,000 kDa) and stored at -80°C until use. The quality of the recombinant proteins was determined by SDS-PAGE and Coomassie blue staining.

4.1.15 Sodium dodecyl sulfate-polyacrylamide gel electrophoresis (SDS-PAGE)

SDS-PAGE is used for separation of proteins based on their molecular size. Self made discontinuous acrylamide gels containing a stacking gel (4% acrylamide) and a separation gel (8% or 10% acrylamide) or gradient gels (10% to 20% acrylamide) (GE Healthcare) were used. Protein samples were heated in SDS-sample buffer for 5 to 10 minutes at 95° and transferred into the sample pockets of the stacking gel. The electrophoresis was performed in BioRad electrophoresis chambers at 100 V for 20

Methods

minutes and afterwards at 200 V until the bromphenol blue line reached down to the bottom of the gel. Gels were subsequently subjected to Western blot analysis.

4.1.6 Coomassie blue staining of SDS polyacrylamide gels

SDS polyacrylamide gels were stained in Roti-Blue staining solution (30 ml H₂O; 10 ml methanol; 10 ml 5x Roti-Blue staining solution (Carl Roth) overnight at room temperature with constant agitation. Then the staining solution was removed and the gel was washed with H₂O until the blue background disappeared.

4.1.17 Western blot analysis

In Western blot analysis, proteins are transferred from the acrylamide gel onto a PROTRAN nitrocellulose membrane (Schleicher and Schuell) and detected with corresponding antibodies. For blotting, a Mini Transblot apparatus (BioRad) was used. The blotting “sandwich” was assembled according to the manufacturer’s instructions. Proteins were transferred electrophoretically for 90 minutes in blotting buffer at constant 100 V on ice. After this protein transfer, the nitrocellulose membrane was placed in a glass jar and the membrane was blocked for one hour in blocking solution (4% skim milk powder in PBST) at room temperature. The membrane was incubated overnight at 4°C on a shaking platform with a primary antibody, which was diluted in blocking solution. The primary antibody was removed and the membrane was washed six times for 5 minutes with PBST at room temperature. Afterwards, the membrane was incubated for one hour at room temperature on a shaking platform with a secondary antibody coupled to horseradish peroxidase (HRP), which was diluted in blocking solution. The secondary antibody was also removed and the membrane washed six times with PBST. Immunoreactivity was visualized with Lumigen™ TMA-6 (GE Healthcare) and detected with ImageQuant™ LAS 4000 mini (GE Healthcare).

4.1.18 Stripping of a nitrocellulose membrane

To incubate the nitrocellulose membrane a second time with a primary antibody, it was necessary to strip the old antibodies from the membrane. The nitrocellulose membrane was placed in a glass jar right-side up and incubated for 10 minutes with the stripping solution at room temperature. Afterwards, the acidic pH was neutralized with 1 M Tris (pH 8.0) and the membrane was blocked for one hour in blocking solution (4% skim milk powder in PBST) at room temperature and stained with the primary antibody.

4.2 Cell biology

4.2.1 Cell lines

In this work were uses Chinese hamster ovary (CHO) K1 cells, human embryonic kidney (HEK) 293 cells and Neuro 2a (N2a) cells. CHO K1 cells are derived from ovary of the Chinese hamster, HEK 293 cells are originally derived from human embryonic kidney cells and N2a is a neural crest-derived cell line from the mouse. They were grown in 20 ml cell medium in 175 cm² culture flasks (Sarstedt) or with 2 ml medium per well in 6 well plates (Sarstedt) in an incubator with 95% relative humidity and 5% CO₂ at 37°C. Every four days, cells were passaged when they reached confluence. During this procedure, cells were washed with pre-warmed (37°C) HBSS without calcium and magnesium (PAA Laboratories) and incubated for 5 minutes with Trypsin-EDTA (PAA Laboratories) and re-suspended in fresh medium and seeded in a new flask or 6-well plate in a dilution of 1:10.

Methods

4.2.2 Primary cell culture

4.2.2.1 Cell culture of primary cerebellar granule cells

For cerebellar granule cell culture, C57BL/6J (wild-type) or NCAM-deficient mice of postnatal day 6 to 7 were used. Mice were decapitated and their cerebellum was removed carefully with a forceps from the skulls. The cerebella were cleaned and cut into 3 pieces per cerebellum. The cerebella pieces were washed twice with ice cold HBBS (PAA Laboratories) and incubated with trypsin and DNase I in HBSS for 15 minutes at room temperature. After removal of the trypsin solution, the cerebella pieces were washed three times with ice cold HBBS, dissociated in HBSS containing DNase I with fire polished glass Pasteur pipettes. Afterwards cells were taken up in ice cold HBSS and centrifuged for 15 minutes at 4°C with 100 g. The cell pellet was dissolved in cerebellum medium and the cells were counted in a Neubauer chamber. Cells were plated on poly-L-lysine (PLL)-coated glass cover slips for immunostainings or seeded in PLL-coated 6-well culture plates with different densities (2 million cells per ml for biochemistry and immunostainings; 150,000 cells per ml for neurite outgrowth). Cells were maintained for 24 hours in a culture incubator (Heracel; Thermo-Fisher Scientific) at 37°C, 5% CO₂ and a humidified atmosphere.

4.2.2.2 Explants of the cerebellum

Cerebella were dissected as described in chapter 4.2.3.1, washed three times with ice cold HBSS and the tissue was dissociated with a metal net (mesh size: 150 µm). The tissue pieces or explants were washed three times with ice-cold HBBS and diluted in cerebellum medium with 10% horse serum and 10% fetal calf serum (1 ml per brain). The explants were plated overnight onto PLL-coated plastic cover slips in a small 50 µl medium and maintained in a culture incubator at 37°C and 5% CO₂ in a humidified atmosphere. On the next day, 200 µl cerebellum medium without serum were added to the coverslips and explants are maintained in culture for further 24 hours.

Methods

4.2.2.3 Cell culture of primary hippocampal cells

For hippocampal cell culture, C57BL/6J (wild-type) or NCAM-deficient mice of a postnatal day 0 to 2 were used. Mice were decapitated and their brain removed from the skulls. The brains were fixed with fine needles in the cerebellum and cut along the midline. The two hemispheres were opened like a book and the two hippocampi removed, cleaned and cut into 1 mm pieces. The hippocampi were washed once with dissection solution and incubated with trypsin and DNase I in digestion solution for five minutes at room temperature. After removal of the digestion solution, the digestion reaction was stopped by treatment with trypsin inhibitor in dissection solution and the hippocampi were washed twice with dissection solution. The hippocampi were then dissociated in dissection solution containing DNase I with fire polished glass Pasteur pipettes. Afterwards, dissection solution was added to the cells and the cells were centrifuged for 15 minutes at 4°C and 100 g. The cell pellet was dissolved in hippocampus medium and the cells were counted in a Neubauer chamber. Cells were plated on PLL-coated glass cover slips for immunostainings or seeded in PLL-coated well plates with different densities (2 million cells per ml for biochemistry and immunostainings; 150,000 cells per ml for neurite outgrowth).

4.2.3 Calcium imaging experiments

One million hippocampal neurons were seeded on PLL-coated glass cover slips and maintained in hippocampus medium with or without 10% horse serum overnight at 37°C and 5% CO₂ in a humidified atmosphere. Afterwards, cells were washed three times with pre-warmed dissection solution and maintained for at least 30 minutes in dissection solution containing 5 µM Fluo-4 AM (Life Technologies). Then, cover slips were transferred in petri dishes containing 3 ml dissection solution. During the live imaging the cells were kept in an incubation chamber (37°C, 5% CO₂, 70% humidity). Imaging of the calcium concentrations in the cells were performed with a confocal microscope OlympusFV1000. Images were taken with a 20x objective every second. Cells were triggered with antibodies against the ECD of NCAM or L1 and then

Methods

imaged for 1,000 seconds. The intensity of the Fluo-4 signal was measured from at least 20 cell somata using ImageJ software and related to the first image before stimulation (0 seconds).

4.2.4 Immunocytochemistry

Hippocampal or cerebellar neurons were seeded onto PLL-coated glass cover slips with a density of one million cells per ml and maintained in culture for 24 or 48 hours. Cells were fixed with 4% paraformaldehyde (PFA) in PBS for 15 minutes at 37°C. Afterwards, they were washed three times with PBS, permeabilized and blocked with 0.2% Triton X-100, 2% goat serum and 1% BSA in PBS for one hour at room temperature and incubated over night at 4°C with primary antibodies. Cells were washed three times for 5 minutes at room temperature with PBS and incubated with secondary antibodies diluted with a ration of 1:200 in PBS for 30 minutes at room temperature. Again, cells were washed three times for 5 minutes at room temperature with PBS and their nuclei were stained with bis-benzamide. Coverslips were mounted on glass slides with Fluoromount-G (SouthernBiotech) and stored in the darkness at 4°C.

4.2.5 Live staining

For live staining, a monoclonal antibody (1:50) against an epitope within the extracellular part of NCAM (H28) or against PSA (735) were incubated with living cells for 10 minutes at room temperature. Then the corresponding secondary antibody was applied and the cells were maintained for another 20 minutes in the incubator. Cells were fixed with 4% PFA in PBS for 15 minutes at 37°C. Afterwards they were washed three times with PBS, permeabilized and blocked with 0.2% Triton X-100, 2% goat serum and 1% BSA in PBS for one hour at room temperature and incubated overnight at 4°C with primary antibodies. Then cells were washed three times for 5 minutes at room temperature with PBS. For F-actin staining, cells were

Methods

incubated for 30 minutes at room temperature with Alexa 594-phalloidin (Life technologies) diluted 1:50 in PBS. Subsequently, cells were washed three times for 5 minutes at room temperature with PBS and incubated with secondary antibodies diluted 1:200 in PBS for 30 minutes at room temperature. Cells were washed three times for 5 minutes at room temperature with PBS and their nuclei were stained with bis-benzamide. Coverslips were mounted on glass slides with Fluoromount-G (SouthernBiotech) and stored in the dark at 4°C.

4.2.6 Fluorescence resonance energy transfer

Twenty four hours after transfection of CHO cells or hippocampal neurons, the dye linked carbohydrates were added to the medium for 15 minutes. Afterwards, the cover slip was transferred into a petri dish with 3 ml pre-warmed dissection solution. During live imaging cells were kept in an incubation chamber (37°C, 5% CO₂, 70% humidity). FRET analysis was performed with the confocal laser scanning microscope Olympus FV1000 using the sensitized emission method. As donor HiLyte Fluor™ 405 hydrazide was used and the acceptor was the GFP-tag of the MARCKS constructs.

4.2.7 Neurite outgrowth

Hippocampal or cerebella granule neurons were seeded at a density of 150,000 cells per ml in PLL-coated 48-well plates. The cells were maintained in culture medium without serum in an incubator (37°C, 5% CO₂, 95% humidity) for 20 to 24 hours. Afterwards, cells were fixed with 2.5% glutaraldehyde in culture medium for 30 minutes at 37°C. The medium with glutaraldehyde was removed and cells were washed three times with H₂O and stained with staining solution (1% toluidine blue and 1% methylene blue in 1% sodium tetraborate) for one hour at room temperature. Then the staining solution was removed, cells were washed three times with H₂O and plates with cells were dried at room temperature. The total length was measured from all neurites of single neurons which were at least as long as the cell body and

Methods

summarized for every cell using an Axiovert 135 microscope (Carl Zeiss) with Axiovision 4.6 imaging system.

4.2.8 Migration assay

Cerebella explants were maintained in cerebellum medium without serum in an incubator (37°C, 5% CO₂, 95% humidity) for 24 hours. Afterwards, explants were fixed with 2.5% glutaraldehyde in culture medium for 30 minutes at 37°C. The medium with glutaraldehyde was removed and explants were washed three times with H₂O and stained with staining solution (1% toluidine blue and 1% methylene blue in 1% sodium tetraborate) for one hour at room temperature. Then the staining solution was removed, explants were washed three times with H₂O and cover slips were dried at room temperature and mounted on microscopic slides using Eukit (Sigma-Aldrich) mounting solution. All cells migrating from the explants were counted using ImageJ software.

4.2.9 Coating of glass cover slips with poly-L-lysine

Glass cover slips were incubated for 30 minutes with 3 M HCl in an Erlenmeyer flask at room temperature with gentle agitation. Cover slips were washed twice with H₂O and incubated for 3 hours under gently shaking with acetone at room temperature. Afterwards, cover slips were washed five times with H₂O, twice with ethanol and sterilized at 200°C. Then the cover slips were coated overnight under gently shaking with PLL (0.01% in H₂O) at 4°C. Finally, cover slips were washed three times with H₂O, dried on sterile tinfoil under the laminar hood and incubated 30 minutes under UV light.

4.2.10 Transfection of cells with Fugene 6TM

One million cells per ml medium without serum were seeded onto PLL-coated glass cover slips or in 6-well plates. After 24 hours, according to the manufacturer's

Methods

instructions (Fugene 6™, Roche) a transfection solution was prepared. For every million of cultured cells, 2 µg plasmid DNA was mixed with 6 µl Fugen 6™ transfection reagent in 100 µl culture medium without serum. The transfection solution was mixed, kept for 20 minutes under the clean bench at room temperature and added drop wise to the cells. After transfection, cells were maintained in culture for further 24 to 48 hours.

4.2.11 Transfection of cells with calcium phosphate

One million hippocampal neurons per ml medium without serum were seeded on PLL-coated glass cover slips. After 24 hours, according to the manufacturer's instructions of the CalPhos mammalian transfection kit (Clontech), a transfection solution was prepared. For every million cultured cells, 3 µg plasmid DNA was mixed with 100 µl 25 mM calcium solution and this solution was mixed together with 100 µl 2x HBS. The transfection solution was mixed, kept for 20 minutes under the clean bench at room temperature and added drop wise to the cells. After transfection, cells were maintained in culture for further 24 to 48 hours.

4.3 Molecular biology

4.3.1 Polymerase chain reaction (PCR)

Vectors coding for the full length TRPC1, 4 and 5 cDNA in pcDNA3 were kindly provided from Dr. Markus Delling (Cardiology, Children's Hospital, Boston, USA). The intracellular N- and C-termini of TRPC1, 4 and 5 were amplified by PCR using following primers: TRPC1 N-Terminus: forward 5'-AAA CCC GGG ATG ATG GCG GCC CTG TAC CCG A-3', reverse 5'-TTT CCC GGG TTT CAT AAA AGG TGT GTG AAT GAT TCT-3'; TRPC1 C-Terminus: forward 5'-AAA CCC GGG ACC AAA CTG CTG GTG GCA ATG CT-3', reverse 5'-TTT CCC GGG ATT TCT TGG ATA AAA CAT AGC ATA TTT AG-3'; TRPC4 N-Terminus: forward 5'-AAA CCC GGG ATG GCT CAG TTC TAT TAC AAA AGA AAT-3', reverse 5'-TTT CCC GGG CTT CAC

Methods

CGC CCA GTG TCT TCT C-3'; TRPC4 C-Terminus: forward 5'-AAA CCC GGG AAT AAT TCT TAC CAA CTA ATT GCC GA-3', reverse 5'-TTT CCC GGG CAA TCT TGT GGT CAC ATA ATC TTC G-3'; TRPC5 N-Terminus: forward 5'-AAA CCC GGG ATG GCC CAA CTG TAC TAC AAA AAG G-3', reverse 5'-TTT CCC GGG CTT GAC TAC CCA GTG TTT CCG CC-3'; TRPC5 C-Terminus: forward 5'-AAA CCC GGG AAC AAC TCC TAT CAG CTT ATT GCC G-3', reverse 5'-TTT CCC GGG GAG GCG AGT TGT AAC TTG TTC TTC-3'.

The PCR solution contained:

DNA template (plasmid):	1 μ l
Primer forward (20 pM):	5 μ l
Primer reverse (20 pM):	5 μ l
dNTPs (2 mM each):	4 μ l
Tag-polymerase:	1 μ l
10x PCR buffer:	5 μ l
MgCl ₂ (50 mM):	2 μ l
H ₂ O:	27 μ l

Total:	50 μ l

The following program was used for the amplification:

cycles	temperature	time
1	95°C	5 minutes
31	95°C	30 seconds
31	65°C	30 seconds
31	72°C	1.5 minutes
1	72°C	7 minutes
1	4°C	forever

Methods

4.3.2 Horizontal agarose gel electrophoresis

1-2% agarose gels were prepared with TAE buffer in an electrophoresis chamber (BioRad). The DNA samples were diluted with 5x sample buffer with orange-G and loaded in the pocket of the agarose gel. The samples were run at constant 100 V until the orange-G dye reaches the end of the gel. The gel was stained in an ethidium bromide staining solution for 20 minutes and bands were visualized using an E.A.S.Y UV-light documentation system (Herolab).

4.3.3 Linearization of the pGEX-3X vector

The vector, in which the PCR products were inserted, had to be linearized. For this, the following restriction enzyme solutions were prepared:

<u>Vector pGEX-3X:</u>	
DNA:	2 μ l
NEB4:	2.5 μ l
10xBSA:	2.5 μ l
SmaI:	2 μ l
H ₂ O:	15 μ l

Total:	25 μ l

The restriction enzyme digestion time took one hour at 37°C. At the end the enzymes were deactivated for 20 minutes at 65°C.

Methods

4.3.4 Dephosphorylation of the pGEX-3X vector

To increase the possibility for a successful ligation, the linearized vector was dephosphorylated with following mixture:

Restriction product:	25 μ l
SAP buffer:	3 μ l
H ₂ O:	1.5 μ l
SAP:	3 μ l

Total:	32.5 μ l

The dephosphorylation time took one hour at 37°C.

4.3.5 Ligation of the insert into the pGEX-3X vector

For the ligation the following solution was incubated overnight at 4°C:

pGEX-3X vector	1 μ l
Insert	29 μ l
Polyethylene glycol [PEG] (5%)	4 μ l
T4-buffer	4 μ l
T4-DNA-Ligase	2 μ l

Total	40 μ l

Methods

4.3.6 Extraction of DNA from agarose gel

Bands were visualized with an UV lamp and carefully cut out of the gels and transferred to Eppendorf reaction tubes. The DNA was extracted from the agarose using the QIAquick Gel extraction kit (Qiagen).

4.3.7 Transformation of *Escherichia coli*

100 µl of competent strains of *Escherichia coli* were thawed on ice, 50-100 ng plasmid DNA were added and bacteria were maintained on ice for further 20 minutes. After heat shock at 42°C (DH5α for 2 minutes; BL21 for 20 seconds), bacteria were kept on ice for one minute. Afterwards 900 µl LB medium was added and cells were kept for 30 minutes at 37°C. The cells were centrifuged (4,000g, 2 minutes, room temperature) and the cell pellet was resuspended in 100 µl LB medium and plated on LB plates containing appropriate antibiotics. The bacteria were grown overnight at 37°C until single colonies were apparent.

4.3.8 Plasmid isolation from *Escherichia coli* culture

The preparation of plasmid DNA was based on alkaline lysis of bacteria, denaturation of protein by chaotropic salts and the isolation of DNA from contaminants using a glass fiber matrix. For small scale plasmid isolation, a single colony was added to 3 ml LB medium containing appropriate antibiotics and incubated for overnight at 37°C with constant shaking. Cells were harvested by centrifugation at 8,000 g for 1 min at RT. Plasmids were isolated with a Miniprep kit (Life Technologies). To prepare large amounts of plasmid DNA, 500 ml bacteria culture were taken to isolate plasmids using the Maxiprep kit (Qiagen) with the same principle.

4.3.9 Determination of DNA concentration

DNA concentrations were determined using the NanoDrop (Spectrophotometer ND-1000, Peqlab). The absorption at 260 nm and 280 nm was measured. The absorption at 260 nm displays the DNA concentration. The ratio of the absorbance at 260 and 280 nm was used to monitor the purity of DNA. A ratio of A₂₆₀/A₂₈₀ between 1.8 and 2.0 indicated sufficient purity of DNA for further experiments.

4.3.10 DNA sequencing

DNA sequencing was performed by the sequencing facility of the ZMNH (step-by-step protocols for DNA sequencing with SequenaseTM-version 2.0, 5th ed., USB, 1990).

4.3.11 Site directed mutagenesis

Mutations of the ED of MARCKS, by which the phenylalanine residues were exchanged by alanine residues, were generated using the GeneArt Site-Directed Mutagenesis System (Life Technologies) according to the instructions of the manufacturer. The mutations were generated in two steps. In the first step the forward primer 5'-ACG CCG AAA AAA AAA AAG AAG CGC GCT TCC GCT AAG AAG TCT TTC AAG-3' and the reverse primer 5'-GCC GCT CAG CTT GAA AGA CTT CTT AGC GGA AGC GCG CTT CTT TTT TTT-3' were used. In the second step the forward primer 5'-AAG AAG TCT TTC AAG CTG AGC GGC GCT TCC GCT AAG AAG AAC AAG AAG-3' and the reverse primer 5'-TGC CTC CTT CTT GTT CTT CTT AGC GGA AGC GCC GCT CAG CTT GAA AGA-3' were used.

5. Results

5.1 NCAM interacts with TRPC1, 4 and 5

Opening of non-selective cation channels (NSCC) and NSCC-induced calcium influx into the cell have been shown to depend on NCAM (Kiryushko *et al.*, 2006). In addition, the antagonist of the TRPC family SKF96365 can block this NCAM- and NSCC-dependent calcium entry. Interestingly, TRPC channels and NCAM share common interaction partners such as the dopamine receptor D2 (Xiao *et al.*, 2010; Hannan *et al.*, 2008) and the receptor tyrosine kinase TrkB (Cassens *et al.*, 2010; Li *et al.*, 1999). Based on these findings, it was conceivable that NCAM and TRPC channels interact with each other in protein complexes with the D2 receptor, TrkB and other proteins.

To test this hypothesis, I first performed co-immunoprecipitation experiments with mouse brain homogenates using antibodies against different members of the TRPC family (Fig. 5.1) or against NCAM (Fig. 5.2). The immunoprecipitates were then subjected to Western blot analysis with an NCAM180-specific antibody (Fig. 5.1A) or antibodies against NCAM140/180 (Fig. 5.1B) or different members of the TRPC family (Fig. 5.2).

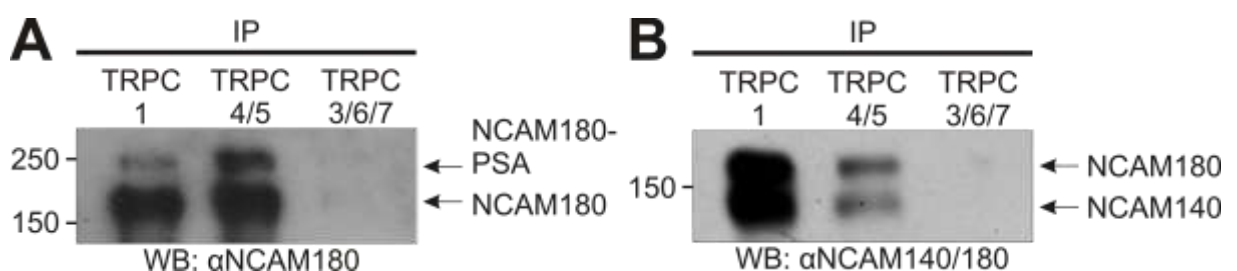


Figure 5.1: NCAM co-immunoprecipitates with TRPC1, 4 and/or 5. Antibodies against TRPC1 (H-105), TRPC4/5 (H-80) and TRPC3/6/7 (H-100) were used for immunoprecipitations (IP) from brain homogenate of adult wild-type mice. The immunoprecipitates were subjected to the SDS-PAGE and Western blot analysis and co-precipitated proteins were detected with antibodies against NCAM180 (D3) (A) or NCAM140/180 (NCAM 5B8) (B).

Results

Western blot with antibody 5B8 recognizing both transmembrane forms of NCAM showed NCAM140 and NCAM180 in immunoprecipitates with antibodies against TRPC1 and TRPC4/5, but not with antibodies against TRPC3/6/7 (Fig. 5.1). With the NCAM180-specific antibody D3, a ~180 kDa band and an additional ~250 kDa band which may represent PSA carrying NCAM180 was detected (Fig. 5.1A). TRPC1, 4 and 5, but not TRPC3, 6 and 7, were immunoprecipitated with antibodies against NCAM (Fig. 5.2). Since shorter splice variants of TRPC1 and 4 were described (Dedman *et al.*, 2011; Mery *et al.*, 2001), the double bands of TRPC1 in the immunoprecipitate from wild-type mice (A) and of TRPC4 in brain homogenate (B) could represent different splice variants of these channels. The results from immunoprecipitation experiments suggest that NCAM interacts with TRPC1, 4 and/or 5 channels.

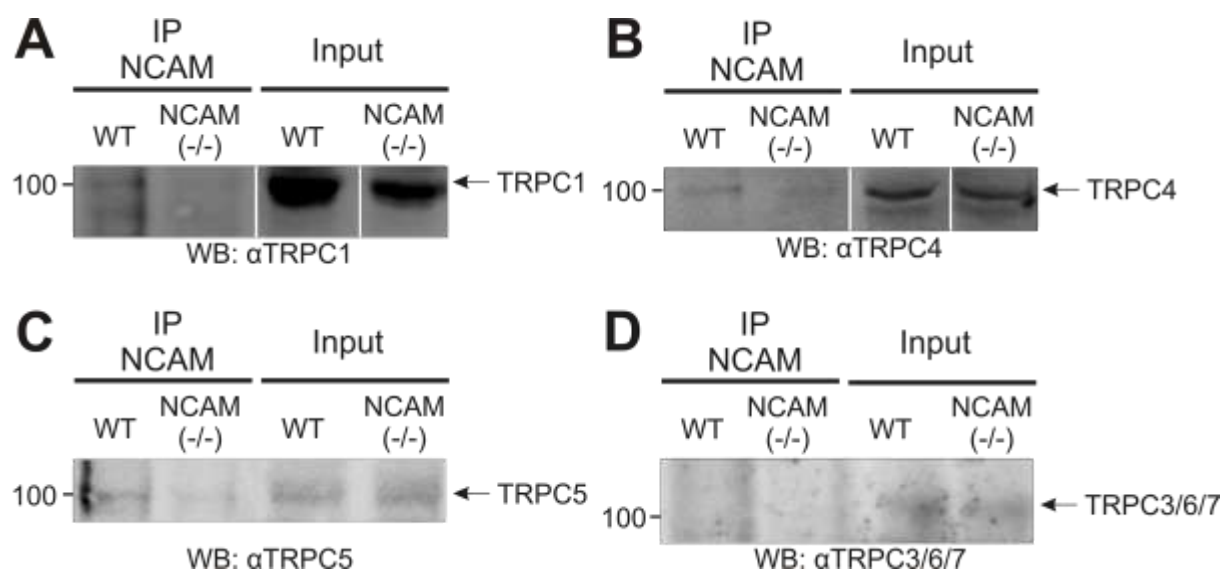


Figure 5.2: TRPC1, 4 and 5 co-immunoprecipitate with NCAM. Antibodies against the ECD of NCAM (NCAM H28; IP; NCAM) and brain homogenates of wild-type (WT) and NCAM-deficient mice (NCAM (-/-)) were used for immunoprecipitations. The immunoprecipitates (IP) and brain homogenates (input) were subjected to SDS-PAGE and Western blot analysis with antibodies against the TRPC subfamilies TRPC1 (H-105) (A), TRPC4 (N77/15) (B), TRPC5 (N67/15) (C) and TRPC3/6/7 (H-100) (D).

5.2 NCAM co-localizes with TRPC1, 4 and/or 5 at the cell surface of hippocampal neurons

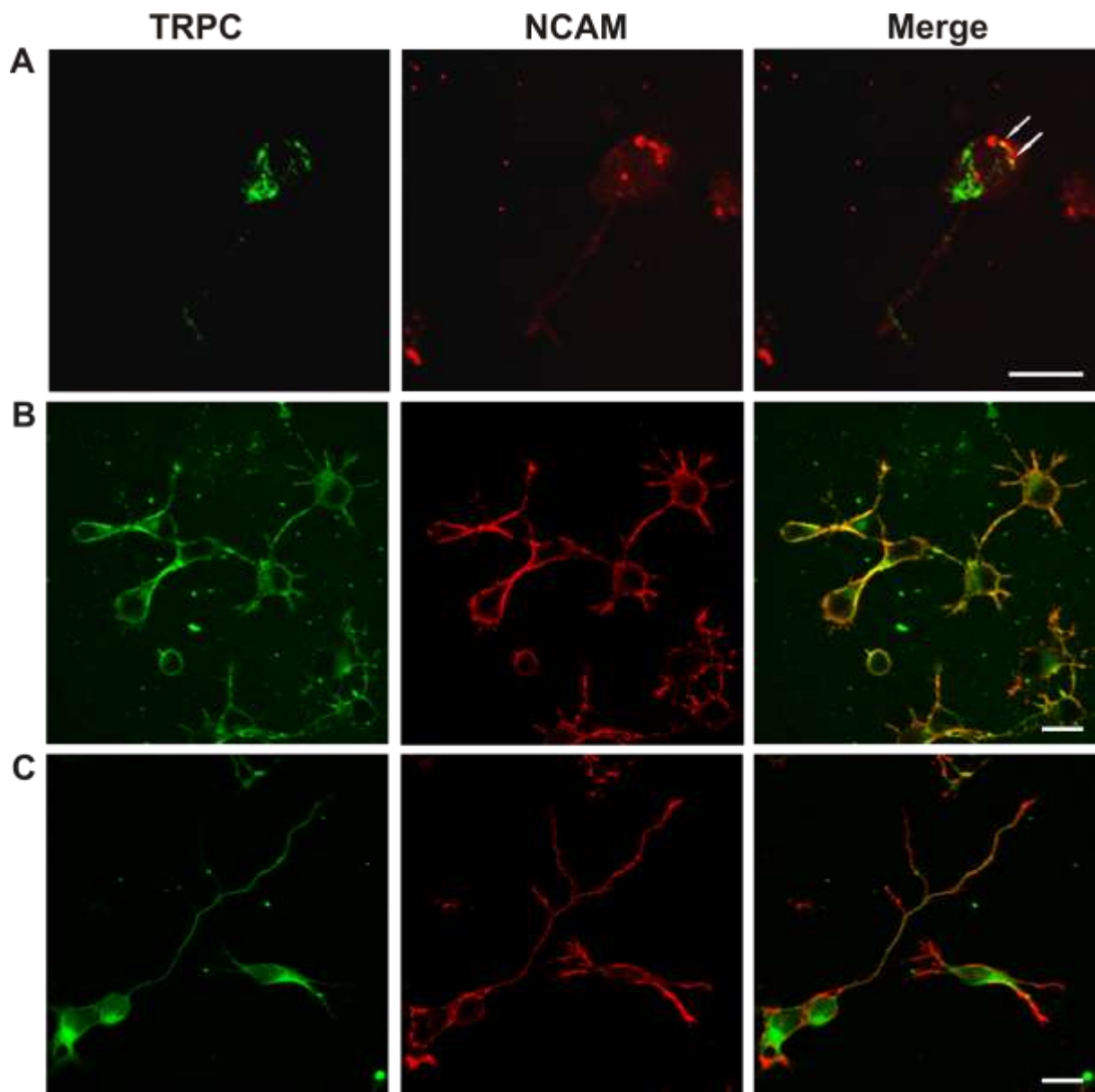


Figure 5.3: TRPC1, 4 and/or 5 co-localize with NCAM on live hippocampal neurons. NCAM was clustered on living cells with the monoclonal antibody H28 against an epitope in the extracellular part of NCAM and a secondary Cy3-labeled anti-rat antibody. Cells were fixed, permeabilized and stained with antibodies against TRPC1 (H-105) (A); TRPC4/5 (H-80) (B) or TRPC3/6/7 (H-100); (C). The immunofluorescence images show a partial co-localization (arrows) of TRPC1 and NCAM (A), a co-localization of TRPC4/5 and NCAM (B) and no co-localization of TRPC3/6/7 and NCAM (C). The scale bars represent 20 μm .

Results

To further substantiate the evidence for an NCAM-TRPC interaction, immunostainings of live hippocampal neurons with antibodies against members of the TRPC family and the ECD of NCAM were performed (Fig. 5.3).

After live staining with NCAM antibody, neurons were fixed, permeabilized and stained with antibodies against the intracellular part of distinct members of the TRPC family. The immunofluorescence images showed a partial co-localization of NCAM with TRPC1 (Fig. 5.3A, arrows) and a prominent co-localization of NCAM with TRPC4/5 (Fig. 5.3B), but not with TRPC 3/6/7 (Fig. 5.3C), indicating that NCAM and TRPC1/4/5 are co-localized at the cell surface.

5.3 TRPC1, TRPC4/5 and TRPC3/6/7 interact with Kir3.3 and PrP, but not with TrkB

Since NCAM interacts with TRPC channels and PrP (Santuccione *et al.*, 2005) and since Kir3.3 and TrkB interact in a competitive manner with the ICD of NCAM (Cassens *et al.*, 2010; Kleene *et al.*, 2010) it was interesting to investigate, if TRPC channels also associate with the NCAM interaction partners TrkB, Kir3.3 and/or PrP.

To this aim, immunoprecipitations from mouse brain homogenates were performed using antibodies against Kir3.3, PrP and TrkB and non-immune anti-goat antibody (Fig. 5.4). Western blot analysis with TRPC antibodies showed that Kir3.3 and PrP, but not TrkB, were precipitated with the antibodies against TRPC1, 4 and/or 5 (Fig. 5.4). These findings suggest that the NCAM interaction partners Kir3.3 and PrP could also interact with TRPC channels, probably within one protein complex.

Results

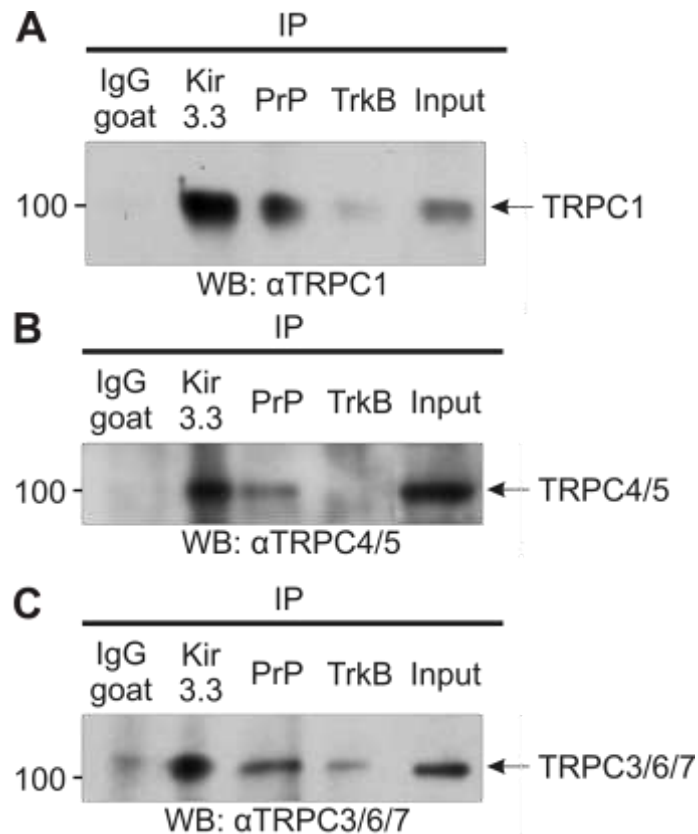


Figure 5.4: Kir3.3 and PrP, but not TrkB were co-immunoprecipitated with TRPC1, 4 and/or 5 channels. For immunoprecipitations, brain homogenates from wild-type mice and antibodies against Kir3.3 (C-18), PrP (M-20), TrkB (N-20) or non-immune goat control antibody (IgG; goat) were used. The immunoprecipitates (IP) and homogenates (Input) were subjected to SDS-PAGE and Western blot analysis with antibodies against TRPC1 (H-105) (A), TRPC4/5 (H-80) (B) and TRPC3/6/7 (H-100) (C).

5.4 TRPC proteins play an important role in NCAM-mediated neurite outgrowth from hippocampal neurons

Since NCAM interacts with TRPC1, 4 and/or 5, the question arises whether this interaction is of functional relevance. Therefore, I analyzed if NCAM-mediated neurite outgrowth can be modulated by the interaction of NCAM with TRPC1, 4 and/or 5 (Fig. 5.5).

Primary hippocampal neurons were maintained on PLL or on substrate-coated ECDs of NCAM, L1 or close homolog of L1 (CHL1) fused to human Fc and in the absence or presence of the TRPC inhibitor SKF96365, the TRPC1 inhibitory antibody T1E3 (Kwan *et al.*, 2009) or control pre-immune rabbit antibody.

Results

NCAM-, but not L1- or CHL1-enhanced neurite outgrowth, was inhibited with the TRPC inhibitor SKF96365 and the inhibitory antibody against TRPC1 when compared to neurite outgrowth observed in the absence of additives (Fig. 5.5). This suggests that the NCAM-TRPC interaction modulates NCAM-mediated neurite outgrowth.

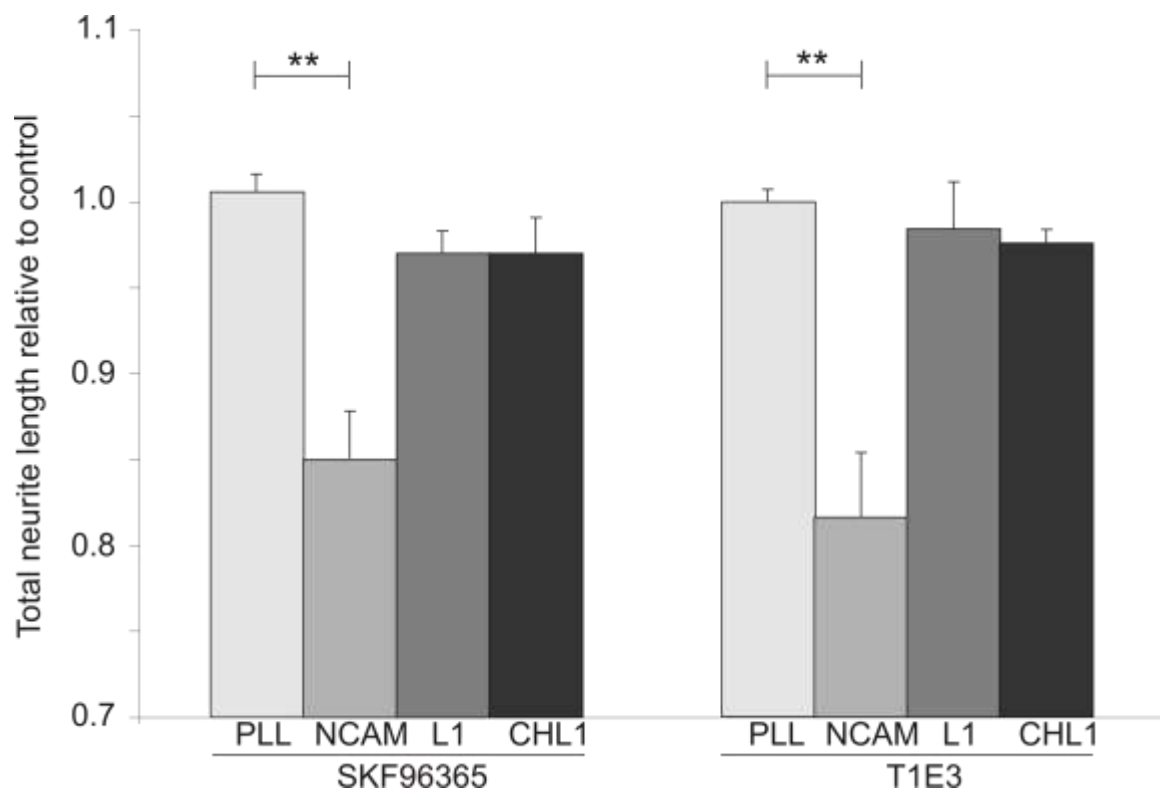


Figure 5.5: TRPC inhibitor SKF96365 and an inhibitory TRPC1 antibody block the NCAM-mediated neurite outgrowth. Primary hippocampal neurons were seeded on PLL substrate or NCAM-, L1- or CHL1-Fc. The cells were treated one hour after seeding with 2 μ M TRPC inhibitor SKF96365, 1.25 μ g/ml of an the inhibitory TRPC1 antibody (T1E3) or 1.25 μ g/ml of control pre-immune rabbit antibody. Non-treated neurons were used as control. The total lengths of neurites from the cells were measured. Ratios between values obtained for neurite outgrowth in the presence of inhibitor or antibodies and in the absence of additives were calculated. Mean values from three experiments are shown and the statistical analyses was performed with the Student's t-test (** $p < 0.01$). The error bars represent the standard error of the mean.

Results

5.5 Treatment of hippocampal neurons with antibodies against the extracellular domain of NCAM or L1 triggers different calcium responses

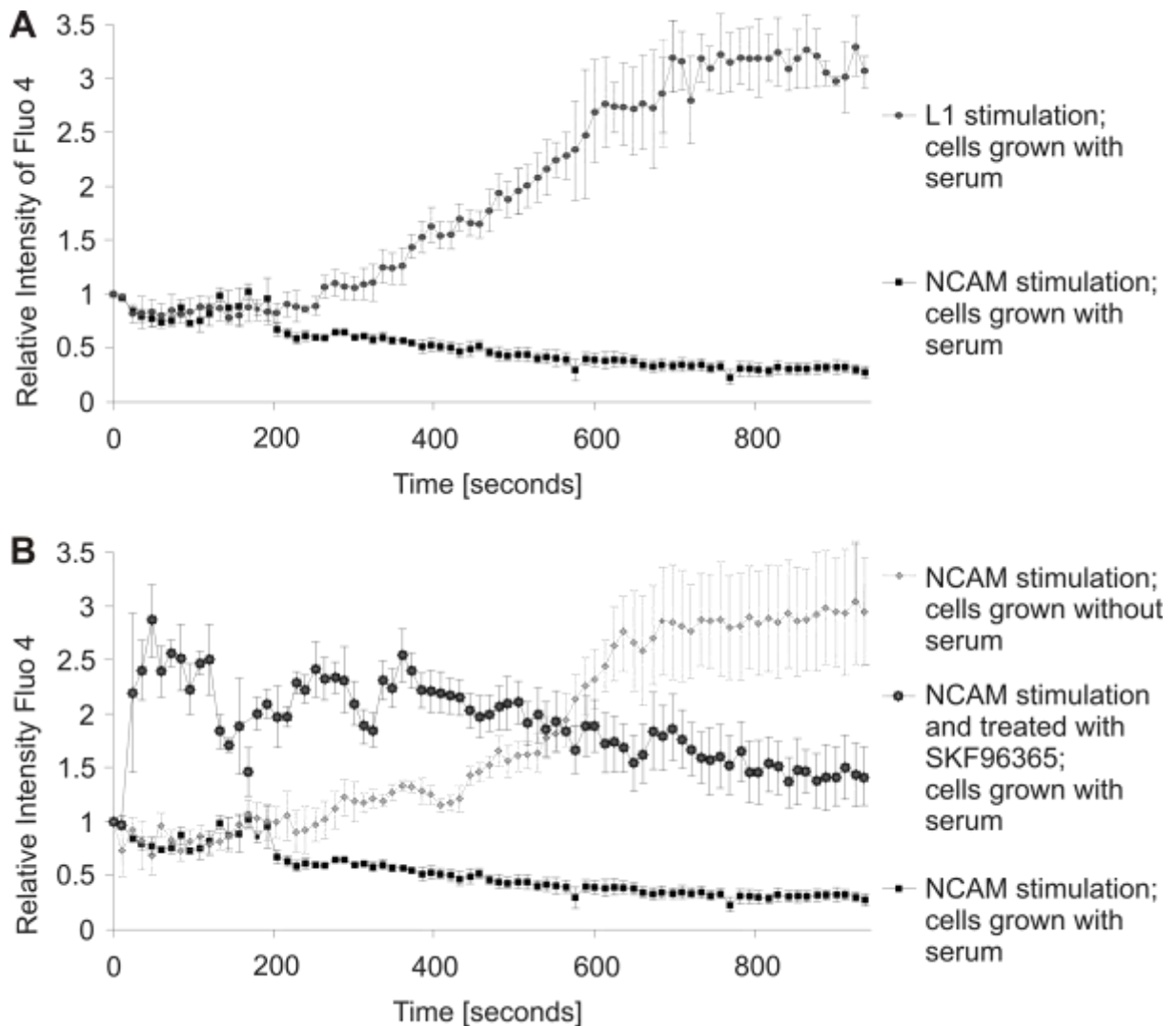


Figure 5.6: Stimulation of hippocampal neurons with an antibody against the ECD of NCAM leads to opening of TRPC channels in the cell membrane. The graphs show the intensity of Fluo-4 signal in primary hippocampal neurons after stimulation with an antibody against the ECD of NCAM (A; B) or L1 (A) related to the intensity before stimulation. The cells were maintained in medium with (A; B) or without (B) 10% horse serum. To inhibit calcium flux mediated by TRPCs 5 μ M SKF96365 was added together with the antibody against NCAM (B). The fluorescence intensity of the calcium signal was measured in soma of at least twenty cells using ImageJ. The live cell images were taken with a confocal microscope (Olympus FV 1000). Shown are mean values and the error bars depict the standard error of the mean.

Results

It has been shown previously that the calcium response of cells is induced by application of the ECDs of cell adhesion molecules or antibodies directed against these ECDs or peptides derived from parts of the ECDs (Kiryushko *et al.*, 2006; Schuch *et al.*, 1989). Moreover, this induced calcium influx leads to an enhanced neurite outgrowth (Kiryushko *et al.*, 2006; Klinz *et al.*, 1995). Since TRPC1, 4 and/or 5 are able to modulate calcium entry into the cell (Liu *et al.*, 2003) and due to the finding that TRPCs and NCAM interact with each other; it was conceivable to test whether the inhibition of TRPC function affects the calcium response of hippocampal neurons stimulated with antibodies against NCAM.

To this aim, calcium imaging experiments were performed with hippocampal neurons. Neurons were loaded with the calcium indicator Fluo-4 and then maintained in a calcium- and magnesium-free medium. Live cell images were taken on a confocal microscope over a time period of 900 seconds. At a defined time point, stimulation with a polyclonal antibody against the ECD of NCAM or L1 was performed. The intensity of Fluo-4 signals within the cell soma was determined and referred to the intensity of Fluo-4 signal before antibody application (Fig. 5.6A, B).

I first investigated whether the calcium response from hippocampal neurons maintained in medium with horse-serum, would differ after NCAM- or L1- antibody treatment (Fig. 5.6A). After stimulation of L1, the signal intensity indicating cytosolic calcium concentration increased until it reached a plateau and remained constant during the rest of the measurement (Fig. 5.6A). In contrast, NCAM stimulation leads to a significant calcium efflux out of the cells (Fig. 5.6).

It seems that two different mechanisms are triggered after NCAM-antibody or L1-antibody stimulation. If the cells were treated with the TRPC inhibitor SKF96365, the intracellular calcium concentration increased rapidly after NCAM-antibody stimulation, decreased afterwards slightly and stayed constant for the rest of the measured time frame (Fig. 5.6B). Neurons that had been kept in medium without horse-serum showed a calcium response after NCAM stimulation that was similar to the calcium response after L1 stimulation: the signal intensity increased until it reached a plateau (Fig. 5.6B).

Results

5.6 TRPC4 and 5 are localized at the cell surface of cultured primary hippocampal neurons

The results from the calcium imaging experiments imply that application of serum might lead to subcellular re-distribution of TRPC channels, so that they can be transported to the cell surface in order to modulate the cellular calcium flux.

To investigate this, cell surface biotinylation of hippocampal neurons which were kept in serum-free medium or medium containing 10% horse serum was performed. After biotinylation, cells were lysed; biotinylated proteins were isolated using Streptavidin beads and then subjected to Western blot analysis using antibodies against different TRPC channels.

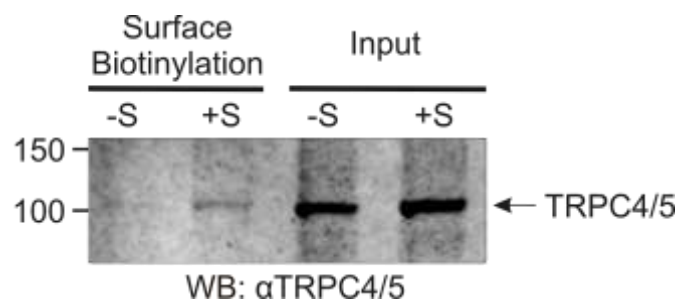


Figure 5.7: Cell surface expression of TRPC4/5 on primary hippocampal neurons is modulated by serum components. Cells were grown overnight with (+ S) or without (- S) 10% horse serum before cell surface biotinylation. Biotinylated proteins were isolated with streptavidin beads (surface) and subjected to Western blot analysis using an antibody against TRPC4/5 (H-80).

The expression levels of TRPC4/5 in cell lysates (input) were not changed upon application of serum (Fig. 5.7). In contrast to this, cells grown in medium containing 10% serum exhibited increased levels of TRPC4/5 at the cell surface compared to cells maintained in serum-free medium (Fig. 5.7), suggesting that application of serum leads to translocation of TRPC4/5 to the cell surface.

5.7 NCAM and TrkB regulate the localization of Kir3.1/3.3 heteromers at the cell surface

In immunoprecipitations experiments TRPC1, 4 and 5 could be co-precipitated with Kir3.3. Moreover, NCAM interacts with TrkB and Kir3.3 (Cassens *et al.*, 2010; Kleene *et al.*, 2010a), and as a consequence the activity of the Kir3.3 channel increases (Kleene *et al.*, 2010a). Hence, it seemed reasonable to investigate whether NCAM and/or TrkB co-expression could also influence the cell surface expression of Kir3.3.

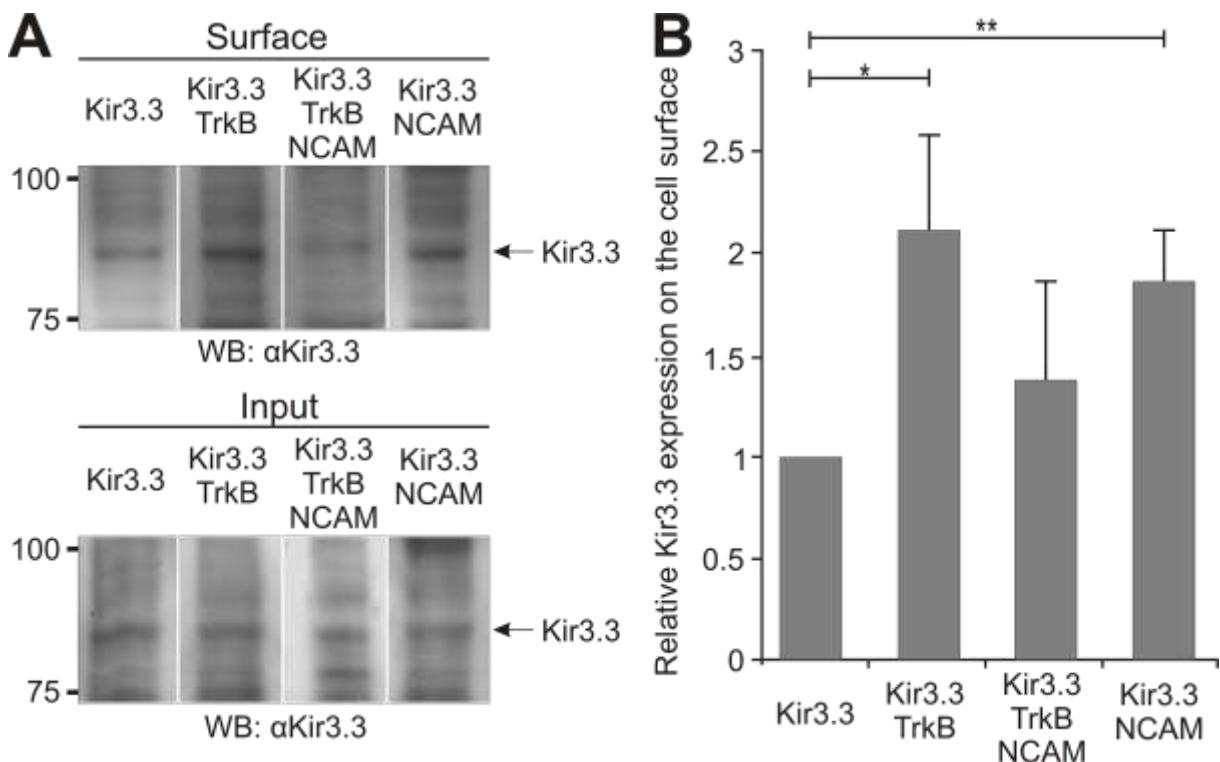


Figure 5.8: NCAM and TrkB regulate the cell surface expression of Kir3.3. CHO cells were transfected with concatameric Kir3.1/3.3 alone (Kir3.3), or co-transfected with TrkB (Kir3.3 + TrkB), TrkB and NCAM (Kir3.3 + TrkB + NCAM) or NCAM (Kir3.3 + NCAM). After cell surface biotinylation, cells were lysed (Input) and biotinylated proteins were isolated using streptavidin beads (Surface) and subjected to Western Blot analysis (A, upper panel: cell surface proteins; A, lower panel: input). Both blots were detected with an antibody directed against Kir3.3 (C-18) and the intensity of bands was quantified by densitometry using TINA software. Values from all conditions were related to values obtained after the transfection with Kir3.3 alone. In the diagram (B) the mean values from three blots are shown. The statistical analysis was performed with the Student's t-test (* $p < 0.05$; ** $p < 0.01$). The error bars represent the standard deviation.

Results

To determine if TrkB and/or NCAM modulate the surface localization of Kir3.3, CHO cells were transfected with concatameric Kir3.1/3.3 alone or co-transfected with Kir3.1/3.3 and TrkB or NCAM140 or with Kir3.1/3.3 and TrkB and NCAM140. After transfection, a cell surface biotinylation assay was performed (Fig. 5.8) and biotinylated proteins were isolated using streptavidin beads. The isolated proteins were subjected to Western blot analysis with an antibody against Kir3.3.

Levels of biotinylated Kir3.3 were significantly higher in CHO cells co-transfected with Kir3.1/3.3 and TrkB or NCAM140 than levels in CHO cells transfected with concatameric Kir3.1/3.3 alone. Kir3.1/3.3-positive CHO cells transfected either with TrkB or NCAM showed significantly higher expression levels of biotinylated Kir3.3 than CHO cells co-transfected with Kir3.1/3.3, TrkB and NCAM together. These results indicate that the cell surface expression of Kir3.3 is enhanced due to the presence of NCAM or TrkB and reduced due to NCAM-TrkB interaction when both proteins are co-expressed.

5.8 The intracellular domains of NCAM140/180 interact with the N- terminus of TRPC1

To narrow down which regions in NCAM and TRPC channels are necessary for the interaction between NCAM and TRPCs mouse brain homogenates were used for pull-down experiments with the ICDs of NCAM140/180 (Fig. 5.9). His-tagged ICDs of NCAM140/180 and truncated ICDs of NCAM140, in which the C-terminus, middle part or N-terminus (ΔC , ΔM or ΔN) (Fig. 5.9A) is missing (Daniel Novak, PhD thesis, Hamburg), were used as bait to precipitate TRPCs from mouse brain homogenates. Additionally, recombinant N- and C-terminus of TRPC1 containing a GST-tag were used as bait to precipitate NCAM from mouse brain homogenates. The ID of L1 was used as a control.

The ICDs of NCAM140/180 as well as the truncated ICD of NCAM140 lacking the middle part of the NCAM-ICD (ΔM), but not the truncated ICDs lacking the C- or N-termini (ΔC and ΔN) or the L1-ICD, precipitated TRPC1 from mouse brain

Results

homogenates (Fig. 5.9B). Moreover, only the N-terminus of TRPC1 could precipitate NCAM (Fig. 5.10A), but not L1 (Fig. 5.10B), from mouse brain homogenates. This result suggests that the ICDs of NCAM140/180 and TRPC1 interact with each other and that both ends of the ICD of NCAM140 are important for the NCAM-TRPC1 interaction.

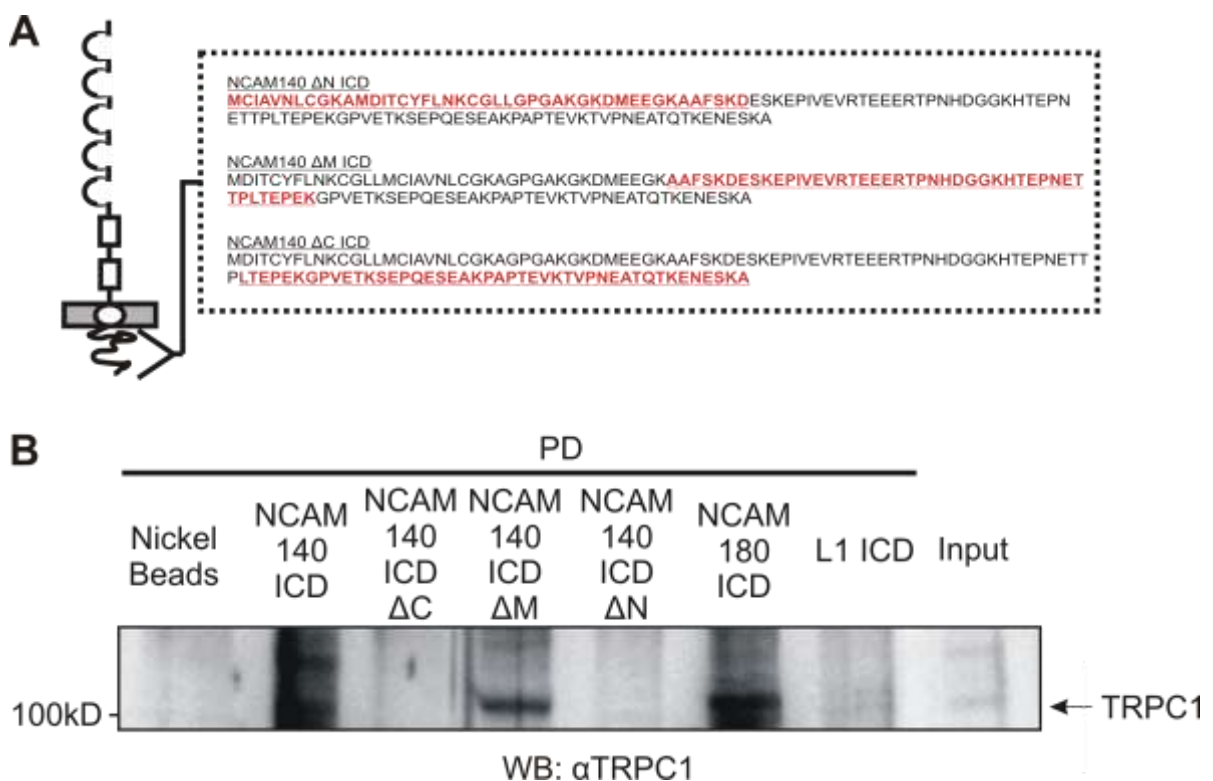


Figure 5.9: TRPC1 is pulled down with the ICD of NCAM140/180, but not with the ICD of L1. For pull-down experiments the ICDs of NCAM140/180, L1 or truncated ICDs of NCAM140 (B) were used and incubated with a protein extract from brain homogenate of wild-type mice (Input). The truncated ICDs were missing the C-terminus (Δ C), the middle part (Δ M) or the N-terminus (Δ N) of the ICDs (A: red and underlined highlights truncated parts). All ICDs contain a His-tag. As negative control only nickel beads (B) were incubated with protein extract. The precipitates were analyzed by SDS-PAGE and Western blot. The blot was incubated with an antibody against TRPC1 (E-6).

Due to the fact that the ICDs of NCAM140/180 contain a binding motif for calmodulin (Kleene *et al.*, 2010b), like all TRPC channels (Vazquez *et al.*, 2004), it was conceivable that calmodulin could mediate the interaction between the ICDs of NCAM140/180 and TRPC1.

Results

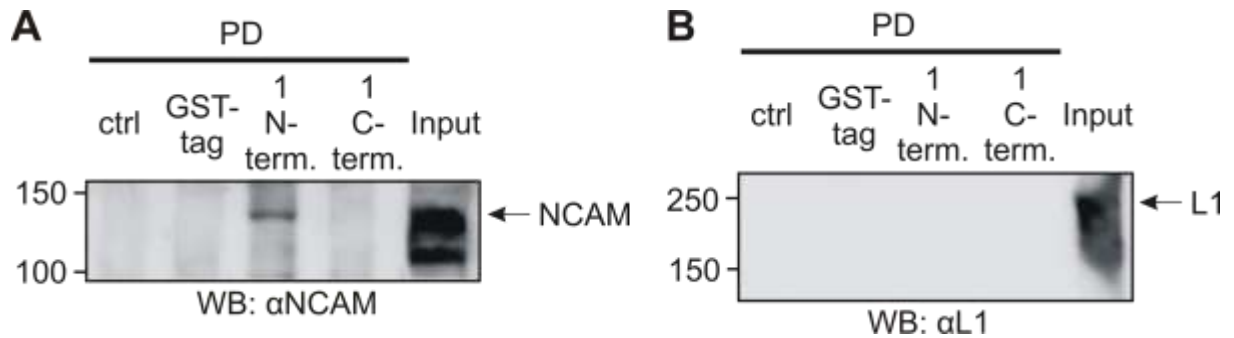


Figure 5.10: NCAM, but not L1, is pulled down with the N-terminus of TRPC1. For pull-down experiments, brain homogenates of wild-type mice (Input) and the cytoplasmic N- and C- termini of TRPC1 (1 N-Term.; 1 C-Term.) with a glutathione sulfotransferase (GST)- tag or as control only beads (ctrl) or GST alone (GST-tag) (A) or wild-type and mutated ICDs of NCAM140/180 (A, B) were used. The precipitates were subjected to SDS-PAGE and Western blot analysis with antibodies against NCAM (5B8) (A) or L1 (557) (B).

To prove this, mouse brain homogenates were used for pull-down experiments with ICDs of wild-type NCAM140/180 and of NCAM ICDs with mutated calmodulin binding motif (Kleene *et al.*, 2010b). TRPC1 co-precipitated with the wild-type and the mutated ICDs of NCAM140.

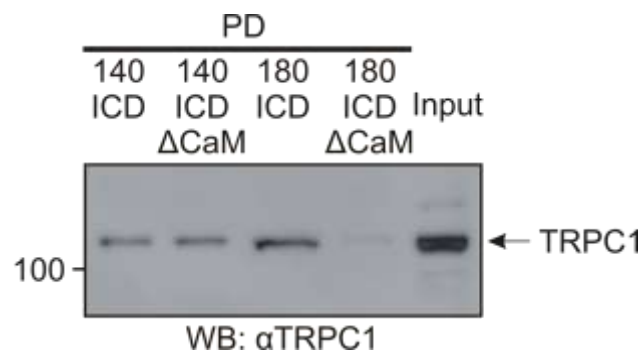


Figure 5.11: TRPC1 is pulled down with the ICD of NCAM140 with and without calmodulin binding motif and with the ID of NCAM180 containing the calmodulin binding motif. For pull-down experiments, brain homogenates of wild-type mice (Input) and wild-type and mutated ICDs of NCAM140/180 were used. The mutated ICDs contained a mutated calmodulin binding motif (Δ CaM) which prohibits the binding of calmodulin. The precipitates were subjected to SDS-PAGE and Western blot analysis with TRPC1 antibody.

Interestingly, the wild-type ICD of NCAM180, but not the mutated ICD of NCAM180, to which calmodulin cannot bind, precipitated TRPC1 (Fig. 5.11). These findings

Results

provide evidence that the NCAM180-TRPC1 interaction is calmodulin-dependent, whereas the NCAM140-TRPC1 interaction does not depend on calmodulin.

5.9 The interaction between the intracellular domain of NCAM180 and the N-terminus of TRPC5 is calmodulin-dependent

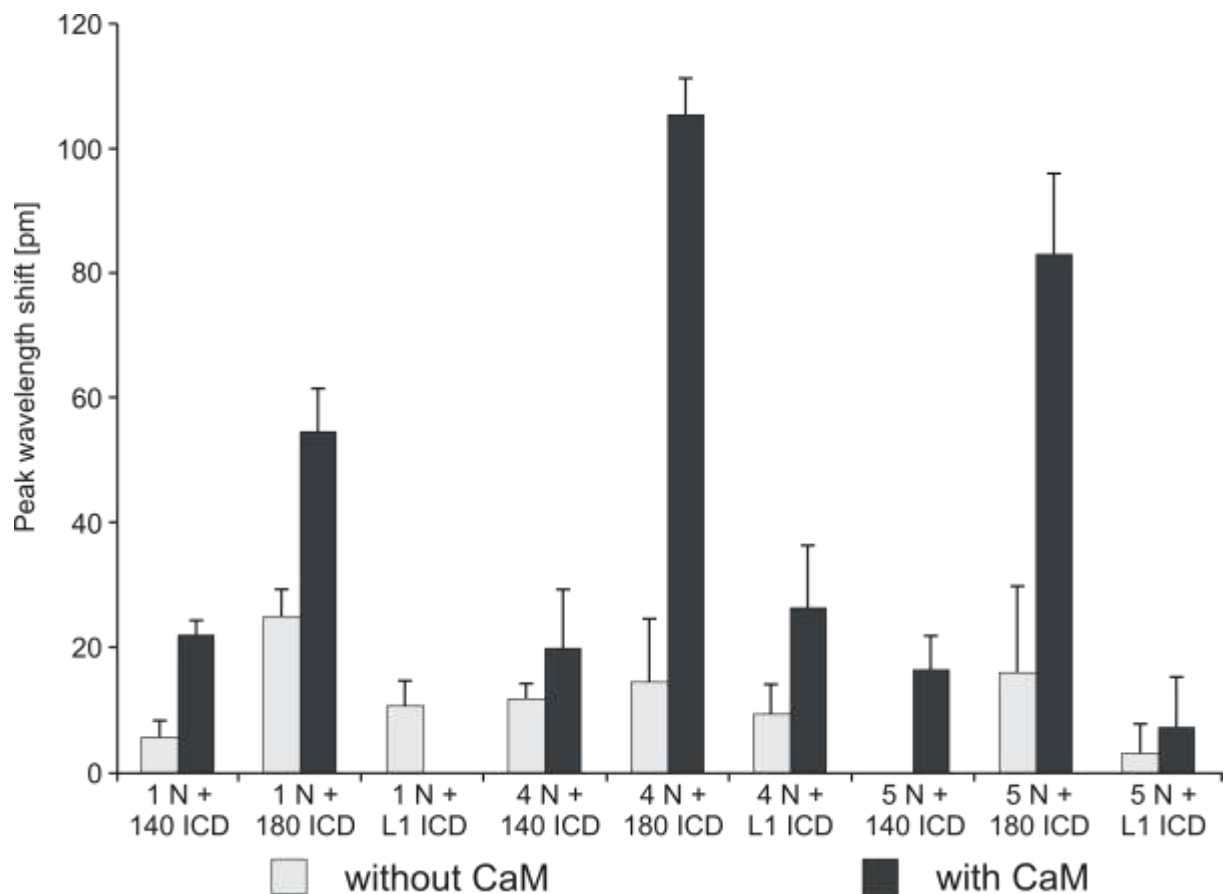


Figure 5.12: Calmodulin-dependent binding of the ICD of NCAM180 to the N-termini of TRPC1, 4 and 5. A label-free binding assay was performed with the N-termini of TRPC1, 4 or 5 (1N, 4N, and 5N) and the ICDs of NCAM140, NCAM180, or L1 (140 ICD, 180 ICD and L1 ICD). The N-termini of TRPC1, 4 and 5 were immobilized overnight at 4°C. The ICDs of the adhesion molecules were pre-incubated with or without calmodulin (CaM) for 30 minutes at 37°C and added as interaction partners to the substrates. The shift in the reflected wavelength (Peak wavelength shift [pm]) upon binding is shown. An increased shift is the result of a binding of the interaction partner to the immobilized substrate. The graph shows mean values from 4 wells per condition and the error bars represent the standard error of the mean.

Results

Next, I investigated whether NCAM140/180 and TRPCs bind directly to each other or if this binding is mediated by calmodulin and thus indirect. A label-free binding assay was performed with the N-termini of TRPC1, 4 and 5 as substrate coats and the ICDs of NCAM pre-incubated with calmodulin. As controls, mock-treated ICDs and ICDs of L1 were used (Fig. 5.12). Binding was analyzed by recording the peak wavelength shifts.

The ICD of NCAM180 showed a strong calmodulin-dependent binding to the N-termini of TRPC1, 4 and 5 (Fig. 5.12), whereas no binding was seen in the absence of calmodulin. The ICDs of NCAM140 and L1 showed only very weak or no binding to the N-termini of TRPC1, 4 and 5 in this assay. The results indicate that the NCAM180-TRPC1/4/5-interaction is calmodulin-dependent and confirm the previous results obtained in the pull-down experiments.

5.10 Inhibition of TRPC by SKF96365 reduces the nuclear import of the 50 kDa NCAM fragment

NCAM is proteolytically cleaved at the plasma membrane generating a 50 kDa NCAM fragment, which translocates into the nucleus in a calcium- and calmodulin-dependent manner (Kleene *et al.*, 2010b). Since calmodulin binds to the ICDs of NCAM140/180 (Kleene *et al.*, 2010b) and NCAM interacts with TRPCs, it was interesting to examine if the TRPC inhibitor SKF96365 affects the nuclear import of the 50 kDa NCAM fragment upon NCAM specific stimulation.

For this purpose, N2A cells, which express endogenous NCAM, were treated without or with 5 μ M or 10 μ M SKF9636 and triggered with an antibody against the ECD of NCAM (1 β 2). Non-stimulated cells were used as a control. After stimulation with NCAM antibody, nuclear fractions containing either nucleoplasmic or chromatin-associated proteins were isolated with the Qproteome™ Nuclear Protein Kit from Qiagen and subjected to Western blot analysis.

Results

As expected, the 50 kDa NCAM fragment was detectable in nuclear fractions upon NCAM-specific stimulation and it was not present in nuclear fractions of non-stimulated N2A cells (Fig. 5.13). The levels of the 50 kDa NCAM fragment in the fraction of chromatin-associated proteins were reduced in the presence of SKF96365 when compared to stimulated cells incubated without inhibitor (Fig. 5.13), indicating that inhibition of TRPCs impairs nuclear import of the 50 kDa NCAM fragment.

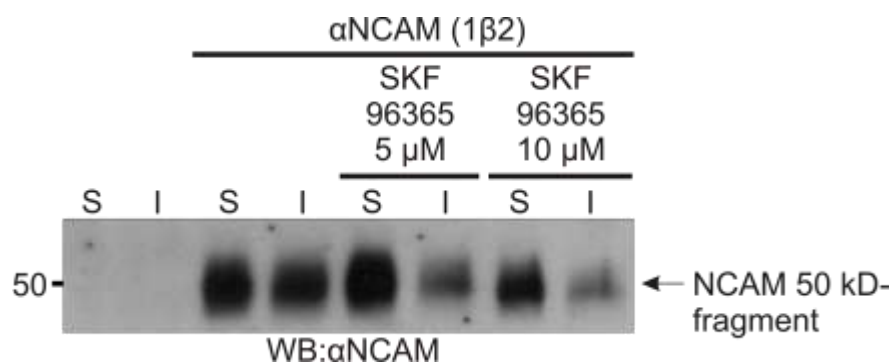


Figure 5.13: The TRPC inhibitor SKF96365 reduces the nuclear import of the 50 kDa fragment of NCAM in a concentration dependent manner. N2A cells were maintained two hours in serum-free medium. Afterwards 5 μM or 10 μM of the TRPC inhibitor SKF96365 were applied to the cells. Twenty minutes later, cells were incubated for one hour with an antibody against the ECD of NCAM (1β2) or cells were not treated. The nucleoplasmic (S) and chromatin-associated (I) proteins were isolated and subjected to SDS-PAGE and Western blot analysis. Nuclear NCAM proteins were detected with an antibody against the ICD of NCAM (P61).

5.11 PSA and HNK-1 are found in the nucleus upon NCAM stimulation

The ECD of NCAM has been found to carry PSA and HNK-1 (Finne *et al.*, 1983; Kruse *et al.*, 1984). Moreover, the 50 kDa NCAM fragment, which is imported into the nucleus after NCAM-specific stimulation, contains part of the extracellular region of NCAM (Kleene *et al.*, 2010b). Hence, I analyzed if PSA and HNK-1 are imported into the nucleus after NCAM specific stimulation and if the nuclear 50 kDa NCAM fragment carries these carbohydrates.

Results

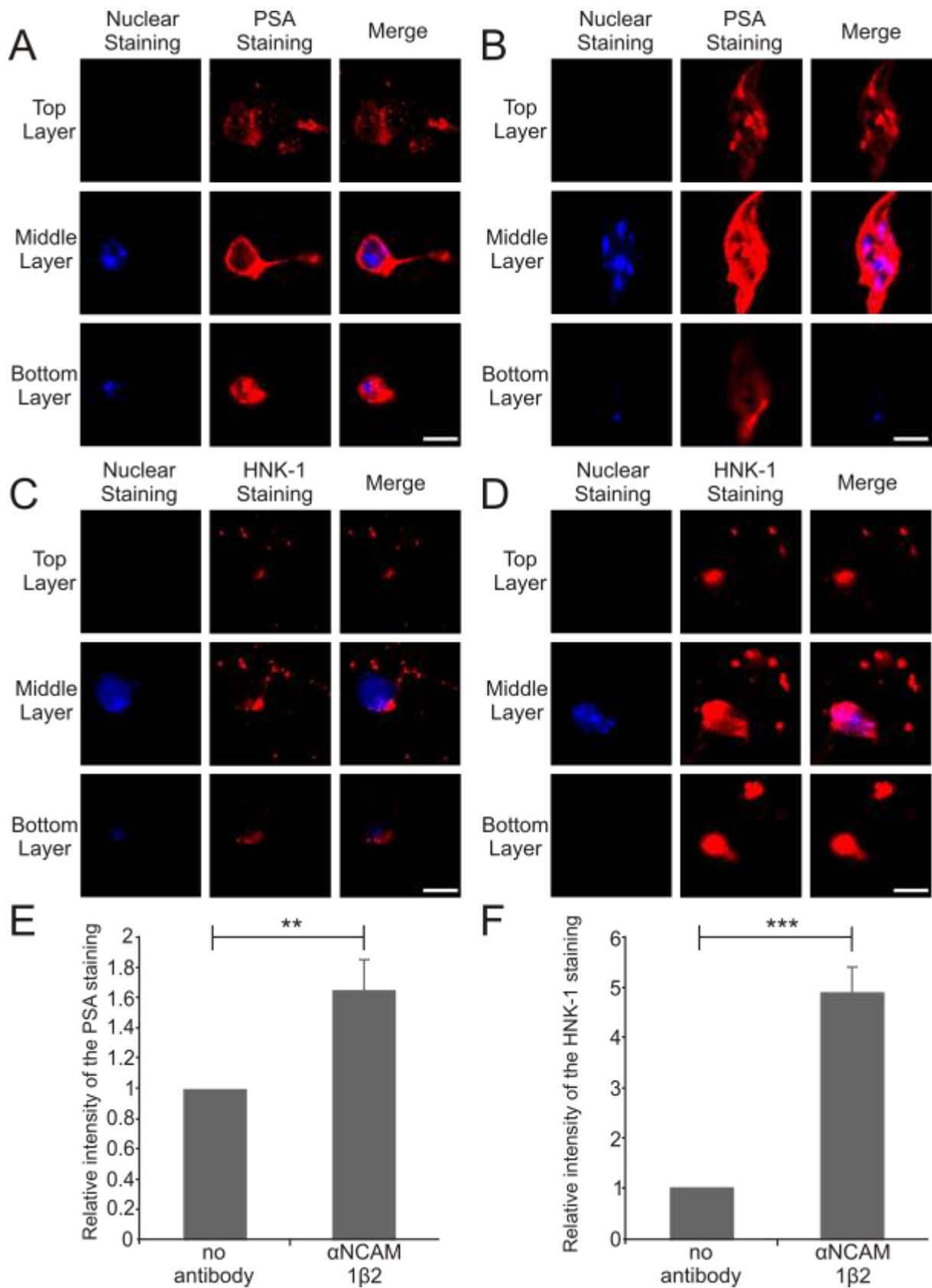


Figure 5.14: Immunostaining of PSA and HNK-1 in the nucleus increases upon NCAM stimulation. Cultured cerebellar neurons from wild-type mice maintained overnight in serum-

Results

containing medium were incubated in serum-free medium for 4 hours. The cells were fixed and permeabilized after treatment without or with an antibody against the ECD of NCAM (1 β 2) for 30 minutes. Cells were stained with PSA antibody 735 (A and B) or HNK-1 antibody 412 (C and D) and Cy2 labelled secondary antibodies. Bis-benzamide was used for staining of nuclei. The top layer (the focus of the microscope is at the surface of the cell), the middle layer (focus is in the plane of the nucleus) and the bottom layer (the focus is at the attachment site of the cell) of representative neurons without antibody treatment (A and C) or after antibody treatment (B and D) are shown. (E and F) The intensities of the carbohydrate stainings from treated cells were related to the intensities of the carbohydrate stainings from non-treated cells. The graphs show the mean value of relative fluorescent intensities of the PSA (E) or HNK-1 (F) staining in the nuclear regions from the middle layer of non-treated and antibody-treated cells. The error bars show the standard error of the mean and the statistical significant differences were obtained by the Student's t-test (** $p < 0.01$; *** $p < 0.001$; $n = 20$). The fluorescence intensity was measured with ImageJ for every single cell. The scale bars represent 20 μm .

Two different methods were used to approach this. First, immunostainings with antibodies against PSA and HNK-1 were performed using cultured cerebellar neurons upon triggering of NCAM signaling with an NCAM antibody against the ECD.

The intensity of the PSA and HNK-1 positive signals were significantly increased in nuclear areas of NCAM-stimulated neurons when compared to signals in nuclear areas of non-stimulated neurons (Fig 5.14). This result indicates that triggering of NCAM leads to nuclear import of proteins carrying PSA and/or HNK-1.

To further substantiate this notion, nuclear fractions containing either nucleoplasmic or chromatin-associated proteins from NCAM-stimulated cerebellar neurons of NCAM-deficient or wild-type littermates were isolated and subjected to Western blot analysis using antibodies against PSA (735) (Fig. 5.15A, B) or HNK-1 (412) (Fig. 5.15C, D).

After stimulation of NCAM, a diffuse PSA-positive band was detected only in the fraction of chromatin-associated proteins from wild-type cerebellar neurons, but not in the fraction of nucleoplasmic or chromatin-associated proteins from NCAM-deficient neurons. In fractions of chromatin-associated proteins from wild-type neurons, levels of PSA were significantly increased after NCAM stimulation compared to basal levels of PSA seen in non-stimulated neurons (Fig. 5.15A, B). This result confirms the notion that PSA is imported into the nucleus after NCAM stimulation. Similar results were obtained for HNK-1: signal intensities of diffuse HNK-1-positive bands showing a similar molecular size like the PSA-positive bands were enhanced in fractions of

Results

nucleoplasmic proteins from wild-type cerebellar neurons upon NCAM stimulation. Besides this, a distinct a HNK-1-positive band with a molecular weight of 250 kDa was detected in the nuclear fraction from wild-type and NCAM-deficient cerebellar neurons and was detected independently of NCAM-stimulation. (Fig. 5.15C, D), indicating that HNK-1 and PSA carried by NCAM are imported into the nucleus after NCAM stimulation and that HNK-1 reaches the nucleus in a NCAM-dependent and – independent manner.

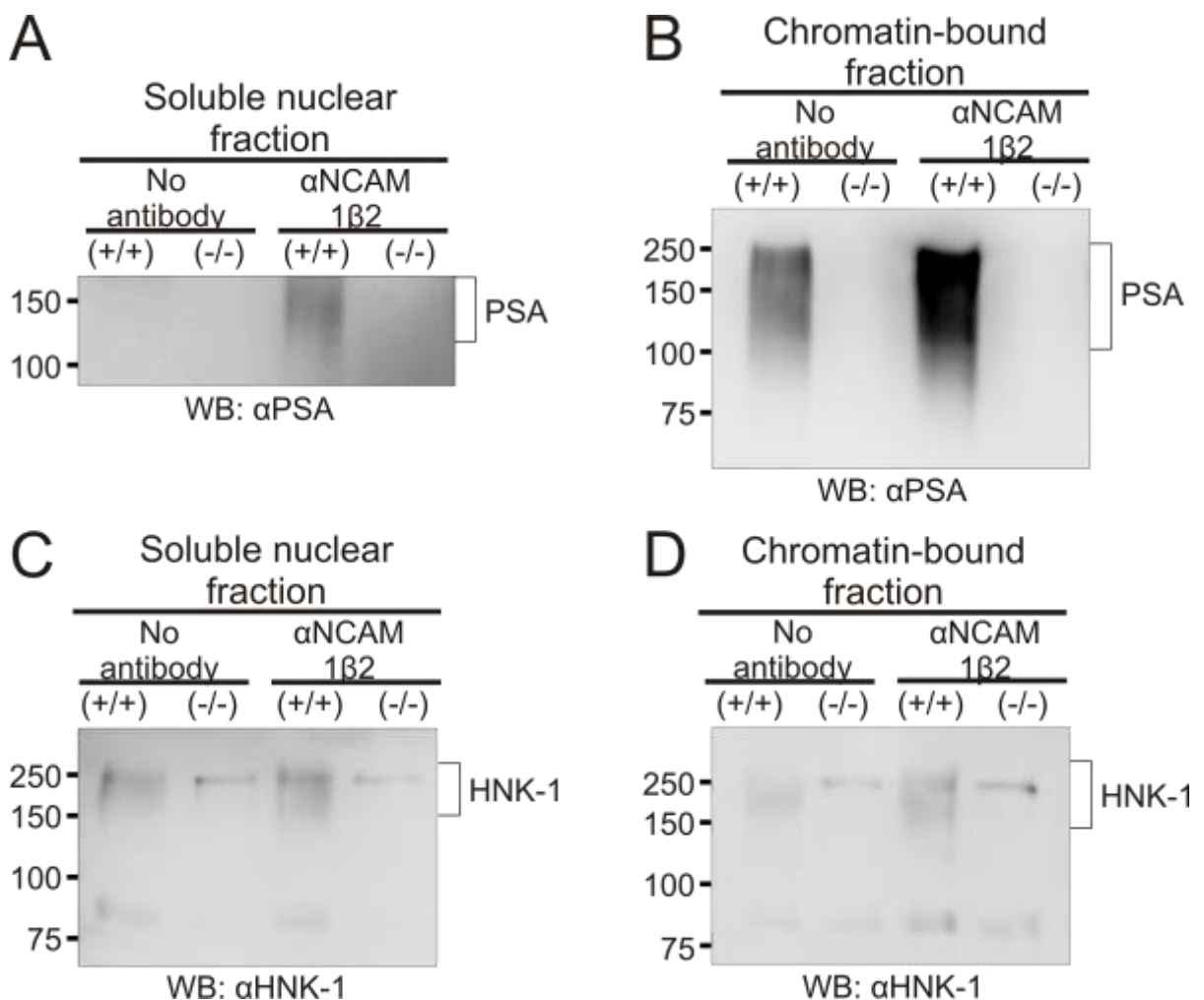


Figure 5.15: Protein fragments carrying PSA and/or HNK-1 appear in the nuclear fraction after treatment of cerebellar neurons with NCAM antibody 1β2. Cerebellar neurons from NCAM-deficient (-/-) mice or wild-type littermates (+/+) were maintained overnight in serum-containing medium. After incubation in serum-free medium for 4 hours, cells were treated for 30 minutes without or with the antibody 1β2 directed against an epitope in the extracellular part of NCAM and subjected to subcellular fractionation using the Qproteome™ Nuclear Protein Kit from Qiagen. Soluble nuclear and chromatin-bound proteins were precipitated from the subcellular fractions using methanol/chloroform and subjected to Western blot analysis. Representative Western blots with the 735 antibody against PSA (A, B) and the 412 antibody against HNK-1 (C, D) are shown.

Results

5.12 A 50 kDa NCAM fragment is present in the nuclear fraction after PSA digestion and NCAM stimulation

Next, I tested whether the nuclear 50 kDa NCAM fragment appears together with PSA in the nucleus. For this aim, cerebellar granule cells were treated with endosialidase (EndoN) – an enzyme which digests PSA and thus removes it from NCAM protein backbone (Gerardy-Schahn *et al.*, 1995) - and then stimulated with a chicken antibody against NCAM. The fractions of nucleoplasmic or chromatin-associated proteins were isolated for Western blot analysis with an antibody against NCAM (P61). Nuclear fractions from NCAM-deficient mice were used as a control.

After EndoN and NCAM antibody treatment, a 50 kDa NCAM fragment was only detected in the fraction of nucleoplasmic proteins from wild-type, but not NCAM-deficient mice (Fig. 5.16).

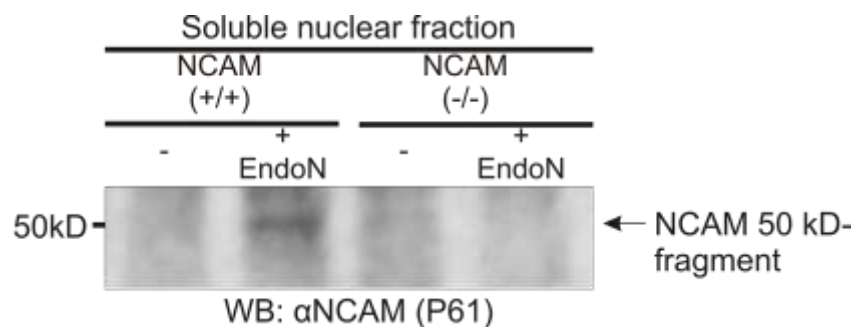


Figure 5.16: A 50 kDa NCAM fragment is present in the nuclear fraction after PSA digestion and NCAM stimulation. Cerebellar neurons from wild-type or NCAM-deficient littermates were maintained overnight in serum-containing medium. After incubation in serum-free medium for 4 hours, cells were not pre-treated (-) or pre-treated 30 minutes with recombinant endosialidase (+ EndoN) and afterwards treated for 30 minutes with an antibody against an epitope of the extracellular part of NCAM and subjected to subcellular fractionation using the Qproteome™ Nuclear Protein Kit from Qiagen. Soluble nuclear fractions were subjected to Western blot analyses using the P61 antibody against NCAM.

5.13. Nuclear PSA-NCAM levels are increased after NCAM stimulation and decrease rapidly after 30 min

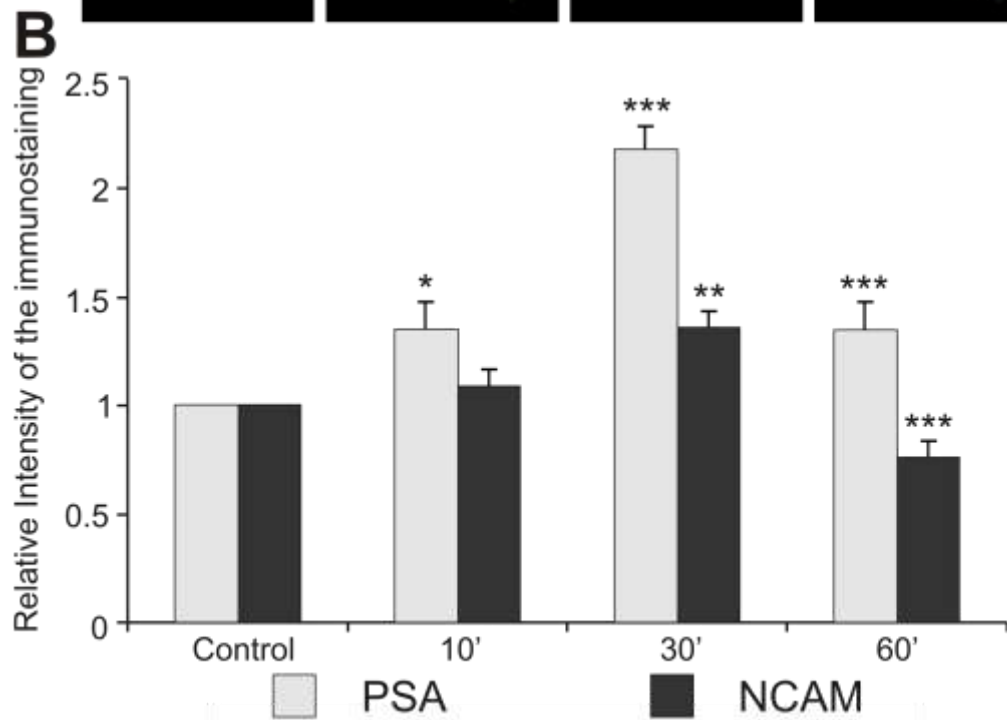
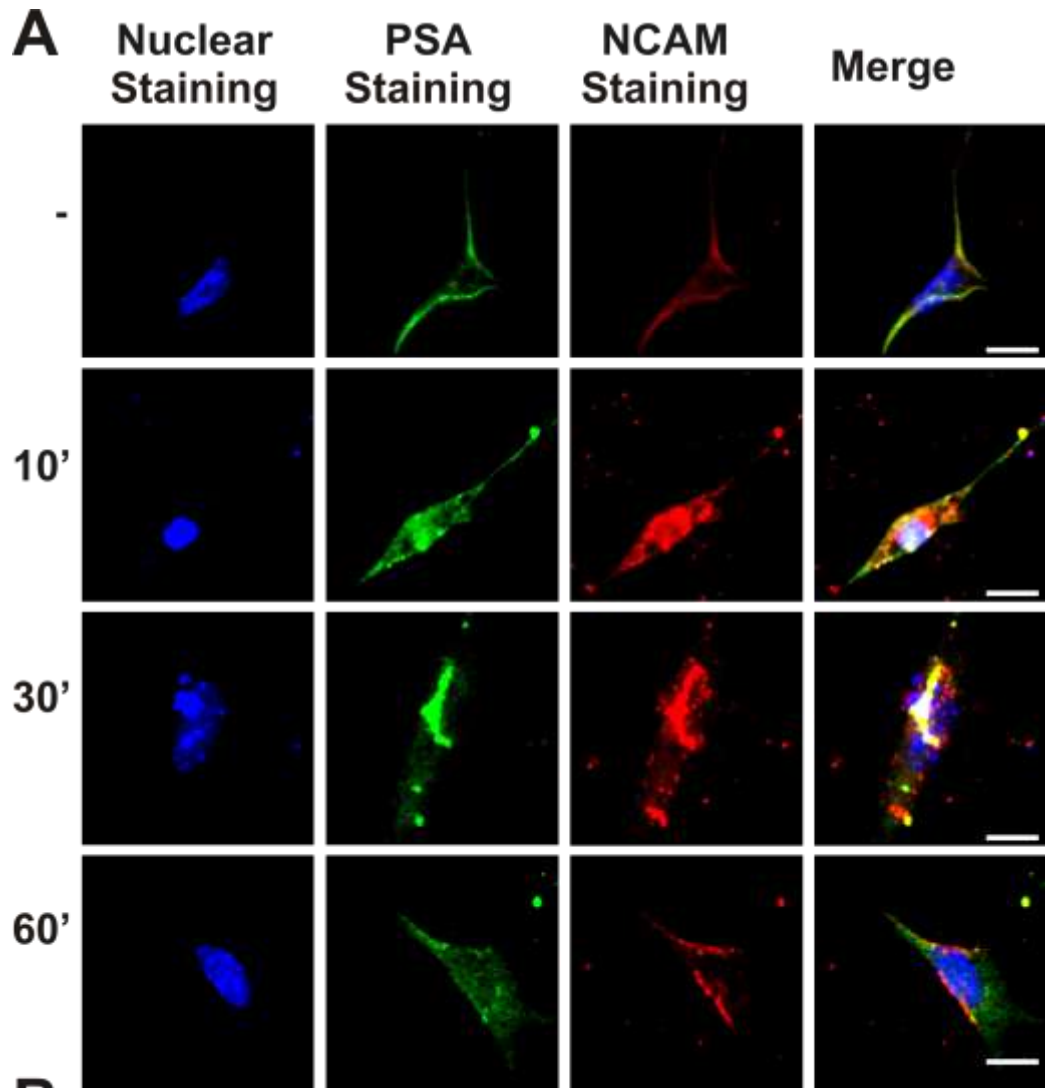
Next, I investigated how PSA/NCAM levels in the nucleus are altered upon NCAM-specific stimulation. To address this question, immunostaining experiments with hippocampal neurons and antibodies against PSA and NCAM were performed. In parallel, the expression levels of NCAM and PSA in nuclear fractions from cerebellar neurons at different time points after stimulation were determined.

Hippocampal neurons were treated with a polyclonal chicken antibody against NCAM for 10, 30 or 60 minutes. For immunostaining, antibodies directed against PSA (735) and NCAM (P61) were used. The nuclei were stained with bis-benzamide (Fig. 5.17). Non-stimulated hippocampal neurons were used as a control. After stimulation and fixation of the neurons, signal intensities of PSA and NCAM staining within nuclear regions were measured with ImageJ software. The intensity of signals in stimulated cells from the three different time points was set in relation to the signal intensity in non-treated cells.

Ten minutes after NCAM stimulation a significant increase in the PSA staining intensity in the nuclear region was detectable compared to signal intensities observed in non-treated cells. The signal intensities of PSA and NCAM reached a maximum at 30 minutes after stimulation and decreased afterwards. After one hour of stimulation, the signal intensity of NCAM was significantly lower than the signal of NCAM in non-treated cells, whereas the signal of PSA was still significantly higher than the control signal (Fig. 5.17).

Since hippocampal neurons do not yield a sufficient amount of nuclear proteins for biochemical analysis, fractions of nucleoplasmic and chromatin-associated proteins were prepared from cerebellar neurons after NCAM stimulation for different time points as described above and subjected to Western blot analysis with PSA antibody (735) (Fig. 5.18A, B).

Results



Results

Figure 5.17: PSA and NCAM levels increase in the nucleus of hippocampal neurons after treatment with an NCAM antibody. Cultured hippocampal neurons from wild-type mice maintained overnight in serum-containing medium were incubated in serum-free medium for 4 hours. After treatment without or with an antibody against the ECD of NCAM (chicken) cells were fixed and permeabilized and incubated with the PSA antibody 735 and NCAM antibody P61 overnight. Bis-benzamide was applied to the cells for the nuclear staining (A). The intensities of the PSA and NCAM staining from cells stimulated with NCAM antibody for 10, 30 and 60 min (10', 30', 60') were compared to the intensities of the PSA and NCAM staining from non-treated cells (Control). The graph shows the mean value of relative fluorescent intensity at different time points (10', 30', 60') of the non-treated or antibody-treated cells (B). The error bars show the standard error of the mean and statistically significant differences were determined by the Student's t-test (* $p < 0.05$; ** $p < 0.01$; *** $p < 0.001$; $n = 20$). The signal intensity was measured with ImageJ for every single cell. The scale bars represent 20 μm .

The amount of PSA in the fraction of nucleoplasmic proteins from cerebellar neurons was increased after 10 min of NCAM stimulation and remained for up to 60 minutes (Fig. 5.18A). In contrast, the PSA expression reached a maximum 10 minutes after treatment in the fractions of chromatin-associated proteins and decreased to similar levels seen in the control (Fig. 5.18B).

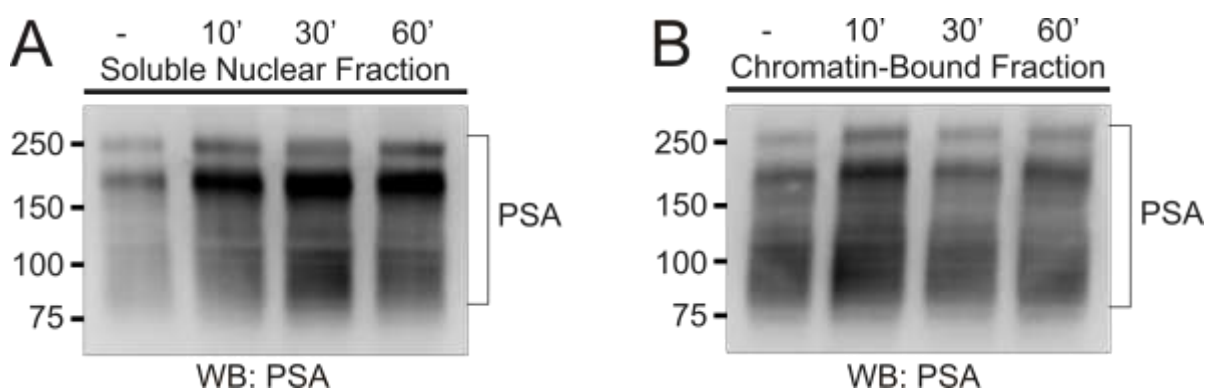


Figure 5.18: Levels of PSA-carrying NCAM forms are enhanced in the nuclear fractions after treatment with an NCAM antibody. Cerebellar neurons from wild-type mice were maintained overnight in serum-containing medium. After incubation in serum-free medium for 4 hours, cells were not treated (-) or treated for 10, 30 or 60 minutes (10', 30', 60') with an antibody against an epitope in the extracellular part of NCAM (chicken) and subjected to subcellular fractionation using the Qproteome™ Nuclear Protein Kit from Qiagen. Soluble nuclear and chromatin-bound proteins were precipitated from the subcellular fractions using methanol/chloroform and subjected to Western blot analysis. Representative Western blots with the 735 antibody against PSA are shown (A, B).

These experiments revealed that the import of PSA already takes place within ten minutes after NCAM stimulation. Moreover, these results indicate that the presence of PSA and NCAM changes spatiotemporally: PSA and NCAM are enhanced in the

Results

fraction of chromatin-associated proteins only 10 min after stimulation, but persist longer in the fraction of nucleoplasmic proteins.

5.14. NCAM stimulation leads to changes in DNA methylation and hydroxymethylation

PSA and the 50kDa NCAM fragment are imported into the nucleus of hippocampal and cerebellar neurons after NCAM stimulation (Figs. 5.16, 5.17, 5.18). Since PSA and the NCAM fragment were found in the nuclear fraction of neurons, it was possible that nuclear PSA-carrying NCAM could interact with DNA and change the chromatin structure.

As an initial step to test this idea, the levels of DNA methylation or hydroxymethylation were measured in lysates of cerebellar neurons upon NCAM-specific stimulation and after treatment without or with the PSA digesting enzyme EndoN (Fig. 5.19A). In parallel, the soluble and chromatin-bound nuclear fractions obtained from each condition were probed by Western blot analysis with an antibody directed against PSA (Fig. 5.19B).

After combined treatment of cerebellar neurons with EndoN and NCAM antibody, levels of DNA methylation and hydroxymethylation were significantly increased compared to control levels and levels seen after NCAM stimulation alone. In contrast, levels of DNA hydroxymethylation were strongly decreased in cells after treatment with EndoN alone compared to control levels, whereas levels of DNA methylation remained unaltered (Fig. 5.19A). The findings indicate that nuclear import of the PSA-free 50 kDa NCAM fragment affects these epigenetic modifications of DNA. PSA on NCAM seems to prevent a change in DNA methylation or hydroxymethylation.

Results

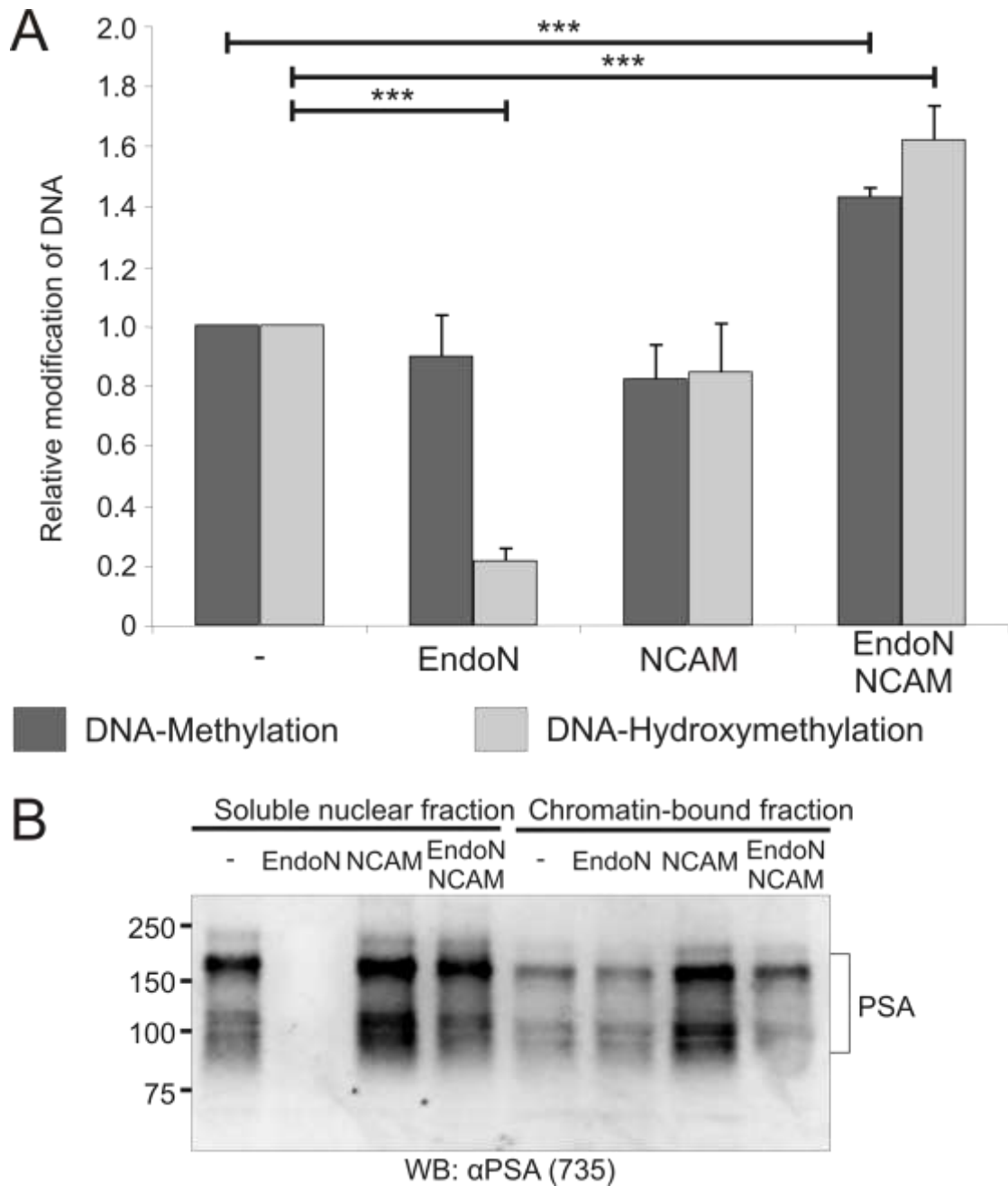


Figure 5.19: Levels of DNA methylation and hydroxymethylation increase significantly after NCAM-stimulation. Cerebellar neurons from wild-type mice were maintained overnight in serum-containing medium. After incubation in serum-free medium for 4 hours, cells were not pre-treated (-) or pre-treated for 30 minutes with recombinant endosialidase (EndoN; EndoN NCAM) and afterwards treated for 30 minutes with an antibody against the extracellular part of NCAM (NCAM; EndoN NCAM). The DNA was isolated and global methylated and hydroxymethylated DNA were quantified. The graph shows/depicts the average relative values from three different experiments ($n=3$) and the different treatments (EndoN; NCAM; EndoN NCAM) related to the untreated control. The error bars show the standard error of the mean and the statistical significant differences were obtained by the Student's t-test (** $p < 0.001$; $n=3$). (B) Cerebellar wild-type neurons were treated like in A and soluble nuclear and chromatin-bound fractions were isolated. Proteins from the subcellular fractions were precipitated using methanol/chloroform and subjected to SDS-PAGE and Western blot analysis. Representative Western blots with an antibody against PSA (735) are shown.

Results

After EndoN treatment, no PSA was detected in fraction of nucleoplasmic proteins from cerebellar neurons. Levels of PSA in fractions of nucleoplasmic and chromatin-associated proteins were increased after NCAM-specific stimulation compared to levels in fractions of nucleoplasmic and chromatin-associated proteins from non-treated cells and cells after combined treatment with NCAM antibody and EndoN (Fig. 5.19B). However, the PSA level only slightly decreased after EndoN treatment and NCAM stimulation. These results could be explained by an incomplete PSA digestion.

5.15 NCAM-mediated neuritogenesis, but not neuronal cell migration, is PSA-dependent

Since NCAM plays an important role in neurite outgrowth and cell migration (Loers and Schachner, 2007; Diestel *et al.*, 2005), it was important to investigate whether these events could be correlated to the results obtained for nuclear import of NCAM and/or PSA-NCAM fragments and DNA methylation and hydroxymethylation after NCAM stimulation and/or Endo N treatment..

Thus, I performed neurite outgrowth experiments with cerebellar and hippocampal neurons and migration assays with cerebellar explants from wild-type mice and NCAM-deficient littermates. Neurons and explants were treated either with EndoN alone, chicken NCAM antibody or with a combination of both EndoN and NCAM antibody.

The average total length of both hippocampal and cerebellar neurons was significantly higher when cells were treated only with the NCAM antibody in comparison to the length of neurites from control neurons (Fig. 5.20A). EndoN treatment alone had no effect on neurite outgrowth. In contrast, the combined treatment of neurons with EndoN and NCAM antibody abolished the NCAM-mediated neurite outgrowth and reduced neurite length to control levels. These results suggest that the NCAM-mediated neuritogenesis depends on PSA or that PSA-NCAM stimulates and PSA-free NCAM inhibit the neurite outgrowth.

Results

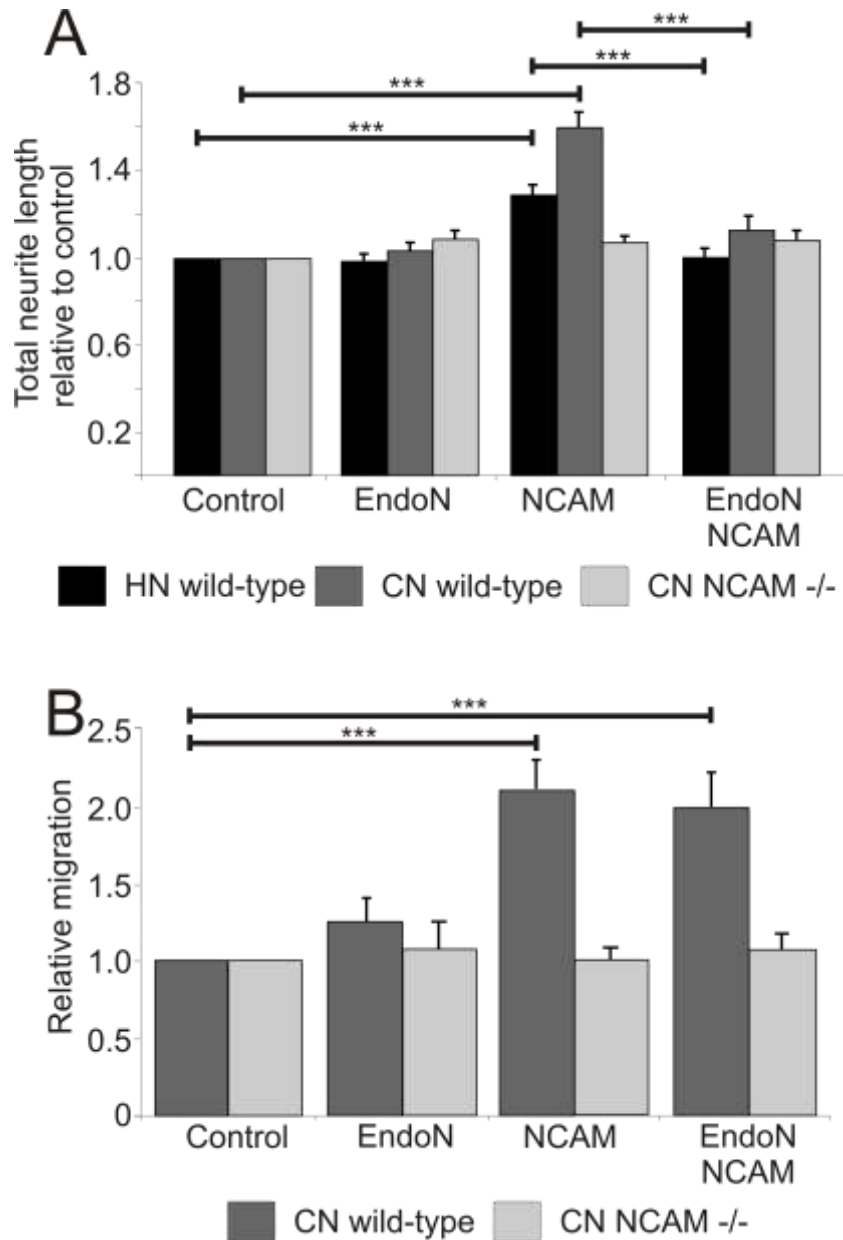


Figure 5.20: NCAM-mediated neurite outgrowth is PSA dependent whereas NCAM-mediated neuronal migration is PSA-independent. For neurite outgrowth experiments (A) hippocampal (HN) or cerebellar (CN) neurons of NCAM-deficient (NCAM^{-/-}) mice or wild-type littermates were cultured overnight in medium without serum. One hour after seeding cells were not treated (Control) or treated with recombinant endosialidase (EndoN) or with an antibody against NCAM (NCAM) or treated with endosialidase and the antibody (NCAM (chicken)) (EndoN NCAM) (A, B). After 24 hours the cells were fixed and stained. The total lengths of neurites from the cells were measured and compared to non-treated cells (Control). The migration assay (B) was performed with explants from the cerebellum of wild-type (CN wild-type) and NCAM-deficient (CN NCAM^{-/-}) littermates. Cells which migrated out of the explants were counted and their numbers compared to the numbers of cells migrating out of untreated explants (Control). The graphs show the mean values from three independent experiments; the statistical analysis was performed with the Student's t-test (***) $p < 0.001$, $n = 3$). The error bars represent the standard error of the mean.

Results

Migration of neurons out of the explant core was accelerated upon NCAM stimulation as well as upon combined treatment with NCAM antibody and EndoN, when compared to neuronal migration in non-treated explants (Fig.5.20 B). Since NCAM-mediated neuronal migration could not be inhibited by EndoN treatment, one can conclude that NCAM-mediated neuronal migration is PSA-independent.

5.16 PSA expression and levels of methylated DNA are significantly reduced during maturation of neurons

Since DNA methylation and hydroxymethylation play an important role in cell differentiation (Takizawa *et al.*, 2001), it seemed plausible to investigate whether expression of PSA and levels of the global DNA methylation and hydroxymethylation are altered in neurons during maturation.

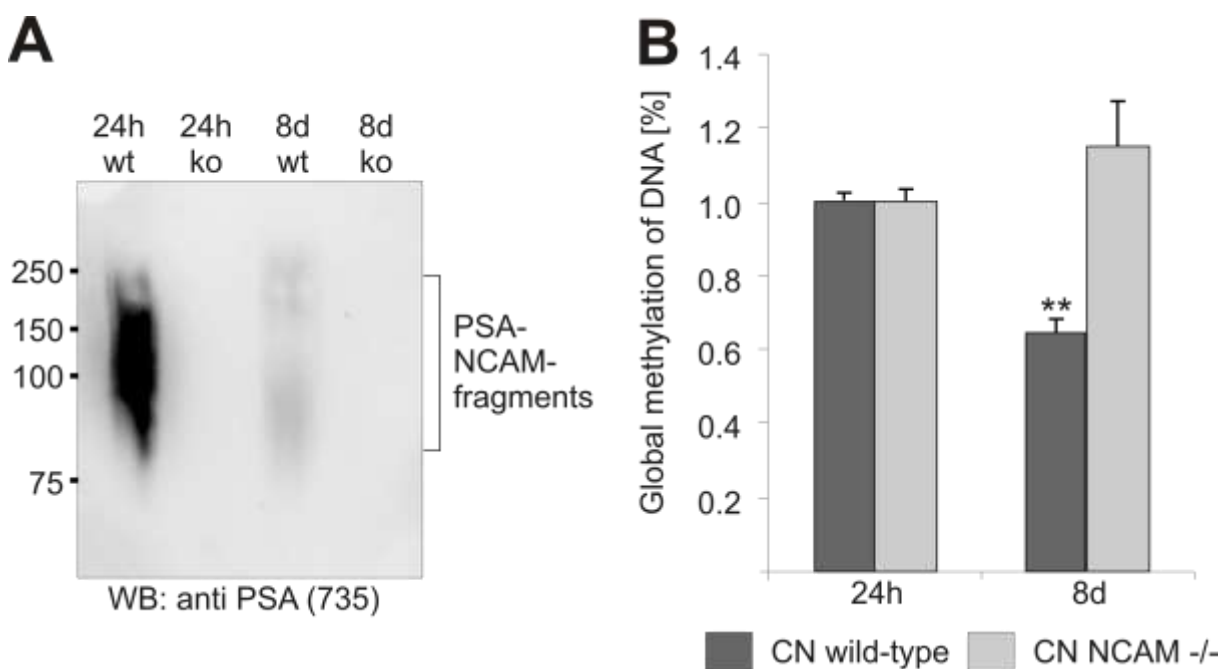


Figure 5.21: The expression of PSA and the level of DNA methylation decrease in cultured cerebellar neurons after 8 days *in vitro*. Cerebellar granule neurons from NCAM-deficient mice and wild-type littermates were maintained for 24 hours or 8 days *in vitro*, lysed and subjected to SDS-PAGE and Western blot analysis with an antibody against PSA (735) (A). Chromosomal DNA was isolated from cerebellar neurons of wild-type and NCAM-deficient mice that were maintained for 24 hours or 8 days *in vitro*. The level of methylated DNA was measured (B). The graph shows the average values from 4 different wells per condition. The error bars show the standard error of the mean and the statistically significant differences were assessed by the Student's t-test (** $p < 0.001$; $n = 4$).

Results

For this purpose, cerebellar neurons from wild-type mice were maintained for 24 hours and 8 days *in vitro*. NCAM-deficient mice were used as control. In parallel, the PSA expression of cerebellar neurons cultured for 1 or 8 days was analyzed by Western blot analysis. Levels of PSA were decreased in lysates from cerebellar neurons after 8 days *in vitro* when compared to levels seen in lysates from neurons maintained in culture for 24 hours (Fig. 5.21A). In addition, levels of the methylated DNA were significantly reduced in lysates from neurons after 8 days in culture in comparison to levels in lysates from neurons maintained in culture for 24 hours (Fig. 5.21B). After either 24 hours or 8 days, levels of the methylated DNA were not altered in NCAM-deficient neurons. The combined results demonstrate that PSA expression and levels of methylated DNA are significantly reduced in neurons during maturation.

5.17 NCAM stimulation leads to the appearance of a high molecular weight complex containing histone H1 in the nucleoplasmic protein fraction

Since histone H1 has been found to interact with PSA at the cell surface of neurons (Mishra *et al.*, 2010) and due to the fact that PSA-NCAM can be found in the nucleus of neurons, I decided to investigate whether NCAM-mediated nuclear import of PSA induces nuclear import of histone H1 and/or changes the cellular localization of histone H1.

To test this possibility, soluble nuclear fractions from wild-type and NCAM-deficient cerebellar neurons were isolated after treatment of cells with an NCAM antibody for 10, 30 or 60 minutes (Fig. 5.22). Non-treated cerebellar neurons were used as a control. The isolated nuclear fractions were subjected to Western blot analysis using histone H1 antibody.

Surprisingly, a histone H1-positive band at approximately 140 kDa was detected in the fractions of nucleoplasmic proteins from wild-type cerebellar neurons, but not in the nuclear fractions obtained from NCAM-deficient neurons (Fig. 5.22A), suggesting

Results

that NCAM stimulation induces a nuclear import of histone H1. Furthermore, a histone H1-positive band was detected at 200 kDa and the levels of this band were steadily increased in fractions of nucleoplasmic proteins after 10, 30 and 60 minutes of NCAM-specific stimulation (Fig. 5.22B). In the nucleoplasmic protein fraction, a histone H1-positive 60 kDa double-band was detected when histone H1 antibody was used (Fig. 5.22B). The signal intensity of the double-band was higher in the nucleoplasmic protein fraction from NCAM-deficient neurons than in the fractions from wild-type cerebellar neurons. Taken together, these results suggest that NCAM-stimulation promotes formation of a histone H1 complex in the nuclei of wild-type cerebellar neurons, while histone H1 dimers are found in nuclei from NCAM-deficient cerebellar neurons.

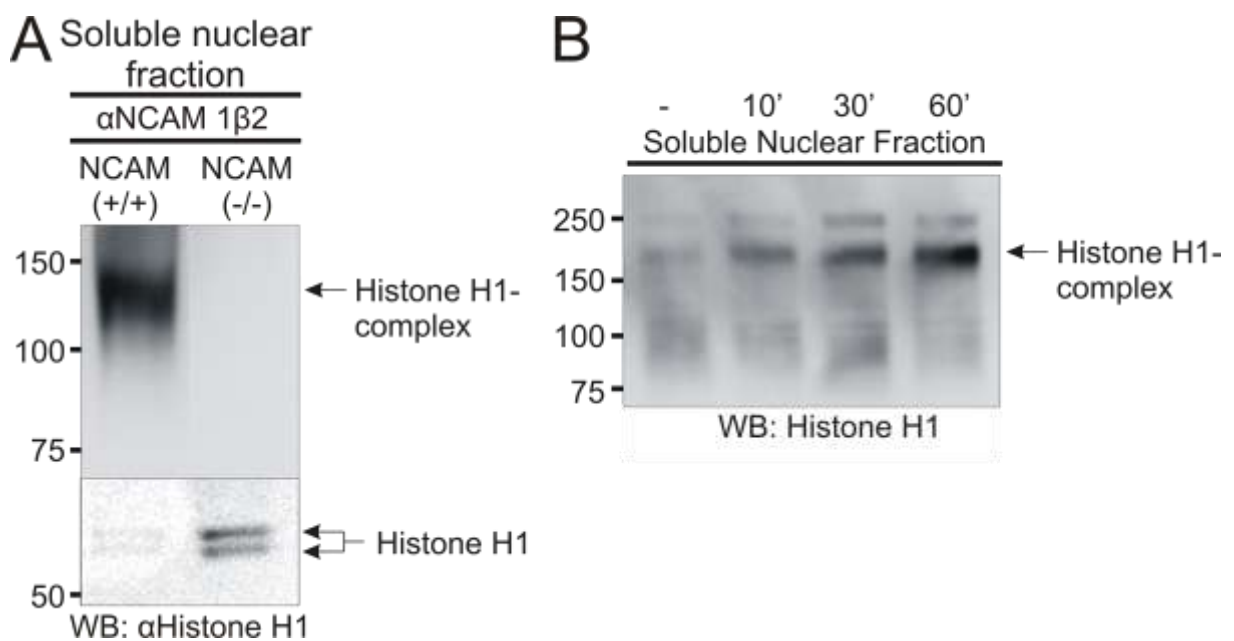


Figure 5.22: High molecular weight histone H1 after treatment of neurons with a polyclonal antibody against NCAM. Cerebellar neurons from wild-type (A, B) or NCAM-deficient (A) littermates were maintained overnight in serum-containing medium. After incubation in serum-free medium for 4 hours, cells were not treated (-) (B) or treated for 10 (B), 30 (B) or 60 minutes (A, B) (10', 30', 60') with an antibody against the extracellular part of NCAM (chicken) and subjected to subcellular fractionation. Soluble nuclear proteins were precipitated from the subcellular fractions using methanol/chloroform and subjected to Western blot analysis. Representative Western blots are detected with an antibody against histone H1 (FL-219) (A, B). In A the lower section of the blot is shown with contrast adjustments using Adobe Photoshop 7.0.

5.18 PSA and MARCKS co-localize in primary hippocampal neurons

Recently, a novel functional interaction between PSA and MARCKS has been observed (Theis *et al.*, 2013). Since a partial co-localization of MARCKS and PSA in an immunostaining experiment has been observed by Bibhudatta Mishra (Theis *et al.*, 2013), it was of interest to investigate whether this co-localization could be altered upon treatment of hippocampal neurons (Fig. 5.23) with a PSA-antibody.

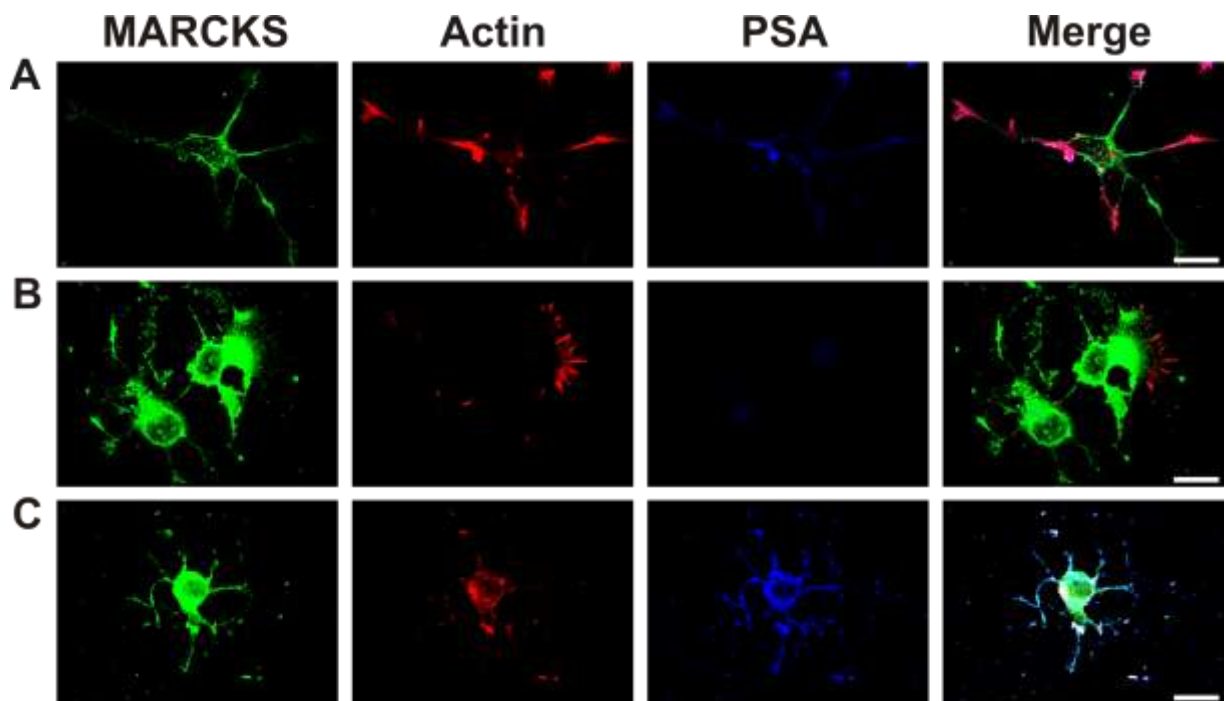


Figure 5.23: MARCKS co-localizes with PSA in hippocampal neurons. Immunostainings were performed with hippocampal neurons from wild-type (A, C) or NCAM-deficient (B) littermates maintained for 24 hours in culture. The cells were fixed with 4% PFA (A, B), the membrane was permeabilized and then cells were incubated with an antibody against MARCKS (rb) (green), and an antibody against PSA (735) (blue). Afterwards, cells were stained for actin (red) with Alexa Fluor® 594 phalloidin. Live cells were incubated with an antibody against PSA (735) for 15 minutes and afterwards for 20 minutes with Cy5-coupled antibody against mouse IgG (C). After live staining the cells were fixed with 4 % PFA, permeabilized and stained for MARCKS and actin as described above. The scale bars represent 20 μ m.

NCAM is the main carrier of PSA and linked through spectrin to the actin-cytoskeleton. Actin is also able to bind MARCKS via its effector domain (ED)

Results

(Hartwig *et al.*, 1992). Because of this, it seems plausible to immunostain actin with MARCKS. Therefore, wild-type and NCAM-deficient hippocampal neurons were stained with antibodies against MARCKS and PSA after or before fixation and permeabilization. The immunostaining after fixation showed a co-localization of PSA and actin, but negligibly weak co-localization of PSA and MARCKS (Fig. 5.23A) – as previously described by Bibhudatta Mishra (Theis *et al.*, 2013). After live cell staining, the PSA-MARCKS co-localization was strongly enhanced when compared to co-localization in immunostainings performed after fixation of cells (Fig. 5.23C). This result implies that PSA and MARCKS interact with each other at the plasma membrane from opposite sides.

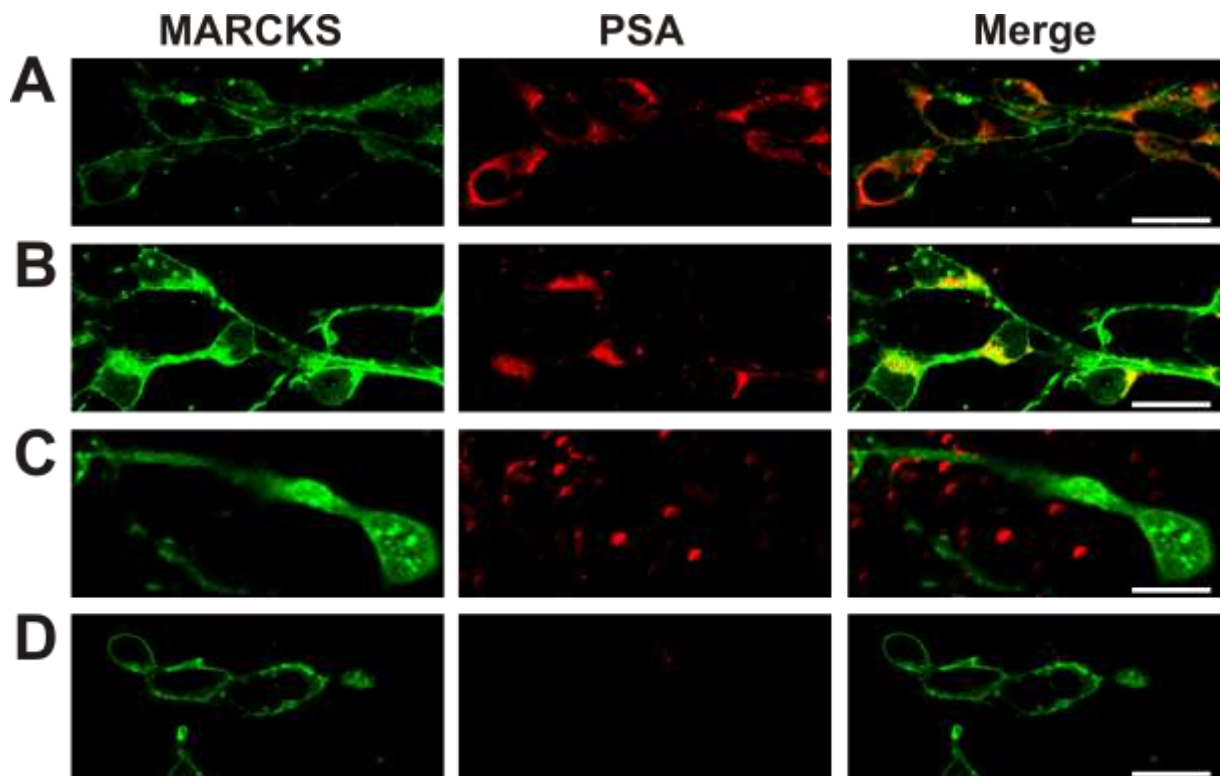


Figure 5.24: MARCKS co-localizes with PSA after treatment of hippocampal neurons with colominic acid, but not with chondroitin sulfate. Hippocampal neurons from wild-type (A-C) or NCAM-deficient (D) littermates were treated for 3 hours with chondroitin sulfate (A), colominic acid/PSA (B, D) or EndoN (C). The cells were fixed; permeabilized and stained with antibodies against total MARCKS (rb) (green) and PSA (735) (red). The scale bars represent 20 μm .

Results

To investigate in more detail, if the co-localization of MARCKS and PSA can be enhanced by addition of soluble PSA, hippocampal neurons from wild-type (Fig. 5.24A-C) or NCAM-deficient mice (Fig. 5.24D) were treated with PSA/colominic acid (Fig. 5.24A and D) or chondroitin sulfate (Fig. 5.24B) or EndoN (Fig. 5.24C) and immunostained for MARCKS and PSA.

The vast majority of PSA co-localized with MARCKS when cells were treated with colominic acid/PSA. After chondroitin sulfate treatment, only a partial co-localization was observed. No co-localization occurred between PSA and MARCKS after PSA digestion with EndoN. In NCAM-deficient neurons, no co-localization between PSA and MARCKS could be observed even after external addition of PSA/colominic acid. These results suggest that addition of PSA to neurons induces an enhancement of PSA-MARCKS interaction.

5.19 PSA interacts with the effector domain of MARCKS within the plasma membrane

The ED of MARCKS mediates the insertion of myristoylated MARCKS into the membrane (Victor *et al.*, 1999; Qin *et al.*, 1996). Exchanging the five phenylalanine residues in the ED with alanine residues or mutation of the myristoylation site prevents the plasma membrane insertion (Spizz *et al.*, 2001). PSA is also able to insert into the membrane via its helical structure (Brisson *et al.*, 1992; Janas *et al.*, 2010, 2001, 2000). A direct binding between the ED of MARCKS and PSA was demonstrated by Bibhudatta Mishra and Gabriele Loers in binding studies (Theis *et al.*, 2013). Since the previous results suggest an interaction between MARCKS, which is a cytoplasmic protein, and PSA, a glycan mainly present on the ECD of NCAM, it seemed reasonable to investigate whether this interaction happens in the membrane.

Results

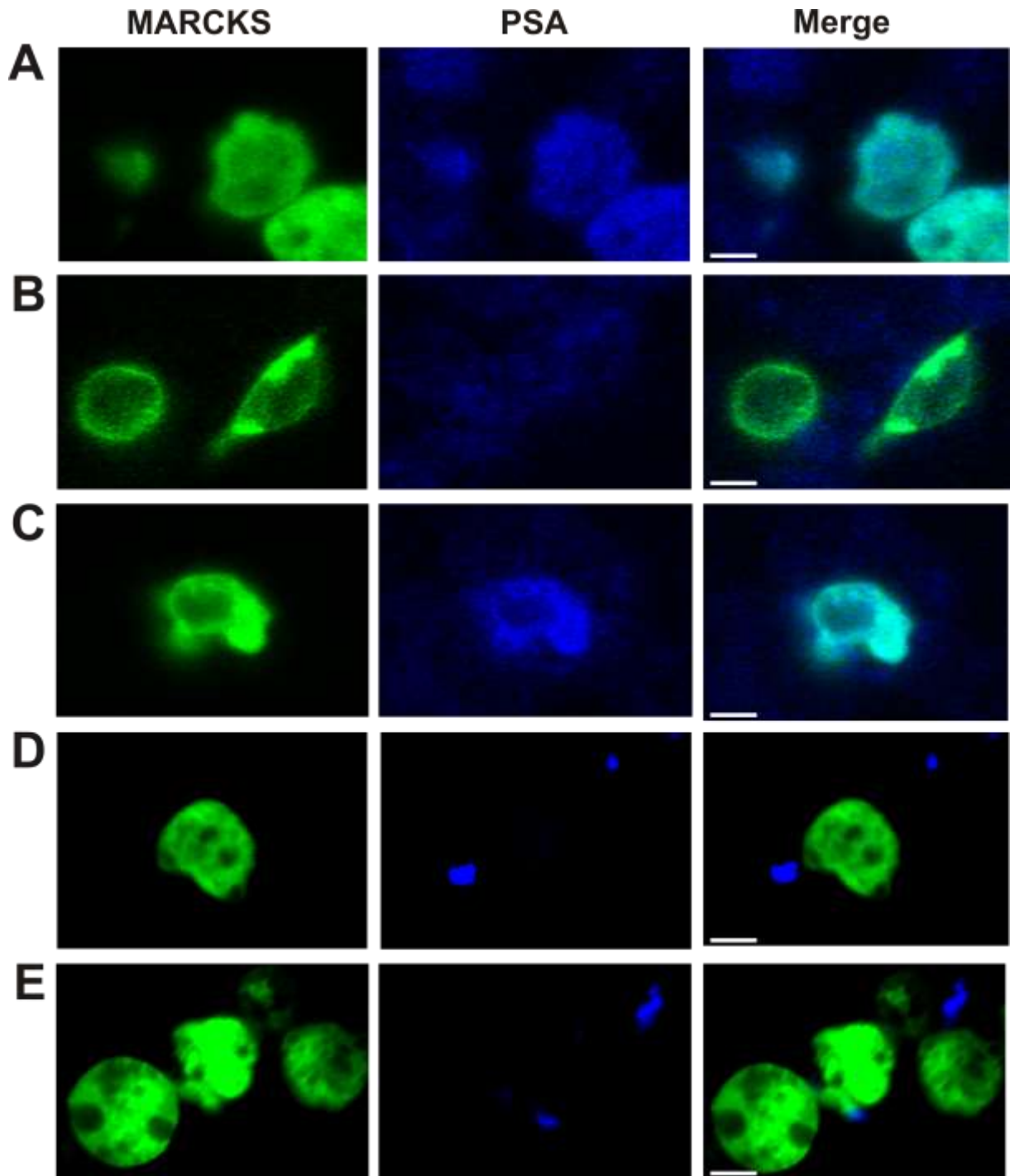


Figure 5.25: MARCKS co-localizes with colominic acid/PSA but not with chondroitin sulfate. CHO cells were transfected with wild-type MARCKS-GFP (A, C, E) or a non-myristoylatable MARCKS mutant (B, D) (green). Twenty minutes before live imaging the cells were treated with different carbohydrates linked to a dye (blue): colominic acid/PSA linked to AMCA (A, B); colominic acid/PSA linked to HiLyte Fluor™ 405 (C, D) or chondroitin sulfate linked to HiLyte Fluor™ 405 (E). The cells were maintained in an incubation chamber (37°C, 5% CO₂ and 70% humidity) during the acquisition of the representative images with an Olympus FV1000 microscope. The scale bars represent 20 µm.

Results

To investigate this putative interaction within the plasma membrane, I analyzed CHO cells by confocal microscopy after transfection with MARCKS-GFP constructs and incubation with colominic acid/PSA which was labeled with the fluorescent dye AMCA (Fig. 5.25A, B) or HiLyte Fluor 405 (Fig. 5.25C, D). In cells which expressed non-mutated MARCKS fused to GFP a co-localization between MARCKS-GFP and labeled colominic acid/PSA (Fig. 5.25A, C) was observed, whereas labeled colominic acid/PSA did not co-localize with MARCKS-GFP in cells which expressed the non-myristoylatable MARCKS-GFP mutant (Fig. 5.25B, D). Chondroitin sulfate labeled with HiLyte Fluor 405 did not co-localize with MARCKS-GFP in cells which expressed non-mutated MARCKS-GFP.

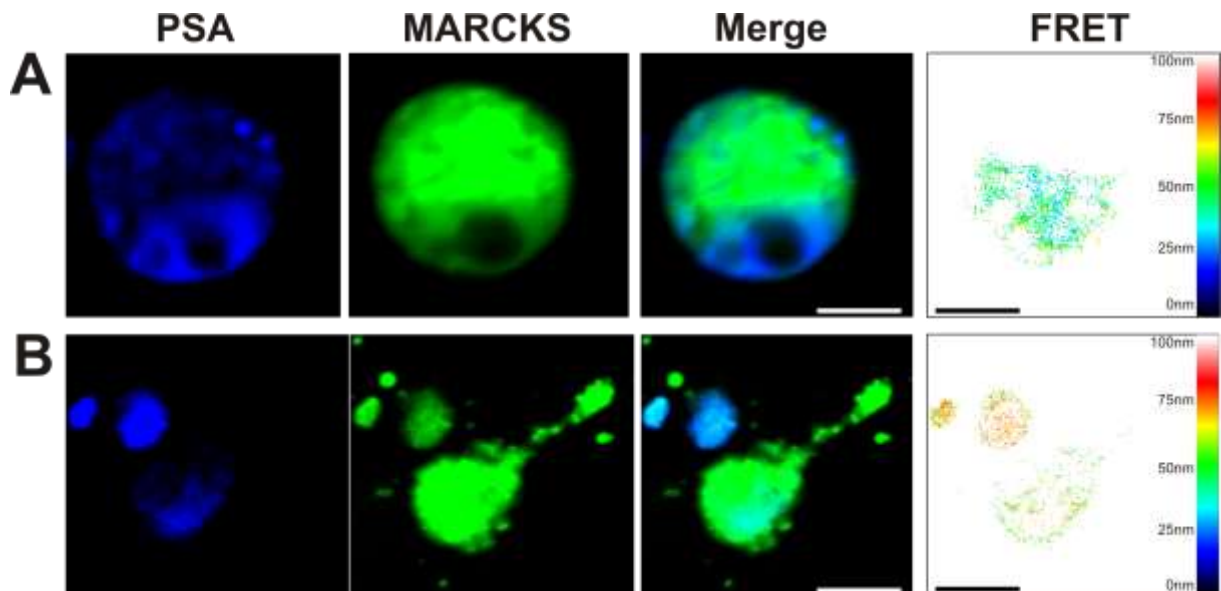


Figure 5.26: The distance between MARCKS-GFP and colominic acid/PSA is less than 50 nm. Fluorescence Resonance Energy Transfer (FRET) between the GFP-tag (green) of the MARCKS constructs and the HiLyte Fluor™ 405 (blue) linked to PSA. CHO cells (A) were transfected with FUGEN one day after seeding or hippocampal neurons from wild-type mice (B) were transfected with the calcium phosphate method two days after seeding. The dye linked carbohydrates were added for 15 minutes to the medium 24 hours after transfection. The FRET analysis was performed with a confocal laser scanning microscope (Olympus FV1000). The donor was the HiLyte Fluor™ 405 hydrazide and the acceptor the GFP-tag of the MARCKS constructs. During the live imaging the cells were maintained in an incubation chamber (37°C, 5% CO₂, 70% humidity). The column of images at the right-hand shows the results of the energy transfer and the distance between the donor and the acceptor in nanometers was calculated with the sensitized emission method. The scale bars represent 20 μm.

Results

To estimate the distance between HiLyte Fluor 405-labeled colominic acid/PSA and non-mutated MARCKS-GFP, FRET analysis was performed using CHO cells (Fig. 5.26A) and hippocampal wild-type neurons (Fig. 5.26B) expressing non-mutated MARCKS fused with GFP and which were treated with HiLyte Fluor 405-labeled colominic acid/PSA. FRET analysis of cells showed an approximate distance of 20-40 nm between the labeled colominic acid/PSA and MARCKS-GFP (Fig. 5.26).

These results show that MARCKS-GFP and labeled colominic acid co-localize and that the distance between their labels is approximately 20-40 nm. Although these results show that MARCKS and PSA are in very close contact, they cannot prove an interaction between MARCKS and colominic acid/PSA within the plasma membrane.

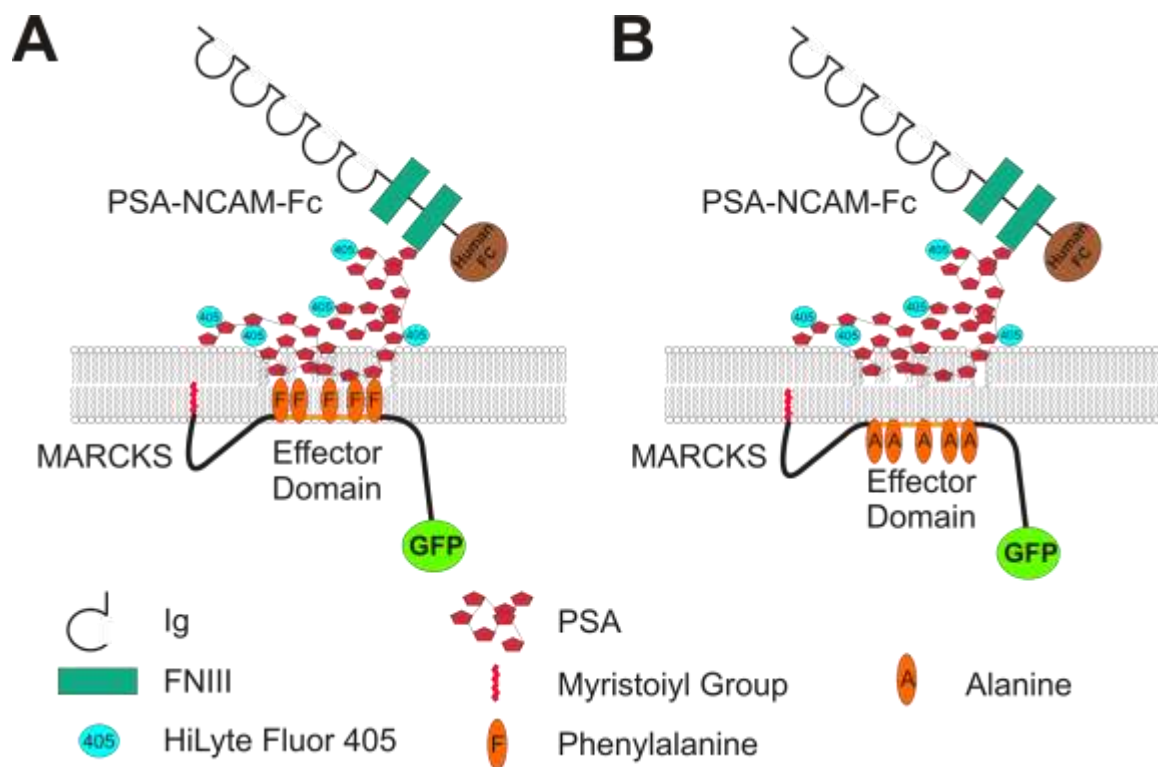


Figure 5.27: Scheme depicting the interaction of MARCKS-GFP and PSA-NCAM-Fc HiLyte Fluor 405. The PSA chain carried by the ECD of NCAM (PSA-NCAM-Fc) and conjugated to HiLyte Fluor 405 penetrates the plasma membrane from the extracellular side. In cells transfected with wild-type MARCKS-GFP (A), the ED of MARCKS is able to penetrate with its phenylalanines from the inside of the cell (cytosol) into the plasma membrane and could thereby interact with PSA within/through the plasma membrane. After excitation of PSA labeled with HiLyte Fluor 405 and interaction of PSA-NCAM with MARCKS-GFP, the GFP would be excited by an energy transfer from HiLyte Fluor 405 to GFP if they are in close vicinity. When cells are transfected with the MARCKS-GFP mutant in which the phenylalanines are exchanged to alanine residues (B), the ED of MARCKS does not penetrate the membrane and therefore no interaction or a reduced interaction between NCAM-PSA and mutant MARCKS takes place leading to reduced FRET or no FRET.

Results

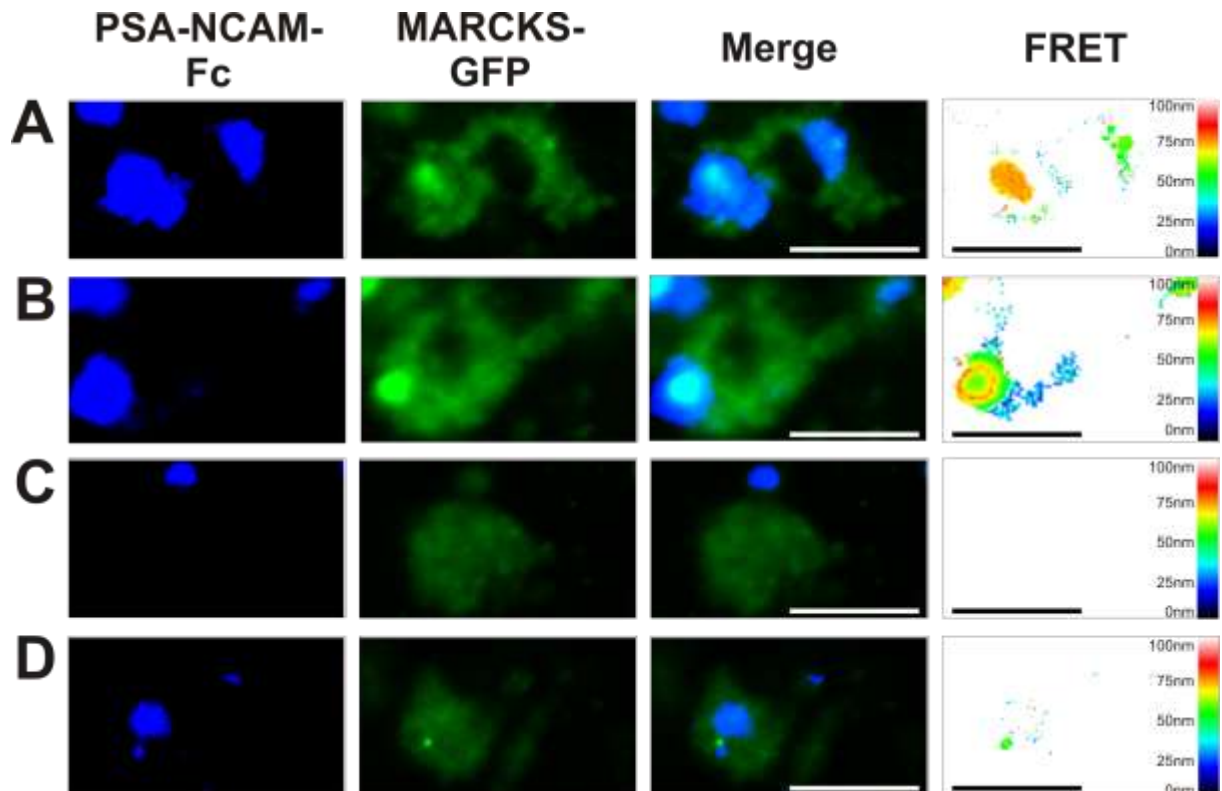


Figure 5.28: Wild-type MARCKS but not MARCKS lacking the F residues in the effector domain interacts with PSA-NCAM-Fc within the plasma membrane. Fluorescence Resonance Energy Transfer (FRET) between the GFP-tag (green) of the MARCKS constructs and HiLyte Fluor™ 405 (blue) linked to PSA which is attached to the ECD of NCAM (NCAM-PSA-Fc). Hippocampal neurons from NCAM-deficient mice were transfected with wild-type MARCKS-GFP (A, B) or with a MARCKS-GFP mutant, in which the five phenylalanine residues of the effector domain were replaced by five alanine residues (C, D). The dye linked PSA-NCAM-Fc was added to the neurons 24 hours after transfection and the cells were incubated with PSA-NCAM-Fc for 20 minutes. The FRET analysis was performed with a confocal laser scanning microscope (Olympus FV1000). The donor was the HiLyte Fluor™ 405 hydrazide and the acceptor the GFP-tag of the MARCKS constructs. During the live imaging the cells were maintained in an incubation chamber (37°C, 5% CO₂, 70% humidity). The column of images at the right-hand shows the results of the energy transfer and the distance between the donor and acceptor was calculated with the sensitized emission method. The scale bars represent 20 µm.

Additionally, FRET analysis was performed with NCAM-deficient hippocampal neurons transfected with non-mutated or mutated MARCKS-GFP containing exchanges of the phenylalanine residues for alanine residues (Fig. 5.27). The cells were incubated with a recombinant soluble NCAM protein which contains the ECD of murine NCAM, PSA labeled with HiLyte Fluor 405 attached to the ECD of NCAM and a human Fc-tag (PSA-NCAM-Fc; Fig. 5.28). In neurons expressing non-mutated MARCKS-GFP, a pronounced co-localization of wild-type MARCKS-GFP and labeled soluble PSA-NCAM-Fc was observed and the calculated distance between wild-type

Results

non-mutated MARCKS-GFP and HiLyte Fluor 405 labeled soluble PSA-NCAM-Fc was 10-30 nm (Fig. 5.28A, B). A co-localization of mutated MARCKS-GFP with labeled soluble PSA-NCAM-Fc could be detected, but either there was no FRET or a strongly reduced FRET between mutated MARCKS-GFP and labeled soluble PSA-NCAM-Fc. The distance between mutated MARCKS-GFP and soluble PSA-NCAM-Fc was 30 nm, and thus, similar to that between wild-type MARCKS-GFP and soluble PSA-NCAM-Fc. These results suggest that soluble PSA-NCAM-Fc interacts with the ED of MARCKS through the plasma membrane and that mutation of the ED leads to disruption or disturbance of this interaction.

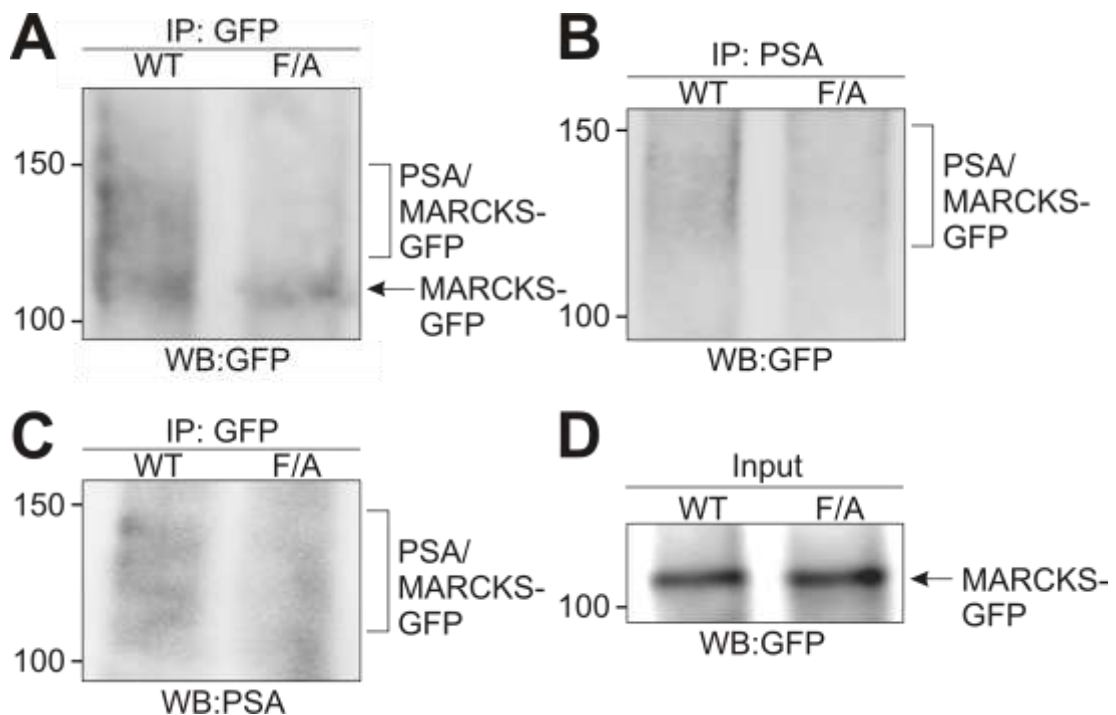


Figure 5.29: MARCKS-GFP directly interacts with colominic acid/PSA. CHO cells were transfected with wild-type (WT) MARCKS-GFP or the MARCKS-GFP mutant in which the five phenylalanines in the ED of MARCKS were replaced with five alanine residues (F/A). The cells were maintained overnight in medium in which the amino residue leucine was replaced against L-photo-leucine. After 24 hours the cells were incubated for 20 minutes with colominic acid (10 μ g per ml) and then exposed for 5 minutes to UV-light of 365 nm. L-photo-leucine residues contain a diazirine ring, which creates a reactive carbene after photo-activation. This leads to a covalent binding to the next atom, if it is closer than 5 \AA to the diazirine ring. The cells were lysed (D, input) and immunoprecipitation with antibodies against GFP (A, C) or PSA (B) was performed. The samples were subjected to SDS-PAGE and Western blot analysis with antibodies against GFP (A, B, D) or PSA (C).

Results

The results of the FRET experiments point to an interaction between PSA and the ED of MARCKS through/within the plasma membrane. To the best of my knowledge, this is the first study demonstrating an interaction between an extracellular carbohydrate and an intracellular cytosolic protein within/through the plasma membrane. It has been traditionally proposed, that the different cellular compartments are strictly separated through membranes and only transmembrane proteins can facilitate a cross-talk between adjacent compartments. To further substantiate the proposed interaction between PSA and MARCKS within/through the plasma membrane, an L-photo-leucine cross-linking approach was performed.

CHO cells were transfected with wild-type MARCKS-GFP or mutated MARCKS-GFP constructs containing exchanges of the phenylalanine residues for alanine residues. The cells were maintained in medium with L-photo-leucine allowing incorporation of this photo-active amino acid into newly synthesized proteins. The cells were exposed to UV light after application of colominic acid/PSA to live cells. Since the ED of MARCKS contains one leucine residue, the lysine in the ED of MARCKS and the extracellular added colominic acid could be covalently linked after exposure of the cells to UV-light, if MARCKS and colominic acid interact within the plane of the plasma membrane. MARCKS-GFP irreversibly cross-linked to colominic acid/PSA could then be detected after immunoprecipitation with an MARCKS or GFP antibody and by staining of the precipitated MARCKS-GFP for PSA and GFP. Furthermore, addition of colominic acid/PSA to MARCKS-GFP should shift its apparent molecular weight to higher kDa values.

In precipitates from cells transfected with wild-type MARCKS, a broad diffuse band ranging from approximately 120-150 kDa and one distinct band of 110 kDa were detected when GFP was used for immunoprecipitation and proteins in Western blots were detected with GFP antibody (Fig. 5.29A). Since the colominic acid/PSA preparation contains molecules of different sizes in a range from 10 to 50 kDa and the MARCKS-GFP fusion protein has an apparent molecular weight of 110 kDa (Fig. 5.29D), this result suggests that the MARCKS bands present at 120 to 150 kDa are MARCKS-GFP proteins carrying PSA of different sizes. In cells expressing mutated MARCKS-GFP, only the GFP-positive 110 kDa band was seen in the GFP

Results

immunoprecipitates (Fig. 5.29A). After staining of blots with the PSA antibody a broad diffuse band between 120 to 150 kDa is detectable in the GFP-immunoprecipitates from cells transfected with wild-type MARCKS-GFP, while only unspecific background staining was detected in GFP-immunoprecipitates from cells expressing the MARCKS-GFP mutant (Fig. 5.29C). When PSA-immunoprecipitates from wild-type MARCKS-GFP transfected cells were analyzed using the GFP antibody, a diffuse band ranging from 120 to 150 kDa could be observed. In contrast to this, only a faint background staining was seen in immunoprecipitates from cells transfected with mutated MARCKS-GFP (Fig. 5.29B). Similar expression levels of both MARCKS-GFP constructs were obtained after transfection (Fig. 5.29D). The predicted shift in the molecular weight of MARCKS-GFP from 110 kDa to 120-150 kDa after cross-linking of colominic acid/PSA was only seen in precipitates from cells transfected with wild-type MARCKS-GFP, but not in precipitates from cells transfected with mutated MARCKS-GFP, which does not insert into the plasma membrane with its ED.

Next, recombinant PSA-NCAM-Fc was used in a cross-linking approach with CHO cells expressing wild-type MARCKS-GFP or mutated MARCKS-GFP. The recombinant PSA-NCAM-FC containing a human Fc-tag was applied to cells and, after cross-linking, PSA-NCAM-Fc and proteins bound to PSA-NCAM-Fc were isolated from the cell lysates with Protein A beads. In the Western blots a PSA-positive band of approximately 220 kDa could be detected in cell lysates from CHO cells expressing wild-type and mutant MARCKS-GFP, while an additional band at a molecular weight of 330 kDa was detectable only in precipitates of cells expressing wild-type MARCKS-GFP (Fig. 5.30A). Importantly, both MARCKS-GFP constructs showed similar expression levels of the 110 kDa MARCKS-GFP (Fig. 5.30B). The 330 kDa band observed only in immunoprecipitates from cells transfected with wild-type MARCKS results from cross-linking of the PSA-NCAM-Fc (220kDa) and wild-type MARCKS-GFP (110 kDa).

Results

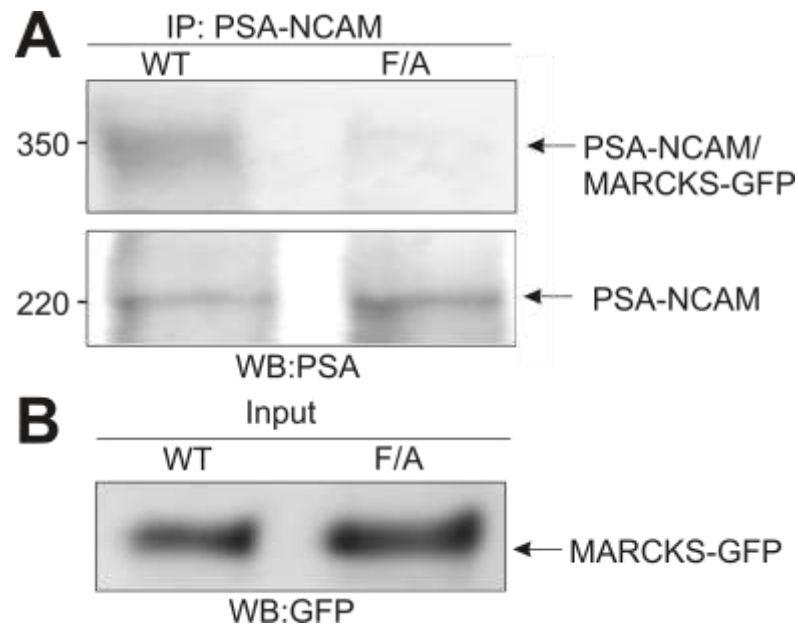


Figure 5.30: Wild-type MARCKS-GFP immunoprecipitates with PSA attached to the ECD of NCAM in a photo-leucine cross-linking approach. CHO cells were transfected with wild-type MARCKS-GFP (WT) or mutant MARCKS-GFP, in which the five phenylalanines in the ED were replaced with five alanine residues (F/A). The cells were maintained overnight in medium, in which the amino residue leucine was replaced against L-photo-leucine. After 24 h in culture the cells were incubated for 20 minutes with PSA-NCAM-Fc (10 μ g per ml). Afterwards cells were incubated under UV light. Then the cells were lysed (B, input) and an immunoprecipitation was performed with protein A agarose beads (Santa Cruz) (A). The samples were subjected to SDS-PAGE and Western blot analysis. The proteins were detected with antibodies against PSA (A) or GFP (B).

Since no FRET from labeled PSA to MARCKS-GFP can be observed when using cells expressing mutated MARCKS-GFP that cannot insert via its ED into the plasma membrane, it is conceivable that the ED of MARCKS tightly interacts with PSA at or within the plasma membrane from opposite sides.

5.20 The interaction between PSA and the ED of MARCKS through an artificial lipid bilayer influences its electrical properties

The FRET results and the cross-linking experiments suggest an interaction of PSA and MARCKS from the opposite sides through/within the plasma membrane. Thus, I next asked whether the electrical properties of the membrane are influenced by this interaction.

To determine whether this might be the case, we used artificial lipid bilayers using the Ionovation Compact V02 system (Fig. 5.31). In this system an artificial lipid bilayer is formed between two adjacent chambers. The capacitance of the bilayer was monitored after addition of colominic acid/PSA or chondroitin sulfate and the MARCKS ED-peptide or the corresponding control peptide to the opposite sides of the bilayer (Fig. 5.31).

I tested the effect of adding colominic acid/PSA or chondroitin sulfate to the cis chamber (Fig. 5.31). This did not lead to a significant alteration in the relative capacitance of the membrane (Fig. 5.32). Subsequent addition of the control peptide to the trans chamber led to a slight increase in the relative capacitance (Fig. 5.32A, B). After addition of the ED-peptide to the opposite side of chondroitin sulfate, the relative capacitance reached a plateau (Fig. 5.32A, C), while addition of the ED-peptide to the opposite side of colominic acid/PSA led to a constant decrease of the capacitance (Fig. 5.32A, B). Finally, the relative capacitance did not change significantly with time, if no peptide or carbohydrate was applied (Fig. 5.32C).

Interestingly, the interaction between the ED of MARCKS and PSA seems to take place through the membrane. This interaction could lead to a connection between the two chambers of the Ionovation system or the cytoplasmic domain and the ECD of the cell. As a consequence, the electrical properties of the artificial membrane or the plasma membrane change.

Results

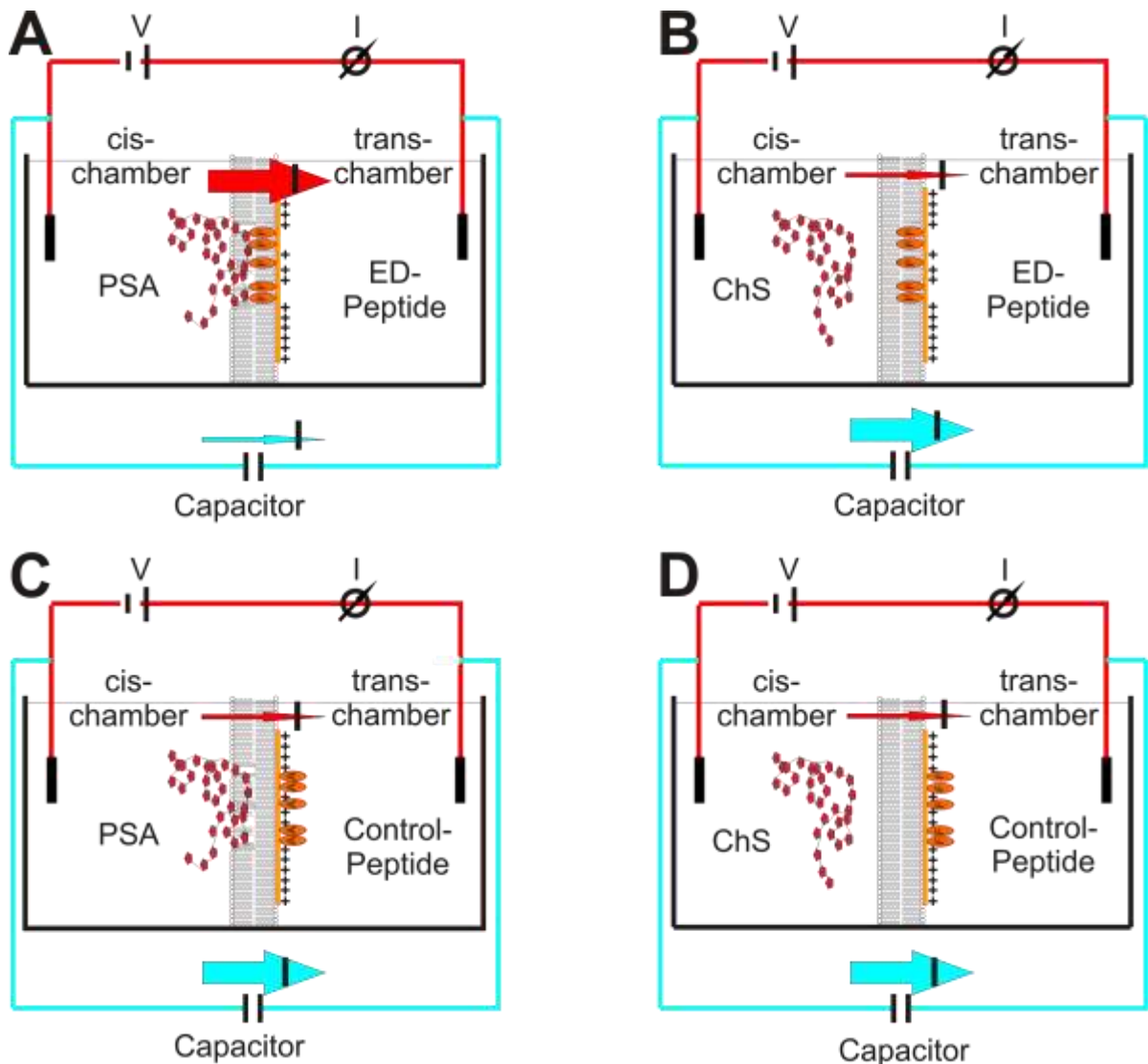


Figure 5.31: Schematic drawing of the setup to measure the capacitance of an artificially lipid bilayer. The Ionovation Compact V02 system was used to build up an artificially lipid bilayer and to measure the capacitance of the bilayer. The lipid bilayer separates adjacent chambers, which were filled with electrode buffer. The artificially lipid bilayer contains a mixture of 1-palmitoyl-2-oleoyl-sn-glycero-3-phosphocholine (POPC) and 1-palmitoyl-2-oleoyl-sn-glycero-3-phosphoethanolamine (POPE) (1:1). In the circuit diagram the resistance circuit (red) and the capacitor circuit (cyan) is shown. The resistance of the red marked circuit is increased when the lipid bilayer is formed. As a consequence more current flows through the capacitor circuit and, thus, lead to an increase of capacitance. When colominic acid and a peptide derived from the ED of MARCKS (ED-Peptide) are added to the trans chamber and the cis chamber, respectively, and if they interact through the lipid bilayer, the lipid bilayer would be more instable from both sides and change its capacitance. Therefore the resistance would decrease and less current would flow through the capacitor circuit which would diminish the capacitance (A). Chondroitin sulfate (ChS) has similar chemical properties as colominic acid, but it is not known that neither it attaches to the membrane nor that it can interact with MARCKS. The control-peptide is also derived from the ED of MARCKS, but the phenylalanine residues were changed to alanine residues. Both were used as controls, which would not penetrate in the lipid bilayer and therefore the bilayer would be stable. The resistance in the red marked circuit would be higher in the controls and therefore more current would flow through the cyan marked circuit followed by an increase of the capacitance (B, C, D).

Results

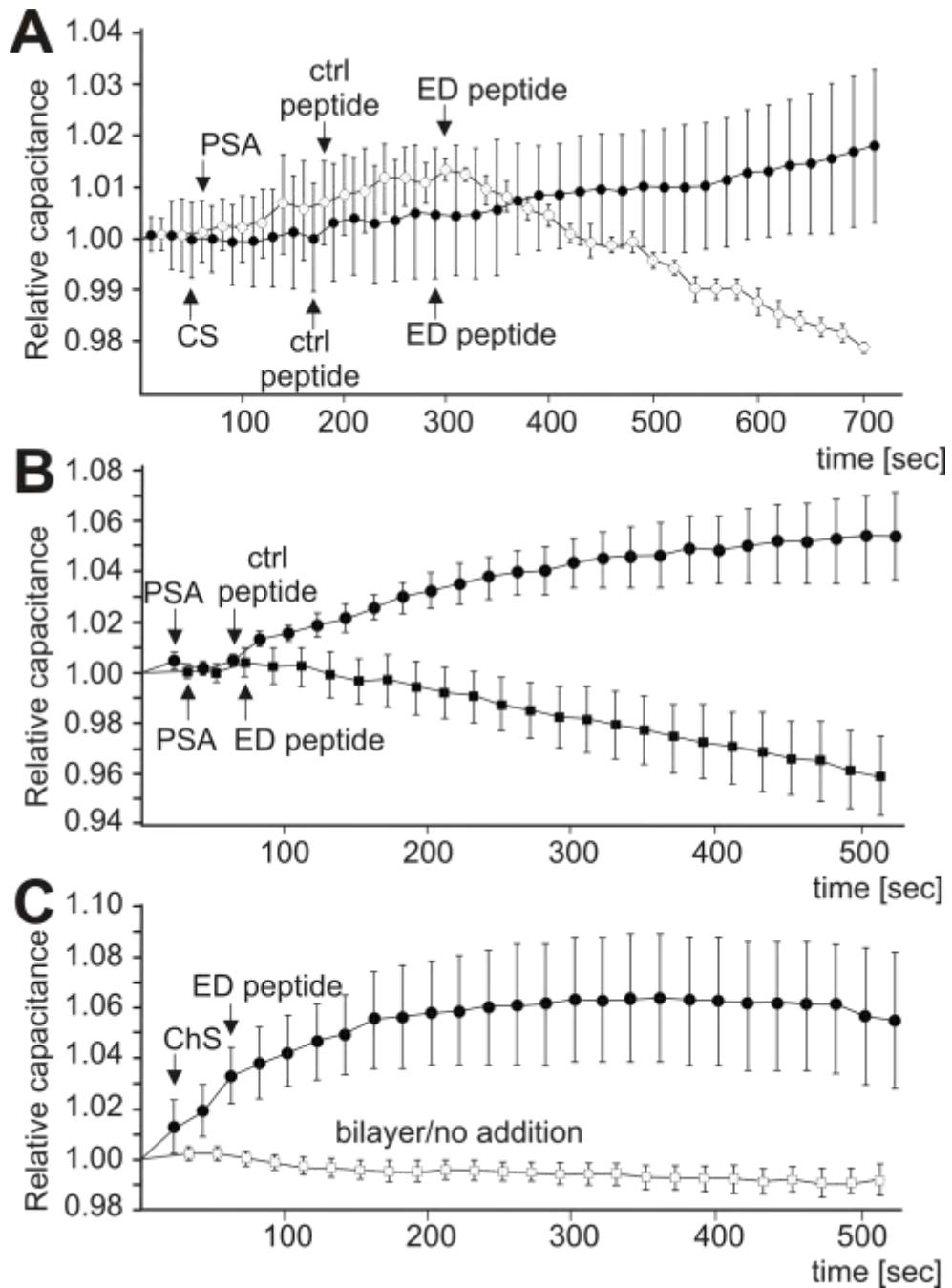


Figure 5.32: The interaction of colominic acid/PSA with MARCKS through an artificial membrane influences the electrical properties of the bilayer. The artificial lipid bilayer which contains a 1:1 lipid mixture of POPE and POPC is formed with the Ionovation Compact V02 system. The capacitance of the lipid bilayer was measured like described in Figure 5.31. The capacitance was recorded over a time period of 520 seconds and compared to the capacitance of the lipid bilayer at the starting point (0 seconds). Colominic acid (PSA) (A, B) or chondroitin sulfate (ChS) (A, C) was added in the trans chamber 30 seconds after the start of the measurements. After further 30 seconds (B, C) or two minutes (A) a peptide derived from the ED of MARCKS (ED peptide) or a control peptide in which the phenylalanines were exchanged to alanines (ctrl peptide) were added to the trans-chamber. As a further control, the capacitance of a lipid bilayer was determined over a time period of 520 seconds without any addition of carbohydrates and peptides (bilayer/no addition).

5.21 The interaction between PSA and MARCKS is necessary for the PSA-mediated neurite outgrowth

Since I could show in previous experiments that NCAM-mediated neurite outgrowth is dependent on PSA (see Fig. 5.15), I next wanted to investigate if the PSA-MARCKS interaction is of functional relevance for NCAM- or PSA-mediated neurite outgrowth.

To investigate whether colominic acid/PSA stimulates neurite outgrowth and the MARCKS-PSA interaction influences this effect, hippocampal neurons from wild-type (Fig. 5.33A) and NCAM-deficient littermates (Fig. 5.33A, B) were transfected with the MARCKS ED or control peptide (Fig. 5.33A) or the peptides were added to the medium (Fig. 5.33B) and the neurons were incubated in the absence or presence of colominic acid, chondroitin sulfate or heparin.

The total neurite length of mock transfected wild-type and NCAM-deficient neurons was increased in the presence of colominic acid/PSA (data not shown). In neurons transfected with the ED-peptide, but not in cells transfected with the control peptide, the stimulatory effect of PSA was abolished (Fig. 5.33A). Since the ED-peptide but not the control-peptide binds *in vitro* to PSA (Theis *et al.*, 2013), it is possible that the ED-peptide, but not the control-peptide, interacted with PSA and disturbed the MARCKS-PSA interaction. A similar effect was observed, if the peptides were applied extracellularly to hippocampal wild-type neurons (Fig. 5.33B). Interestingly, neurite outgrowth was enhanced after chondroitin sulfate treatment and decreased after heparin treatment of NCAM-deficient neurons, but not wild-type neurons. This effect was observed in cells transfected with the ED- or the control- peptide (Fig. 5.33A). An enhanced neurite outgrowth was observed by Bibhudatta Mishra (PhD thesis, Hamburg, 2010) when wild-type neurons were treated only with the ED-peptide. This effect could be abolished after EndoN treatment (Theis *et al.*, 2013). Here we treated NCAM deficient hippocampal neurons with the ED- or control-peptide alone and this led to no enhancement of neurite outgrowth, compared to non-treated cells (Fig. 5.32B).

Results

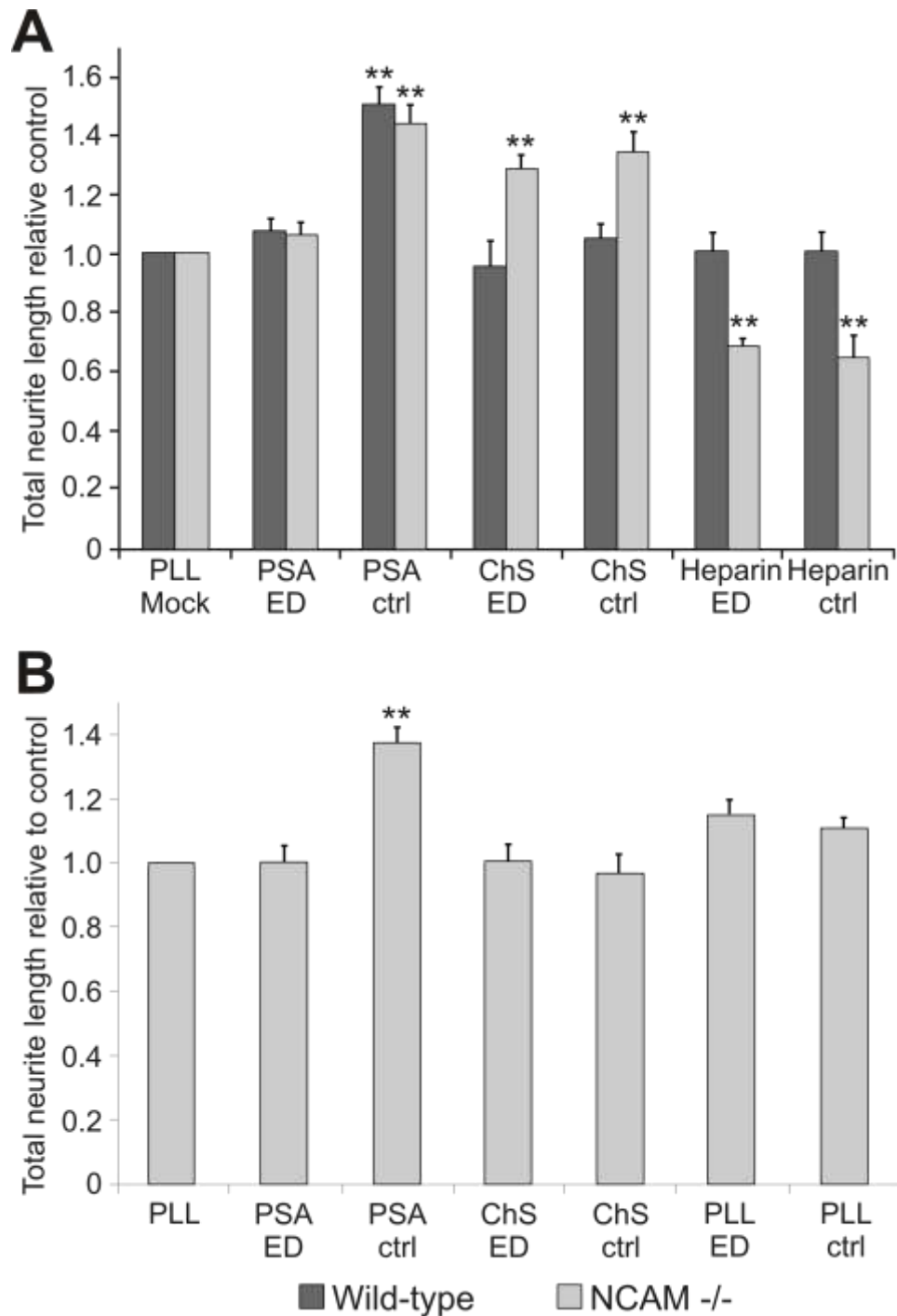


Figure 5.33: MARCKS is involved in PSA-dependent neurite elongation. The length of neurites from wild-type (A) and NCAM-deficient (A and B) neurons was determined. Different carbohydrates (colominic acid (PSA), chondroitin sulfate (ChS) or heparin) were added to the neurons one hour after seeding. In A the cells were transfected with the ED- or ctrl- peptide and co-transfected with GFP as transfection control. In the mock control, cells were only transfected with GFP and not treated with carbohydrates (A). In B the cells were treated with colominic acid (PSA) or chondroitin sulfate (ChS) and additionally the ED- or control (ctrl)-peptides were added to the medium. As controls non-treated cells (PLL) or cells only treated with the peptides (PLL ED; PLL ctrl) were used. The neurite lengths of treated neurons were compared to neurite length of cells cultured on PLL (Mock; A) or PLL (B) control. Mean values are shown. The error bars show the standard error of the mean and statistically significant differences were identified by the Student's t-test (** $p < 0.01$; $n = 100$).

Results

These results indicate that the effect of soluble colominic acid/PSA is independent from endogenous PSA and NCAM, but the effect is mediated by the ED of MARCKS.

5.22 Phosphorylation of the ED of MARCKS is prevented by the interaction between PSA and MARCKS

Since I could prove that MARCKS and PSA interact with each other at the plasma membrane, it seems to be obvious, that colominic acid/PSA treatment leads to recruitment of additional MARCKS to the plasma membrane. Because MARCKS can only be associated with the plasma membrane when its ED is not phosphorylated (Swierczynski *et al.*, 1995), the level of phosphorylated MARCKS should decrease after colominic acid/PSA treatment.

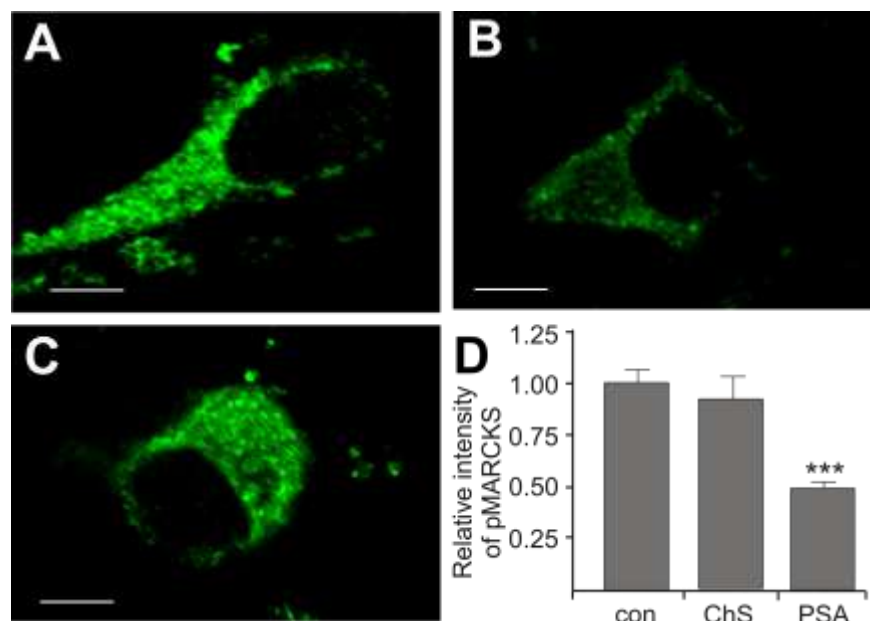


Figure 5.34: PSA/colominic acid treatment reduces the level of phospho-MARCKS in hippocampal neurons. Quantification of the immunofluorescence signal of phospho-MARCKS (A: not treated; B: treated with colominic acid/PSA; C: treated with chondroitin sulfate). Hippocampal neurons which were maintained *in vitro* for 24 hours were fixed, permeabilized and stained with an antibody against phosphorylated MARCKS (p-MARCKS). The intensities of the different stainings were measured with ImageJ and related to the intensity of the phospho-MARCKS staining of non-treated cells (D). The error bars show the standard error of the mean and the statistical significant was analysed by Student's t-test (***) $p < 0.001$; $n = 7$). The scale bars represent 20 μm .

Results

First indications for such an effect were obtained by Bibhudatta Mishra, who observed decreased levels of phosphorylated MARCKS in hippocampal neurons after colominic acid treatment (Theis *et al.*, 2013).

Here, the immunofluorescence signal of phospho-MARCKS from non-treated hippocampal neurons (Fig. 5.34A) was compared to phospho-MARCKS levels in neurons treated with chondroitin sulfate (Fig. 5.34B) or colominic acid (Fig. 5.34C). A significant decrease of phospho-MARCKS could be also observed with this method after colominic acid/PSA treatment, but not after chondroitin sulfate treatment. This result confirms the hypothesis that the MARCKS-PSA interaction prevents the phosphorylation of MARCKS.

6. Discussion

6.1 The interaction between NCAM140/180 and TRPC1, 4 and 5

From immunoprecipitation experiments and immunofluorescence stainings I obtained indications for a possible interaction between NCAM and TRPC1, 4 and 5. Furthermore, label-free binding assays showed calmodulin-dependent binding of TRPC1, 4 and 5 channels to the ICD of NCAM180, whereas no binding between ICD of NCAM140 and TRPC proteins was observed. The calmodulin-dependent interaction between TRPC1 and NCAM180 was confirmed in pull-down assays using wild-type NCAM180 ICD or NCAM180 ICD containing a mutated calmodulin binding site (Mounir M'Zoughi, PhD thesis, Hamburg). Since the ICD of NCAM140 and 180 both have a calmodulin binding motif (Kleene *et al.*, 2010b) it seems that binding of calmodulin to NCAM would mediate interaction of NCAM with TRPC. However, TRPC1 was not only precipitated with the wild-type ICD of NCAM140, but also was precipitated with mutated NCAM140 ICD containing the disrupted calmodulin binding site. The combined results exclude a direct interaction between NCAM and TRPCs and suggest that calmodulin mediates the interaction between NCAM180 and TRPC1, 4 and/or 5. In contrast to NCAM180, the interaction of NCAM140 with TRPCs is not mediated by calmodulin as binding and pull-down assays indicate. Since NCAM140 precipitates with TRPC1 in a pull-down experiment using mouse brain homogenate, it is likely that this interaction is mediated by other proteins. A direct interaction of the ICDs can be excluded, because binding of NCAM140 ICD to ICDs of TRPCs including TRPC1 ICD was not observed in the binding assay.

The different modes of interaction of NCAM140 and 180 with TRPCs suggest that NCAM140 and 180 trigger different TRPC-associated signaling pathways. One well-known cellular response to NCAM signaling is neurite outgrowth. In previous studies, it was reported that NCAM binds to the FGFR (Christensen *et al.*, 2006; Kiselyov *et al.*, 2003) and that NCAM-mediated neuritogenesis requires the FGFR (Niethammer *et al.*, 2002). This NCAM-FGFR interaction induces phosphorylation of FGFR leading

Discussion

to an activation of PLC (Jessen *et al.*, 2001). PLC hydrolyzes PIP₂ yielding IP₃ and DAG. IP₃ binds to the IP₃ receptor in the membrane of the endoplasmic reticulum leading to a calcium release from the intracellular calcium stores. This increased calcium concentration in the cytoplasm could activate TRPC channels (Salido *et al.*, 2009). Since the FGFR interacts with TRPC1 (Fiorio Pla *et al.*, 2005) and since I could show that NCAM-, but not L1- or CHL1- enhanced neurite outgrowth, was inhibited with the TRPC inhibitor SKF96365 and the inhibitory antibody against TRPC1, it is conceivable that the interaction between NCAM140 and TRPC1 is mediated by the FGFR and that this interaction triggers NCAM-dependent neurite outgrowth.

Homophilic NCAM interaction triggers the Fyn/Fak pathway resulting in enhanced neurite outgrowth (Ditlevsen *et al.*, 2010). It was reported that the expression of the growth-associated protein (GAP-43) most likely acts as switch for NCAM180-induced signaling (Korshunova *et al.*, 2007). The binding between NCAM180 and spectrin facilitates the interaction of NCAM180 with GAP-43 and promotes the formation of a NCAM180/spectrin/GAP-43 complex. This interaction regulates NCAM180-mediated neurite outgrowth, which is assumed to be FGFR-dependent, but independent of the Fyn/Fak pathway (Korshunova *et al.*, 2007). It may be possible that interaction of NCAM180 with TRPCs and/or FGFR plays a role in regulating the interaction between NCAM180, spectrin and GAP-43 and thus in regulating or promoting NCAM180-dependent neurite outgrowth.

NCAM-TRPC interactions could also be involved in other physiological processes beside in neurite outgrowth. For example, it is known, that TRPC channels play an important role in SOCE (Liao *et al.*, 2008; 2007). Triggering of signal cascades through transmembrane receptors could lead to depletion of intracellular calcium stores and to a concomitant increase in cytoplasmic calcium concentration. This increased calcium concentration could trigger opening of calcium permeable channels in the plasma membrane resulting in SOCE (Putney *et al.*, 1986). Thus, NCAM-TRPC interactions could also play a role in SOCE. It has been reported that TRPC1 is a prerequisite for SOCE, which mediates the glutamate secretion from astrocytes (Malarkey *et al.*, 2008). Since NCAM is also expressed in astrocytes

Discussion

(Theodosios *et al.*, 1999) and can inhibit astrocyte proliferation (Krushel *et al.*, 1995), it is likely that the interaction of NCAM with TRPC can also regulate cellular functions in astrocytes, such as glutamate secretion and proliferation.

Other physiological functions for the NCAM-TRPC interaction are conceivable: The calmodulin-dependent interaction between NCAM180 and TRPC1, 4 and 5 is probably involved in regulating different cellular responses in the mature nervous system. Since the dopamine receptor D2 interacts with TRPC1, 4 and 5 (Hannan *et al.*, 2008) and with NCAM180 (Xiao *et al.*, 2009), it seems plausible that the interaction between TRPC1, 4, 5 and NCAM180 influences signaling via dopamine receptor D2. Since NCAM180 is involved in activity-dependent internalization of the D2 receptor, it is likely that the interaction between NCAM180 and TRPC1, 4 and/or 5 modulates this internalization.

The NCAM-TRPC interaction could also affect the generation of plateau potentials in cholinergic neurons. Plateau potentials are caused by a persistent cellular ion influx which leads to a lasting depolarization of the plasma membrane. Neurons displaying such plateau potentials fire independently of synaptic excitation (Takai *et al.*, 2004; Lee *et al.*, 2003; Kuzmiski *et al.*, 2001; Fraser *et al.*, 1996; Marder, 1991). NCAM-deficient mice have been shown to display a reduced number of septal cholinergic neurons (Tereshchenko *et al.*, 2011) that are able to generate these plateau potentials. Furthermore, it has been reported that TRPC4 and 5 channels are responsible for generation of non-selective cation influx and therefore generate these plateau potentials in cholinergic neurons (Tai *et al.*, 2011; Zhang *et al.*, 2011). Based on these findings and regarding the fact that NCAM180 and TRPC1, 4 and 5 were shown to interact with each other, NCAM-TRPC interaction might affect the emerging plateau potentials in cholinergic neurons. Calmodulin-dependent binding between NCAM180 and TRPC4/5 may induce an opening of TRPC4 and/or 5 channels in the cell membrane and as a consequence, a constant non-selective cation influx would propagate into the cell generating a lasting depolarized membrane potential. Since NCAM180 is predominantly expressed at sites of cell-cell contacts and in growth cones contacting other cells (Pollerberg *et al.*, 1987; Pollerberg *et al.*, 1986) and homo- or heterophilic NCAM interactions are important for maintenance of these

Discussion

contacts, it is conceivable that NCAM might modulate the functional behavior of its adjacent binding partners and thus the cell-cell contacts.

Binding of NCAM or L1 antibodies to NCAM or L1 at the cell surface could mimic homo- and heterophilic interactions of NCAM or L1. Antibodies against NCAM or L1 directed against their ECDs trigger signaling and lead to an increase in the intracellular calcium concentration (Schuch *et al.*, 1989). In my work, function-triggering polyclonal antibodies were used in calcium imaging and neurite outgrowth experiments and showed an NCAM-mediated response. Calcium imaging and cell surface biotinylation of hippocampal neurons indicated that functional TRPC4 and 5 channels are translocated from the interior of the cell to the surface when the cells are cultured in medium containing serum. This translocation does not take place when the cells are maintained in medium without serum. Several reports have shown translocation of TRPC4 and 5 to the cell surface after treatment with different growth factors such as epidermal growth factor (EGF), BDNF, nerve growth factor (NGF) and insulin-like growth factor-1 (IGF-1) (Bezzarides *et al.*, 2004, Schaefer *et al.*, 2000). Thus, growth factors present in the serum could trigger the translocation of TRPC4 and 5 to the plasma membrane where they function as storage operating calcium channels or in generation of a lasting depolarized membrane potential.

6.2 Functional interplay between NCAM, TRPC1, 4 and 5 with PrP and Kir3.3

The inwardly-rectifying potassium channel Kir3.3 (Kleene *et al.*, 2010a) and the prion protein (PrP) (Santuccione *et al.*, 2005; Schmitt-Ulms *et al.*, 2001) are binding partners of NCAM. Inwardly-rectifying potassium channels maintain the membrane resting potential near to the potassium reversal potential and have a highly stabilizing effect on the resting potential of the cell (Fakler *et al.*, 1995). For the strong inward rectification of these channels a highly voltage-dependent block by intracellular magnesium and an endogenous channel gating process are responsible (Matsuda *et al.*, 1991). The Kir3.3 channel interacts intracellularly with NCAM140 and

Discussion

NCAM180 and this interaction seems to reduce the activity of Kir3.3 and to block the NCAM-mediated neurite outgrowth (Kleene *et al.*, 2010a). Here, I demonstrate that the NCAM-Kir3.3 interaction recruits Kir3.3 to the cell surface.

PrP is a GPI anchored cell surface glycoprotein which is ubiquitously expressed in the brain (Schmitt-Ulms *et al.*, 2001). In a previous study, it has been described that the interaction between NCAM and PrP is important for NCAM-stimulated neurite outgrowth (Santuccione *et al.*, 2005). In immunoprecipitation experiments, I obtained evidences for interactions between Kir3.3 and TRPC1, 3, 4, 5, 6 and/or 7 and between PrP and TRPC1, 3, 4, 5, 6 and/or 7. Since NCAM-enhanced neurite outgrowth depends on PrP- and TRPC- interactions with NCAM and could be blocked with the TRPC inhibitor or a function-blocking TRPC1 antibody, one could speculate that the interaction between PrP and TRPC proteins may modulate NCAM-dependent neuritogenesis.

I observed a calcium efflux from hippocampal neurons after NCAM-stimulation, when the neurons had been cultured in medium with serum. Since the TRPC inhibitor SKF96365 blocks this NCAM-induced calcium efflux and since it has been shown to inhibit inwardly-rectifying potassium current in human endothelial cells (Schwarz *et al.*, 1994), it is likely that the NCAM-induced calcium efflux is mediated by TRPCs and regulated by the functional interplay between NCAM, the TRPCs and the inwardly-rectifying potassium channel Kir3.3. In this functional interplay, Kir3.3 might be activated by the ion flow through the TRPC-channels. One might speculate that the ion flow through the TRPC channels generate a depolarization of the plasma membrane, while the potassium flow through the Kir3.3 channel leads to a change of the potassium reversal potential and a further enhancement in plasma membrane depolarization.

6.3 NCAM-stimulated import of PSA into the nucleus

It has been proposed that triggering of NCAM signaling with an antibody against its ECD leads to oligomerisation of NCAM at the cell surface, an increase in intracellular

Discussion

calcium levels, interaction with calmodulin, and a proteolytic cleavage of NCAM by a serine protease. The proteolytic processing of NCAM results in the generation of two fragments (Kleene *et al.*, 2010b): a soluble 55 kDa fragment with part of the ECD and a membrane bound 50 kDa fragment containing the intracellular and transmembrane domain as well as part of the ECD (Kleene *et al.*, 2010b). In my work, I showed that the import of the 50 kDa NCAM fragment is reduced by the TRPC inhibitor SKF96365, indicating that the calcium-dependent nuclear import of the NCAM fragment requires the opening of TRPC channels.

Taking the apparent molecular weight of NCAM into account, I expect that the cleavage of NCAM by the serine protease activity takes place within the fourth or fifth Ig-like domain distal to the fifth and sixth N-glycosylation sites to which PSA and/or HNK1 are attached (Wuhrer *et al.*, 2003). Thus, it was likely that a PSA- and/or HNK-1-carrying 50 kDa NCAM fragment is imported into the nucleus after NCAM-stimulation. Indeed, PSA-immunopositive staining in the nucleus was observed after NCAM-stimulation of hippocampal neurons. In addition, after NCAM-stimulation of cerebellar neurons, PSA-positive bands of 100-200 kDa were seen in nuclear fraction containing nucleoplasmic or chromatin attached proteins. The enhanced nuclear levels of PSA at the beginning of the NCAM-stimulation decreased and reached the nuclear PSA level of untreated neurons. Since the intensity of the PSA-immunopositive nuclear signal was decreased after one hour of NCAM-stimulation, one could speculate that PSA on NCAM is degraded after it reaches the nucleus or is exported from the nucleus. It is still not clear, whether PSA is attached to the 50 kDa NCAM fragment and thereby reaches the nucleus as a 100-200 kDa protein. Although a 50 kDa NCAM fragment was seen in the fraction of nucleoplasmic proteins after degradation of PSA by treating cerebellar neurons with Endo N before NCAM stimulation, no larger PSA-carrying NCAM forms were detectable in Western blot analysis of mock-treated neurons with the antibody P61 against the intracellular NCAM domain.

The appearance of PSA and/or HNK1 in the nucleus after NCAM stimulation implies that the attached glycans modulate the function of nuclear NCAM, such as affecting chromatin structure and/or regulation of gene expression. Chromatin remodeling is

Discussion

associated with DNA modifications such as methylation and hydroxymethylation (Biran *et al.*, 2012). Since histone H1 plays a role as a linker histone and mediates DNA packaging in nucleosomes (Doenecke *et al.*, 1997), and since PSA interacts with histone H1 (Mishra *et al.*, 2010), PSA may draw histone H1 from the chromosomal DNA leading to modifications of the DNA, such as methylation and hydroxymethylation (Irier *et al.*, 2012). Alternatively, histone H1 might bind to PSA-NCAM at the cell surface (Mishra *et al.*, 2010), and be imported in a complex with PSA-NCAM into the nucleus after NCAM stimulation. Surprisingly, histone H1 was found in a 200 kDa PSA-immunopositive band which may represent a large SDS stable protein complex of histone H1 and PSA-NCAM. Although PSA seems to interact with histone H1 in the nucleus, levels of DNA methylation and hydroxymethylation are not affected by enhancement of the nuclear PSA levels.

On the other hand, increase levels of DNA methylation and hydroxymethylation were observed after PSA digestion and subsequently NCAM-stimulation. These increases are accompanied by the appearance of a 50 kDa NCAM in the fraction of nucleoplasmic proteins, suggesting that this fragment induces modifications of DNA. The 50 kDa NCAM fragment could bind to the chromosomal DNA, and thus, could induce a change in chromatin structure and in DNA modifications. Alternatively, the NCAM fragment could bind to nuclear proteins that are involved in DNA modifications, such as the deoxyribonucleic acid methyltransferases 1, 3a or 3b catalyzing DNA methylation (Rottach *et al.*, 2009; Bestor *et al.*, 2000), to the ten-eleven translocation enzyme catalyzing the oxidation of the methyl group to a hydroxymethyl group (Guo *et al.*, 2011; He *et al.*, 2011; Ito *et al.*, 2011; Tahiliani *et al.*, 2009) or to histones, which are essential for the packaging of the chromatin (Lodén *et al.*, 2005).

6.4 Interaction between MARCKS and PSA

In a previous study, it has been demonstrated that MARCKS and PSA interact with each other (Bibhudetta Mishra, PhD thesis, Hamburg; Maren von der Ohen, PhD thesis, Hamburg). I have further characterized this interaction. Since MARCKS is an

Discussion

intracellular protein and PSA on NCAM is located extracellularly, it seems likely that the interaction between both molecules takes place from opposite sides of the plasma membrane.

The ED of MARCKS attaches to membranes via electrostatic interactions between its positively charged residues and the negatively charged phospholipids of the membrane bilayer. The phenylalanines of MARCKS ED can penetrate in addition through the polar head groups of the lipids of the bilayer into the hydrophobic part of the plasma membrane, and thus, stabilizes the attachment of MARCKS to the plasma membrane (Victor *et al.*, 1999; Qin *et al.*, 1996). The helical and random coiled conformation of PSA (Brisson *et al.*, 1992) facilitates its association with liposomal membranes and its penetration into lipid bilayers (Janas *et al.*, 2000; 2001; 2010). Based on the similar properties of PSA and MARCKS to insert into the membrane, it could be inferred that PSA and MARCKS might thereby interact within the plasma membrane from opposite sites. The results from the cross-linking approach with photo-L-leucine and FRET analysis using different MARCKS-constructs and colominic acid/PSA or PSA-NCAM-Fc support this hypothesis. Furthermore, application of the ED-peptide, to the opposite site colominic acid/PSA application destabilized the bilayer and allowed ions to flow through the bilayer and, therefore, to change the electrical properties of the membrane. Neither chondroitin sulfate nor the control peptide insert into the bilayer and thus do not change the properties of the membrane. This PSA-MARCKS interaction may form hydrophilic pores in the lipid bilayer, which would allow ions to pass the membrane. Since PSA is able to influence the long term potentiation in the brain (Becker *et al.*, 1996; Muller *et al.*, 1996), this observation suggests a novel mechanism of how PSA could modulate the membrane potential to influence cellular processes involved in long term potentiation.

The PSA-enhanced neurite outgrowth in hippocampal neurons was triggered upon colominic acid/PSA incubation (Mehanna *et al.*, 2010; Muller *et al.*, 1994). This PSA-enhanced neurite outgrowth was inhibited by transfection or by extracellular addition of the MARCKS ED peptide, but not by application of the MARCKS control peptide. Moreover, levels of phosphorylated MARCKS in hippocampal neurons were

Discussion

decreased after PSA treatment. Based on this observation, one could speculate that the additionally added colominic acid might recruit more MARCKS at the plasma membrane; in order to prevent the phosphorylation of MARCKS ED. Phosphorylated MARCKS may further trigger a signal cascade, which inhibits neurite outgrowth. Application of additional PSA would then lead to an inhibition of this signal cascade and, consequently, to an enhanced neurite outgrowth. The MARCKS ED peptide may disturb the PSA-MARCKS interaction, which might lead to an increased phosphorylation of MARCKS and, thereby, stimulate the signal cascade, which thereafter inhibits neurite outgrowth.

NCAM-deficient neurons showed a decreased neurite outgrowth after heparin treatment and an enhanced neurite outgrowth after chondroitin sulfate treatment. In contrast, heparin and chondroitin sulfate had no effect on neurite outgrowth of wild-type neurons. In its Ig1 and Ig2 domains NCAM contains one heparin binding motif to which both heparin and chondroitin sulfate can bind (Cole *et al.*, 1989, 1986a, b). One possible explanation, that an effect of heparin and chondroitin sulfate in neurite outgrowth of NCAM-deficient, but not wild-type hippocampal neurons, was observed would be that heparin and chondroitin sulfate could interact with the heparin binding motif of NCAM in wild-type neurons. This might lead to a neutralization of the heparin and chondroitin sulfate effect on neurite outgrowth of wild-type, but not NCAM-deficient hippocampal neurons.

It was reported that the MARCKS ED peptide has an enhancing effect on hippocampal neuritogenesis (Theis *et al.*, 2013). One can assume that the inhibitory effect of the ED peptide on NCAM-mediated neurite outgrowth could be explained by a side effect of this ED peptide, and not disturb a possible PSA-MARCKS interaction. Since the phenylalanine residues in the ED of MARCKS show a high affinity of binding to PIP₂, and thus, regulate the availability of PIP₂ by sequestration of PIP₂ (Gambhir *et al.*, 2004; Laux *et al.*, 2000), which has been implicated in signal transduction (Kwiatkowska *et al.*, 2010), it seems conceivable, that this sequestered of PIP₂ leads to an increased total neurite length of hippocampal neurons. In contrast, the additional treatment of hippocampal neurons with PSA would lead to inhibition of neuritogenesis. The results from this study are contrary to this

Discussion

assumption. Here, the ED peptide had no stimulating effect on neuritogenesis in hippocampal neurons from NCAM deficient mice, which also express PIP₂, but do not PSA. Additionally, the ED peptide was applied to the neurons extracellularly which did not allow the peptide to sequester PIP₂, because PIP₂ is abundantly present in the inner layer of the plasma membrane. Since the ED peptide stimulates neurite outgrowth only in the presence of endogenous PSA, it seems plausible that the ED peptide disturbs the interaction between PSA and MARCKS, and thus, might provide PSA which is accessible for other interaction partners, such as histone H1 or FGF. This interaction of PSA with histone H1 or FGF would lead to an increase of the neurite outgrowth of hippocampal neurons. My assumptions seem controversial. However, endogenous PSA may recruit much less MARCKS at the plasma membrane which prevent MARCKS to be phosphorylated, then additional applied colominic acid/PSA to the neurons. The stimulation of neurite outgrowth triggered by other interaction partners than MARCKS, such as histone H1 or FGF, seems to be stronger than the inhibition of neurite outgrowth by additionally phosphorylated MARCKS.

7. Literature

Aderem A (1992). The MARCKS brothers: a family of protein kinase C substrates. *Cell* 27;71(5):713-6.

Albach C, Damoc E, Denzinger T, Schachner M, Przybylski M, Schmitz B (2004). Identification of N-glycosylation sites of the murine neural cell adhesion molecule NCAM by MALDI-TOF and MALDI-FTICR mass spectrometry. *Anal Bioanal Chem* 378(4):1129-35.

Albert KA, Nairn AC, Greengard P (1987). The 87-kDa protein, a major specific substrate for protein kinase C: purification from bovine brain and characterization. *Proc Natl Acad Sci U S A* 84(20):7046-50.

Alcaraz G, Goridis C (1991). Biosynthesis and processing of polysialylated NCAM by AtT-20 cells. *Eur J Cell Biol* 55(1):165-73.

Allen LH, Aderem A (1995a). A role for MARCKS, the alpha isozyme of protein kinase C and myosin I in zymosan phagocytosis by macrophages. *J Exp Med* 1;182(3):829-40.

Allen LA, Aderem A (1995b). Protein kinase C regulates MARCKS cycling between the plasma membrane and lysosomes in fibroblasts. *EMBO J* 15;14(6):1109-21.

Angata K, Nakayama J, Fredette B, Chong K, Ranscht B, Fukuda M (1997). Human STX polysialyltransferase forms the embryonic form of the neural cell adhesion molecule. Tissue-specific expression, neurite outgrowth, and chromosomal localization in comparison with another polysialyltransferase, PST. *J Biol Chem* 14;272(11):7182-90.

Aonurm-Helm A, Jurgenson M, Zharkovsky T, Sonn K, Berezin V, Bock E, Zharkovsky A (2008). Depression-like behaviour in neural cell adhesion molecule (NCAM)-deficient mice and its reversal by an NCAM-derived peptide, FGL. *Eur J Neurosci* 28(8):1618-28.

Aplin, A. E., Howe, A., Alahari, S. K., Juliano, R. L (1998). Signal Transduction and Signal Modulation by Cell Adhesion Receptors: The Role of Integrins, Cadherins, Immunoglobulin-Cell Adhesion Molecules, and Selectins. *Pharmacol Rev* 50: 197-263.

Arai M, Yamada K, Toyota T, Obata N, Haga S, Yoshida Y, Nakamura K, Minabe Y, Ujike H, Sora I, Ikeda K, Mori N, Yoshikawa T, Itokawa M (2006). Association between polymorphisms in the promoter region of the sialyltransferase 8B (SIAT8B) gene and schizophrenia. *Biol Psychiatry* 59(7):652-9.

Arai M, Itokawa M, Yamada K, Toyota T, Arai M, Haga S, Ujike H, Sora I, Ikeda K, Yoshikawa T (2004). Association of neural cell adhesion molecule 1 gene polymorphisms with bipolar affective disorder in Japanese individuals. *Biol Psychiatry* 15;55(8):804-10.

Arbuzova A, Schmitz AA, Vergères G (2002). Cross-talk unfolded: MARCKS proteins. *Biochem J* 15;362(Pt 1):1-12.

Arbuzova A, Murray D, McLaughlin S (1998). MARCKS, membranes, and calmodulin: kinetics of their interaction. *Biochim Biophys Acta* 10;1376(3):369-79.

Literature

- Barthels D, Vopper G, Wille W (1988). NCAM-180, the large isoform of the neural cell adhesion molecule of the mouse, is encoded by an alternatively spliced transcript. *Nucleic Acids Res* 25;16(10):4217-25.
- Becker CG, Artola A, Gerardy-Schahn R, Becker T, Welzl H, Schachner M (1996). The polysialic acid modification of the neural cell adhesion molecule is involved in spatial learning and hippocampal long-term potentiation. *J Neurosci Res* 45(2):143-52.
- Bestor TH (2000). The DNA methyltransferases of mammals. *Hum Mol Genet* 9(16):2395-402.
- Bezzierides VJ, Ramsey IS, Kotecha S, Greka A, Clapham DE. (2004). Rapid vesicular translocation and insertion of TRP channels. *Nat Cell Biol* 6(8):709-20.
- Battistel MD, Shangold M, Trinh L, Shiloach J, Freedberg DI (2012). Evidence for helical structure in a tetramer of α 2-8 sialic acid: unveiling a structural antigen. *J Am Chem Soc* 134(26):10717-20.
- Bhatnagar RS, Gordon JI (1997). Understanding covalent modifications of proteins by lipids: where cell biology and biophysics mingle. *Trends Cell Biol* 7(1):14-20.
- Blackshear PJ (1993). The MARCKS family of cellular protein kinase C substrates. *J Biol Chem* 25;268(3):1501-4.
- Bodrikov V, Leshchyns'ka I, Sytnyk V, Overvoorde J, den Hertog J, Schachner M (2005). RPTPalpha is essential for NCAM-mediated p59fyn activation and neurite elongation. *J Cell Biol* 3;168(1):127-39.
- Bollimuntha S, Ebadi M, Singh BB (2006). TRPC1 protects human SH-SY5Y cells against salsolinol-induced cytotoxicity by inhibiting apoptosis. *Brain Res* 12;1099(1):141-9.
- Bollimuntha S, Singh BB, Shavali S, Sharma SK, Ebadi M (2005). TRPC1-mediated inhibition of 1-methyl-4-phenylpyridinium ion neurotoxicity in human SH-SY5Y neuroblastoma cells. *J Biol Chem* 21;280(3):2132-40.
- Bonfanti L, Olive S, Poulain DA, Theodosis DT (1992). Mapping of the distribution of polysialylated neural cell adhesion molecule throughout the central nervous system of the adult rat: an immunohistochemical study. *Neuroscience* 49(2):419-36.
- Boutin JA (1997). Myristoylation. *Cell Signal* 9(1):15-35.
- Brisson JR, Baumann H, Imberty A, Pérez S, Jennings HJ (1992). Helical epitope of the group B meningococcal alpha(2-8)-linked sialic acid polysaccharide. *Biochemistry* 31(21):4996-5004.
- Bukalo O, Fentrop N, Lee AY, Salmen B, Law JW, Wotjak CT, Schweizer M, Dityatev A, Schachner M (2004). Conditional ablation of the neural cell adhesion molecule reduces precision of spatial learning, long-term potentiation, and depression in the CA1 subfield of mouse hippocampus. *J Neurosci* 24(7):1565-77.
- Burroughs CL, Watanabe M, Morse DE (1991). Distribution of the neural cell adhesion molecule (NCAM) during heart development. *J Mol Cell Cardiol* 23(12):1411-22.

Literature

Carson W, Caligiuri M (1996). Natural Killer Cell Subsets and Development Methods 9(2):327-43.

Cassens C, Kleene R, Xiao MF, Friedrich C, Dityateva G, Schafer-Nielsen C, Schachner M (2010). Binding of the receptor tyrosine kinase TrkB to the neural cell adhesion molecule (NCAM) regulates phosphorylation of NCAM and NCAM-dependent neurite outgrowth. J Biol Chem 285(37):28959-67.

Chipman PH, Franz CK, Nelson A, Schachner M, Rafuse VF (2010). Neural cell adhesion molecule is required for stability of reinnervated neuromuscular junctions. Eur J Neurosci 31(2):238-49.

Christensen C, Lauridsen JB, Berezin V, Bock E, Kiselyov VV (2006). The neural cell adhesion molecule binds to fibroblast growth factor receptor 2. FEBS Lett 12;580(14):3386-90.

Close BE, Colley KJ (1998). In vivo autopolysialylation and localization of the polysialyltransferases PST and STX. J Biol Chem 273(51):34586-93.

Cole GJ, Akeson R (1989). Identification of a heparin binding domain of the neural cell adhesion molecule N-CAM using synthetic peptides. Neuron 2(2):1157-65.

Cole GJ, Glaser L (1986a). A heparin-binding domain from N-CAM is involved in neural cell-substratum adhesion. J Cell Biol 102(2):403-12.

Cole GJ, Loewy A, Cross NV, Akeson R, Glaser L (1986b). Topographic localization of the heparin-binding domain of the neural cell adhesion molecule N-CAM. J Cell Biol 103(5):1739-44.

Cremer H, Lange R, Christoph A, Plomann M, Vopper G, Roes J, Brown R, Baldwin S, Kraemer P, Scheff S, *et al.* (1994). Inactivation of the N-CAM gene in mice results in size reduction of the olfactory bulb and deficits in spatial learning. Nature 367(6462):455-9.

Cunningham BA, Hemperly JJ, Murray BA, Prediger EA, Brackenbury R, Edelman GM (1987). Neural cell adhesion molecule: structure, immunoglobulin-like domains, cell surface modulation, and alternative RNA splicing. Science 236(4803):799-806.

Curreli S, Arany Z, Gerardy-Schahn R, Mann D, Stamatou NM (2007). Polysialylated neuropilin-2 is expressed on the surface of human dendritic cells and modulates dendritic cell-T lymphocyte interactions. J Biol Chem 282(42):30346-56.

Dedman AM, Majeed Y, Tumova S, Zeng F, Kumar B, Munsch C, Bateson AN, Wittmann J, Jäck HM, Porter KE, Beech DJn (2011). TRPC1 transcript variants, inefficient nonsense-mediated decay and low up-frameshift-1 in vascular smooth muscle cells. BMC Mol Biol 12:30.

D'Eustachio P, Owens GC, Edelman GM, Cunningham BA (1985). Chromosomal location of the gene encoding the neural cell adhesion molecule (N-CAM) in the mouse. Proc Natl Acad Sci U S A 82(22):7631-5.

Literature

- Durbec P, Cremer H (2001). Revisiting the function of PSA-NCAM in the nervous system. *Mol Neurobiol* 24(1-3):53-64.
- Diestel S, Schaefer D, Cremer H, Schmitz B (2007). NCAM is ubiquitylated, endocytosed and recycled in neurons. *J Cell Sci* 120(Pt 22):4035-49.
- Diestel S, Hinkle CL, Schmitz B, Maness PF (2005). NCAM140 stimulates integrin-dependent cell migration by ectodomain shedding. *J Neurochem* 95(6):1777-84.
- Diestel S, Laurini C, Traub O, Schmitz B (2004). Tyrosine 734 of NCAM180 interferes with FGF receptor-dependent signaling implicated in neurite growth. *Biochem Biophys Res Commun* 10;322(1):186-96.
- Ditlevsen DK, Kolkova K (2010). Signaling pathways involved in NCAM-induced neurite outgrowth. *Adv Exp Med Biol* 663:151-68.
- Dityatev A, Dityateva G, Sytnyk V, Delling M, Toni N, Nikonenko I, Muller D, Schachner M (2004). Polysialylated neural cell adhesion molecule promotes remodeling and formation of hippocampal synapses. *J Neurosci* 20;24(42):9372-82.
- Doenecke D, Albig W, Bode C, Drabent B, Franke K, Gavenis K, Witt O (1997). Histones: genetic diversity and tissue-specific gene expression. *Histochem Cell Biol* 107(1):1-10.
- Downward J (1996). Control of ras activation. *Cancer Surv.* 27:87-100.
- Engelke M, Friedrich O, Budde P, Schäfer C, Niemann U, Zitt C, Jüngling E, Rocks O, Lückhoff A, Frey J (2002). Structural domains required for channel function of the mouse transient receptor potential protein homologue TRP1beta. *FEBS Lett* 523(1-3):193-9.
- Euteneuer S, Yang KH, Chavez E, Leichtle A, Loers G, Olshansky A, Pak K, Schachner M, Ryan AF (2012). Glial cell line-derived neurotrophic factor (GDNF) induces neuritogenesis in the cochlear spiral ganglion via neural cell adhesion molecule (NCAM). *Mol Cell Neurosci* 20. pii: S1044-7431(12)00214-X..
- Evans SV, Sigurskjold BW, Jennings HJ, Brisson JR, To R, Tse WC, Altman E, Frosch M, Weisgerber C, Kratzin HD, *et al.* (1995). Evidence for the extended helical nature of polysaccharide epitopes. The 2.8 Å resolution structure and thermodynamics of ligand binding of an antigen binding fragment specific for alpha-(2-->8)-polysialic acid. *Biochemistry* 34(20):6737-44.
- Faber ES, Sedlak P, Vidovic M, Sah P (2006). Synaptic activation of transient receptor potential channels by metabotropic glutamate receptors in the lateral amygdala. *Neuroscience* 137(3):781-94.
- Farag SS, Caligiuri MA (2006). Human natural killer cell development and biology. *Blood Rev* 20(3):123-37.
- Fidziańska A, Kamińska A (1995). Neural cell adhesion molecule (N-CAM) as a marker of muscle tissue alternations. Review of the literature and own observations. *Folia Neuropathol* 33(3):125-8.

Literature

- Filiz S, Dalcik H, Yardimoglu M, Gonca S, Ceylan S (2002). Localization of neural cell adhesion molecule (N-CAM) immunoreactivity in adult rat tissues. *Biotech Histochem* 77(3):127-35.
- Finne J, Finne U, Deagostini-Bazin H, Goridis C (1983). Occurrence of alpha 2-8 linked polysialosyl units in a neural cell adhesion molecule. *Biochem Biophys Res Commun* 29;112(2):482-7.
- Fiorio Pla A, Maric D, Brazer SC, Giacobini P, Liu X, Chang YH, Ambudkar IS, Barker JL (2005). Canonical transient receptor potential 1 plays a role in basic fibroblast growth factor (bFGF)/FGF receptor-1-induced Ca²⁺ entry and embryonic rat neural stem cell proliferation. *J Neurosci* 25(10):2687-701.
- Fowler MA, Sidiropoulou K, Ozkan ED, Phillips CW, Cooper DC (2007). Corticolimbic expression of TRPC4 and TRPC5 channels in the rodent brain. *PLoS One* 2(6):e573.
- Fraser DD, MacVicar BA (1996). Cholinergic-dependent plateau potential in hippocampal CA1 pyramidal neurons. *J Neurosci* 16(13):4113-28.
- Frosch M, Görgen I, Boulnois GJ, Timmis KN, Bitter-Suermann D (1985). NZB mouse system for production of monoclonal antibodies to weak bacterial antigens: isolation of an IgG antibody to the polysaccharide capsules of *Escherichia coli* K1 and group B meningococci. *Proc Natl Acad Sci U S A* 82(4):1194-8.
- Fujimoto I, Bruses JL, Rutishauser U (2001). Regulation of cell adhesion by polysialic acid. Effects on cadherin, immunoglobulin cell adhesion molecule, and integrin function and independence from neural cell adhesion molecule binding or signaling activity. *J Biol Chem* 276(34):31745-51.
- Galuska SP, Rollenhagen M, Kaup M, Eggers K, Oltmann-Norden I, Schiff M, Hartmann M, Weinhold B, Hildebrandt H, Geyer R, Mühlhoff M, Geyer H (2010). Synaptic cell adhesion molecule SynCAM 1 is a target for polysialylation in postnatal mouse brain. *Proc Natl Acad Sci U S A* 107(22):10250-5.
- Gambhir A, Hangyás-Mihályné G, Zaitseva I, Cafiso DS, Wang J, Murray D, Pentylala SN, Smith SO, McLaughlin S (2004). Electrostatic sequestration of PIP₂ on phospholipid membranes by basic/aromatic regions of proteins. *Biophys J* 86(4):2188-207.
- Gennarini G, Rougon G, Deagostini-Bazin H, Hirn M, Goridis C (1984). Studies on the transmembrane disposition of the neural cell adhesion molecule N-CAM. A monoclonal antibody recognizing a cytoplasmic domain and evidence for the presence of phosphoserine residues. *Eur J Biochem* 142(1):57-64.
- Gerardy-Schahn R, Bethe A, Brennecke T, Mühlhoff M, Eckhardt M, Ziesing S, Lottspeich F, Frosch M (1995). Molecular cloning and functional expression of bacteriophage PK1E-encoded endoneuraminidase Endo NE. *Mol Microbiol.* 1995 May;16(3):441-50.
- Glüer S, Schelp C, Madry N, von Schweinitz D, Eckhardt M, Gerardy-Schahn R (1998). Serum polysialylated neural cell adhesion molecule in childhood neuroblastoma. *Br J Cancer* 78(1):106-10.

Literature

- Gower HJ, Barton CH, Elsom VL, Thompson J, Moore SE, Dickson G, Walsh FS (1988). Alternative splicing generates a secreted form of N-CAM in muscle and brain. *Cell* 23;55(6):955-64.
- Greka A, Navarro B, Oancea E, Duggan A, Clapham DE (2003). TRPC5 is a regulator of hippocampal neurite length and growth cone morphology. *Nat Neurosci* 6(8):837-45.
- Grumet M, Flaccus A, Margolis RU (1993). Functional characterization of chondroitin sulfate proteoglycans of brain: interactions with neurons and neural cell adhesion molecules. *J Cell Biol* 120(3):815-24.
- Gumbiner BM (1996). Cell adhesion: The molecular basis of tissue architecture and morphogenesis. *Cell* 84:345–357.
- Guo JU, Su Y, Zhong C, Ming GL, Song H (2011). Hydroxylation of 5-methylcytosine by TET1 promotes active DNA demethylation in the adult brain. *Cell* 29;145(3):423-34.
- Hannan MA, Kabbani N, Paspalas CD, Levenson R (2008). Interaction with dopamine D2 receptor enhances expression of transient receptor potential channel 1 at the cell surface. *Biochim Biophys Acta* 1778(4):974-82.
- Hardie RC, Minke B (1992). The *trp* gene is essential for a light-activated Ca²⁺ channel in *Drosophila* photoreceptors. *Neuron* 8(4):643-51.
- Hartwig JH, Thelen M, Rosen A, Janmey PA, Nairn AC, Aderem A (1992). MARCKS is an actin filament crosslinking protein regulated by protein kinase C and calcium-calmodulin. *Nature* 16;356(6370):618-22.
- He YF, Li BZ, Li Z, Liu P, Wang Y, Tang Q, Ding J, Jia Y, Chen Z, Li L, Sun Y, Li X, Dai Q, Song CX, Zhang K, He C, Xu GL (2011). Tet-mediated formation of 5-carboxylcytosine and its excision by TDG in mammalian DNA. *Science*. 333(6047):1303-7.
- Hildebrandt H, Becker C, Mürau M, Gerardy-Schahn R, Rahmann H (1998). Heterogeneous expression of the polysialyltransferases ST8Sia II and ST8Sia IV during postnatal rat brain development. *J Neurochem* 71(6):2339-48.
- Hinsby AM, Berezin V, Bock E (2004). Molecular mechanisms of NCAM function. *Front Biosci* 9:2227-44.
- Hofmann T, Schaefer M, Schultz G, Gudermann T (2002). Subunit composition of mammalian transient receptor potential channels in living cells. *Proc Natl Acad Sci U S A* 99(11):7461-6.
- Hofmann T, Obukhov AG, Schaefer M, Harteneck C, Gudermann T, Schultz G (1999). Direct activation of human TRPC6 and TRPC3 channels by diacylglycerol. *Nature* 397(6716):259-63.
- Horstkorte R, Schachner M, Magyar JP, Vorherr T, Schmitz B (1993). The fourth immunoglobulin-like domain of NCAM contains a carbohydrate recognition domain for oligomannosidic glycans implicated in association with L1 and neurite outgrowth. *J Cell Biol* 121(6):1409-21.

Literature

Irier HA, Jin P (2012). Dynamics of DNA methylation in aging and Alzheimer's disease. *DNA Cell Biol* 31 Suppl 1:S42-8.

Ito S, Shen L, Dai Q, Wu SC, Collins LB, Swenberg JA, He C, Zhang Y (2011). Tet proteins can convert 5-methylcytosine to 5-formylcytosine and 5-carboxylcytosine. *Science* 333(6047):1300-3.

Janas T, Janas T, Krajiński H (2000). Membrane transport of polysialic acid chains: modulation of transmembrane potential. *Eur Biophys J* 29(7):507-14.

Janas T, Krajiński H, Timoszyk A, Janas T (2001). Translocation of polysialic acid across model membranes: kinetic analysis and dynamic studies. *Acta Biochim Pol* 48(1):163-73.

Janas T, Nowotarski K, Janas T (2010). Polysialic acid can mediate membrane interactions by interacting with phospholipids. *Chem Phys Lipids* 163(3):286-91.

Jessen U, Novitskaya V, Pedersen N, Serup P, Berezin V, Bock E (2001). The transcription factors CREB and c-Fos play key roles in NCAM-mediated neuritogenesis in PC12-E2 cells. *J Neurochem* 79(6):1149-60.

Johnson CP, Fragneto G, Konovalov O, Dubosclard V, Legrand JF, Leckband DE (2005a). Structural studies of the neural-cell-adhesion molecule by X-ray and neutron reflectivity. *Biochemistry* 44(2):546-54.

Johnson CP, Fujimoto I, Rutishauser U, Leckband DE (2005b). Direct evidence that neural cell adhesion molecule (NCAM) polysialylation increases intermembrane repulsion and abrogates adhesion. *J Biol Chem* 280(1):137-45.

Kalus I, Bormann U, Mzoughi M, Schachner M, Kleene R (2006). Proteolytic cleavage of the neural cell adhesion molecule by ADAM17/TACE is involved in neurite outgrowth. *J Neurochem* 98(1):78-88.

Kanato Y, Kitajima K, Sato C (2008). Direct binding of polysialic acid to a brain-derived neurotrophic factor depends on the degree of polymerization. *Glycobiology* 18(12):1044-53.

Klinz SG, Schachner M, Maness PF (1995). L1 and N-CAM antibodies trigger protein phosphatase activity in growth cone-enriched membranes. *J Neurochem* 65(1):84-95.

Kiryushko D, Korshunova I, Berezin V, Bock E (2006). Neural cell adhesion molecule induces intracellular signaling via multiple mechanisms of Ca²⁺ homeostasis. *Mol Biol Cell* 17(5):2278-86.

Kiselyov VV, Skladchikova G, Hinsby AM, Jensen PH, Kulahin N, Soroka V, Pedersen N, Tsetlin V, Poulsen FM, Berezin V, Bock E (2003). Structural basis for a direct interaction between FGFR1 and NCAM and evidence for a regulatory role of ATP. *Structure* 11(6):691-701.

Kleene R, Cassens C, Bähring R, Theis T, Xiao MF, Dityatev A, Schafer-Nielsen C, Döring F, Wischmeyer E, Schachner M (2010a). Functional consequences of the interactions among the neural cell adhesion molecule NCAM, the receptor tyrosine kinase TrkB, and the inwardly rectifying K⁺ channel KIR3.3. *J Biol Chem* 10;285(37):28968-79.

Literature

- Kleene R, Mzoughi M, Joshi G, Kalus I, Bormann U, Schulze C, Xiao MF, Dityatev A, Schachner M (2010b). NCAM-induced neurite outgrowth depends on binding of calmodulin to NCAM and on nuclear import of NCAM and fak fragments. *J Neurosci* 11;30(32):10784-98.
- Kleene R, Schachner M (2004). Glycans and neural cell interactions. *Nat Rev Neurosci* 5(3):195-208.
- Kochlamazashvili G, Senkov O, Grebenyuk S, Robinson C, Xiao MF, Stummeyer K, Gerardy-Schahn R, Engel AK, Feig L, Semyanov A, Suppiramaniam V, Schachner M, Dityatev A (2010). Neural cell adhesion molecule-associated polysialic acid regulates synaptic plasticity and learning by restraining the signaling through GluN2B-containing NMDA receptors. *J Neurosci* 30(11):4171-83.
- Kochlamazashvili G, Bukalo O, Senkov O, Salmen B, Gerardy-Schahn R, Engel AK, Schachner M, Dityatev A (2012). Restoration of synaptic plasticity and learning in young and aged NCAM-deficient mice by enhancing neurotransmission mediated by GluN2A-containing NMDA receptors. *J Neurosci* 32(7):2263-75.
- Kolkova K (2010). Biosynthesis of NCAM. *Adv Exp Med Biol* 663:213-25.
- Kolkova K, Novitskaya V, Pedersen N, Berezin V, Bock E (2000). Neural cell adhesion molecule-stimulated neurite outgrowth depends on activation of protein kinase C and the Ras-mitogen-activated protein kinase pathway. *J Neurosci* 20(6):2238-46.
- Komminoth P, Roth J, Saremaslani P, Matias-Guiu X, Wolfe HJ, Heitz PU (1994). Polysialic acid of the neural cell adhesion molecule in the human thyroid: a marker for medullary thyroid carcinoma and primary C-cell hyperplasia. An immunohistochemical study on 79 thyroid lesions. *Am J Surg Pathol* 18(4):399-411.
- Koutsoudaki PN, Hildebrandt H, Gudi V, Skripuletz T, Škuljec J, Stangel M (2010). Remyelination after cuprizone induced demyelination is accelerated in mice deficient in the polysialic acid synthesizing enzyme St8sialV. *Neuroscience* 171(1):235-44.
- Krog L, Bock E (1992). Glycosylation of neural cell adhesion molecules of the immunoglobulin superfamily. *APMIS Suppl* 27:53-70.
- Krushel LA, Sporns O, Cunningham BA, Crossin KL, Edelman GM (1995). Neural cell adhesion molecule (N-CAM) inhibits astrocyte proliferation after injury to different regions of the adult rat brain. *Proc Natl Acad Sci U S A* 92(10):4323-7.
- Kruse J, Mailhammer R, Wernecke H, Faissner A, Sommer I, Goridis C, Schachner M (1984). Neural cell adhesion molecules and myelin-associated glycoprotein share a common carbohydrate moiety recognized by monoclonal antibodies L2 and HNK-1. *Nature* 13-19;311(5982):153-5.
- Kuzmiski JB, MacVicar BA (2001). Cyclic nucleotide-gated channels contribute to the cholinergic plateau potential in hippocampal CA1 pyramidal neurons. *J Neurosci* 21(22):8707-14.

Literature

- Kwan HY, Shen B, Ma X, Kwok YC, Huang Y, Man YB, Yu S, Yao X (2009). TRPC1 associates with BK(Ca) channel to form a signal complex in vascular smooth muscle cells. *Circ Res* 104(5):670-8.
- Kwiatkowska K (2010). One lipid, multiple functions: how various pools of PI(4,5)P(2) are created in the plasma membrane. *Cell Mol Life Sci* 67(23):3927-46.
- Lantuejoul S, Moro D, Michalides RJ, Brambilla C, Brambilla E (1998). Neural cell adhesion molecules (NCAM) and NCAM-PSA expression in neuroendocrine lung tumors. *Am J Surg Pathol* 22(10):1267-76.
- Latorre R, Zaelzer C, Brauchi S (2009). Structure-functional intimacies of transient receptor potential channels. *Q Rev Biophys* 42(3):201-46.
- Laux T, Fukami K, Thelen M, Golub T, Frey D, Caroni P (2000). GAP43, MARCKS, and CAP23 modulate PI(4,5)P(2) at plasmalemmal rafts, and regulate cell cortex actin dynamics through a common mechanism. *J Cell Biol* 149(7):1455-72.
- Lee YM, Kim BJ, Kim HJ, Yang DK, Zhu MH, Lee KP, So I, Kim KW (2003). TRPC5 as a candidate for the nonselective cation channel activated by muscarinic stimulation in murine stomach. *Am J Physiol Gastrointest Liver Physiol* 284(4):G604-16.
- Lepage PK, Lussier MP, Barajas-Martinez H, Bousquet SM, Blanchard AP, Francoeur N, Dumaine R, Boulay G (2006). Identification of two domains involved in the assembly of transient receptor potential canonical channels. *J Biol Chem* 281(41):30356-64.
- Leshchyns'ka I, Sytnyk V, Morrow JS, Schachner M (2003). Neural cell adhesion molecule (NCAM) association with PKCbeta2 via beta1 spectrin is implicated in NCAM-mediated neurite outgrowth. *J Cell Biol* 161(3):625-39.
- Leshchyns'ka I, Tanaka MM, Schachner M, Sytnyk V (2011). Immobilized pool of NCAM180 in the postsynaptic membrane is homeostatically replenished by the flux of NCAM180 from extrasynaptic regions. *J Biol Chem* 286(26):23397-406.
- Li HS, Xu XZ, Montell C (1999). Activation of a TRPC3-dependent cation current through the neurotrophin BDNF. *Neuron* 24(1):261-73.
- Liao Y, Erxleben C, Abramowitz J, Flockerzi V, Zhu MX, Armstrong DL, Birnbaumer L. (2008). Functional interactions among Orai1, TRPCs, and STIM1 suggest a STIM-regulated heteromeric Orai/TRPC model for SOCE/Icrac channels. *Proc Natl Acad Sci U S A* 105(8):2895-900.
- Liao Y, Erxleben C, Yildirim E, Abramowitz J, Armstrong DL, Birnbaumer L. (2007). Orai proteins interact with TRPC channels and confer responsiveness to store depletion. *Proc Natl Acad Sci U S A* 104(11):4682-7.
- Liman ER, Innan H (2003). Relaxed selective pressure on an essential component of pheromone transduction in primate evolution. *Proc Natl Acad Sci U S A* 100(6):3328-32.
- Lintschinger B, Balzer-Geldsetzer M, Baskaran T, Graier WF, Romanin C, Zhu MX, Groschner K (2000). Coassembly of Trp1 and Trp3 proteins generates diacylglycerol- and Ca²⁺-sensitive cation channels. *J Biol Chem* 275(36):27799-805.

Literature

- Little EB, Edelman GM, Cunningham BA (1998). Palmitoylation of the cytoplasmic domain of the neural cell adhesion molecule N-CAM serves as an anchor to cellular membranes. *Cell Adhes Commun* 6(5):415-30.
- Liu X, Bandyopadhyay BC, Singh BB, Groschner K, Ambudkar IS (2005). Molecular analysis of a store-operated and 2-acetyl-sn-glycerol-sensitive non-selective cation channel. Heteromeric assembly of TRPC1-TRPC3. *J Biol Chem* 280(22):21600-6.
- Liu X, Singh BB, Ambudkar IS (2003). TRPC1 is required for functional store-operated Ca²⁺ channels. Role of acidic amino acid residues in the S5-S6 region. *J Biol Chem* 278(13):11337-43.
- Lobaugh LA, Blackshear PJ (1990). Neuropeptide Y stimulation of myosin light chain phosphorylation in cultured aortic smooth muscle cells. *J Biol Chem* 265(30):18393-9.
- Lodén M, van Steensel B (2005). Whole-genome views of chromatin structure. *Chromosome Res.* 2005;13(3):289-98.
- Loers G, Schachner M (2007). Recognition molecules and neural repair. *J Neurochem* 101(4):865-82.
- Lyles JM, Amin W, Bock E, Weill CL (1993). Regulation of NCAM by growth factors in serum-free myotube cultures. *J Neurosci Res* 15;34(3):273-86.
- Lyles JM, Linnemann D, Bock E (1984). Biosynthesis of the D2-cell adhesion molecule: post-translational modifications, intracellular transport, and developmental changes. *J Cell Biol* 99(6):2082-91.
- Malarkey EB, Ni Y, Parpura V (2008). Ca²⁺ entry through TRPC1 channels contributes to intracellular Ca²⁺ dynamics and consequent glutamate release from rat astrocytes. *Glia* 56(8):821-35.
- Marder E (1991). Plateaus in time. *Curr Biol* 1(5):326-7.
- McNamara RK, Stumpo DJ, Morel LM, Lewis MH, Wakeland EK, Blackshear PJ, Lenox RH (1998). Effect of reduced myristoylated alanine-rich C kinase substrate expression on hippocampal mossy fiber development and spatial learning in mutant mice: transgenic rescue and interactions with gene background. *Proc Natl Acad Sci U S A* 95(24):14517-22.
- Mendiratta SS, Sekulic N, Hernandez-Guzman FG, Close BE, Lavie A, Colley KJ (2006). A novel alpha-helix in the first fibronectin type III repeat of the neural cell adhesion molecule is critical for N-glycan polysialylation. *J Biol Chem* 281(47):36052-9.
- Mery L, Strauss B, Dufour JF, Krause KH, Hoth M (2002). The PDZ-interacting domain of TRPC4 controls its localization and surface expression in HEK293 cells. *J Cell Sci* 115(Pt 17):3497-508.
- Mery L, Magnino F, Schmidt K, Krause KH, Dufour JF (2001). Alternative splice variants of hTrp4 differentially interact with the C-terminal portion of the inositol 1,4,5-trisphosphate receptors. *FEBS Lett* 5;487(3):377-83.

Literature

- Milev P, Friedlander DR, Sakurai T, Karthikeyan L, Flad M, Margolis RK, Grumet M, Margolis RU (1994). Interactions of the chondroitin sulfate proteoglycan phosphacan, the extracellular domain of a receptor-type protein tyrosine phosphatase, with neurons, glia, and neural cell adhesion molecules. *J Cell Biol* 127(6 Pt 1):1703-15.
- Mio K, Ogura T, Hara Y, Mori Y, Sato C (2005). The non-selective cation-permeable channel TRPC3 is a tetrahedron with a cap on the large cytoplasmic end. *Biochem Biophys Res Commun* 333(3):768-77.
- Miragall F, Kadmon G, Husmann M, Schachner M (1988). Expression of cell adhesion molecules in the olfactory system of the adult mouse: presence of the embryonic form of N-CAM. *Dev Biol* 129(2):516-31.
- Mishra B, von der Ohe M, Schulze C, Bian S, Makhina T, Loers G, Kleene R, Schachner M (2010). Functional role of the interaction between polysialic acid and extracellular histone H1. *J Neurosci* 30(37):12400-13.
- Muller D, Wang C, Skibo G, Toni N, Cremer H, Calaora V, Rougon G, Kiss JZ (1996). PSA-NCAM is required for activity-induced synaptic plasticity. *Neuron* 17(3):413-22.
- Munsch T, Freichel M, Flockerzi V, Pape HC (2003). Contribution of transient receptor potential channels to the control of GABA release from dendrites. *Proc Natl Acad Sci U S A* 100(26):16065-70.
- Murray D, Ben-Tal N, Honig B, McLaughlin S (1997). Electrostatic interaction of myristoylated proteins with membranes: simple physics, complicated biology. *Structure* 5(8):985-9.
- Mühlenhoff M, Eckhardt M, Gerardy-Schahn R (1998). Polysialic acid: three-dimensional structure, biosynthesis and function. *Curr Opin Struct Biol* 8(5):558-64.
- Mosavi LK, Cammett TJ, Desrosiers DC, Peng ZY (2004). The ankyrin repeat as molecular architecture for protein recognition. *Protein Sci* 13(6):1435-48.
- Nakayama J, Angata K, Ong E, Katsuyama T, Fukuda M (1998). Polysialic acid, a unique glycan that is developmentally regulated by two polysialyltransferases, PST and STX, in the central nervous system: from biosynthesis to function. *Pathol Int* 48(9):665-77.
- Nelson RW, Bates PA, Rutishauser U (1995). Protein determinants for specific polysialylation of the neural cell adhesion molecule. *J Biol Chem* 270(29):17171-9.
- Newton AC, Johnson JE (1998). Protein kinase C: a paradigm for regulation of protein function by two membrane-targeting modules. *Biochim Biophys Acta* 1376(2):155-72.
- Nguyen C, Mattei MG, Mattei JF, Santoni MJ, Goridis C, Jordan BR (1986). Localization of the human NCAM gene to band q23 of chromosome 11: the third gene coding for a cell interaction molecule mapped to the distal portion of the long arm of chromosome 11. *J Cell Biol* 102(3):711-5.
- Niethammer P, Delling M, Sytnyk V, Dityatev A, Fukami K, Schachner M (2002). Cosignaling of NCAM via lipid rafts and the FGF receptor is required for neurite outgrowth. *J Cell Biol* 157(3):521-32.

Literature

- Ohmori S, Sakai N, Shirai Y, Yamamoto H, Miyamoto E, Shimizu N, Saito N (2000). Importance of protein kinase C targeting for the phosphorylation of its substrate, myristoylated alanine-rich C-kinase substrate. *J Biol Chem* 275(34):26449-57.
- Oltmann-Norden I, Galuska SP, Hildebrandt H, Geyer R, Gerardy-Schahn R, Geyer H, Mühlenhoff M (2008). Impact of the polysialyltransferases ST8SialI and ST8SialIV on polysialic acid synthesis during postnatal mouse brain development. *J Biol Chem* 283(3):1463-71.
- Ono K, Tomasiewicz H, Magnuson T, Rutishauser U (1994). N-CAM mutation inhibits tangential neuronal migration and is phenocopied by enzymatic removal of polysialic acid. *Neuron* 13(3):595-609.
- Ono S, Hane M, Kitajima K, Sato C (2012). Novel regulation of fibroblast growth factor 2 (FGF2)-mediated cell growth by polysialic acid. *J Biol Chem* 287(6):3710-22.
- Quimet CC, Wang JK, Walaas SI, Albert KA, Greengard P (1990). Localization of the MARCKS (87 kDa) protein, a major specific substrate for protein kinase C, in rat brain. *J Neurosci* 10(5):1683-98.
- Owens GC, Edelman GM, Cunningham BA (1987). Organization of the neural cell adhesion molecule (N-CAM) gene: alternative exon usage as the basis for different membrane-associated domains. *Proc Natl Acad Sci U S A* 84(1):294-8.
- Paratcha G, Ledda F, Ibáñez CF (2003). The neural cell adhesion molecule NCAM is an alternative signaling receptor for GDNF family ligands. *Cell* 113(7):867-79.
- Papastefanaki F, Chen J, Lavdas AA, Thomaidou D, Schachner M, Matsas R (2007). Grafts of Schwann cells engineered to express PSA-NCAM promote functional recovery after spinal cord injury. *Brain* 130(Pt 8):2159-74.
- Plappert CF, Schachner M, Pilz PK (2006). Neural cell adhesion molecule (NCAM^{-/-}) null mice show impaired sensitization of the startle response. *Genes Brain Behav* 5(1):46-52.
- Plattner H, Kissmehl R (2005). Molecular aspects of rapid, reversible, Ca²⁺-dependent dephosphorylation of pp63/parafusin during stimulated exo-endocytosis in Paramecium cells. *Cell Calcium* 38(3-4):319-27.
- Pollerberg GE, Burridge K, Krebs KE, Goodman SR, Schachner M (1987). The 180-kD component of the neural cell adhesion molecule N-CAM is involved in cell-cell contacts and cytoskeleton-membrane interactions. *Cell Tissue Res* 250(1):227-36.
- Pollerberg GE, Schachner M, Davoust J (1986). Differentiation state-dependent surface mobilities of two forms of the neural cell adhesion molecule. *Nature* 324(6096):462-5.
- Porumb T, Crivici A, Blackshear PJ, Ikura M (1997). Calcium binding and conformational properties of calmodulin complexed with peptides derived from myristoylated alanine-rich C kinase substrate (MARCKS) and MARCKS-related protein (MRP). *Eur Biophys J* 25(4):239-47.

Literature

Poteser M, Graziani A, Rosker C, Eder P, Derler I, Kahr H, Zhu MX, Romanin C, Groschner K (2006). TRPC3 and TRPC4 associate to form a redox-sensitive cation channel. Evidence for expression of native TRPC3-TRPC4 heteromeric channels in endothelial cells. *J Biol Chem* 281(19):13588-95.

Probstmeier R, Bilz A, Schneider-Schaulies J (1994). Expression of the neural cell adhesion molecule and polysialic acid during early mouse embryogenesis. *J Neurosci Res* 37(3):324-35.

Qin Z, Cafiso DS (1996). Membrane structure of protein kinase C and calmodulin binding domain of myristoylated alanine rich C kinase substrate determined by site-directed spin labeling. *Biochemistry* 35(9):2917-25.

Reyes AA, Small SJ, Akeson R (1991). At least 27 alternatively spliced forms of the neural cell adhesion molecule mRNA are expressed during rat heart development. *Mol Cell Biol* 11(3):1654-61.

Rønn LC, Doherty P, Holm A, Berezin V, Bock E (2000). Neurite outgrowth induced by a synthetic peptide ligand of neural cell adhesion molecule requires fibroblast growth factor receptor activation. *J Neurochem* 75(2):665-71.

Rosen A, Keenan KF, Thelen M, Nairn AC, Aderem A (1990). Activation of protein kinase C results in the displacement of its myristoylated, alanine-rich substrate from punctate structures in macrophage filopodia. *J Exp Med* 172(4):1211-5.

Rottach A, Leonhardt H, Spada F (2009). DNA methylation-mediated epigenetic control. *J Cell Biochem* 110(1):43-51.

Rutishauser U, Thiery JP, Brackenbury R, Sela BA, Edelman GM (1976). Mechanisms of adhesion among cells from neural tissues of the chick embryo. *Proc Natl Acad Sci U S A* 73(2):577-81.

Sadoul K, Meyer A, Low MG, Schachner M (1986). Release of the 120 kDa component of the mouse neural cell adhesion molecule N-CAM from cell surfaces by phosphatidylinositol-specific phospholipase C. *Neurosci Lett* 23;72(3):341-6.

Saimi Y, Kung C (2002). Calmodulin as an ion channel subunit. *Annu Rev Physiol* 64:289-311.

Salido GM, Sage SO, Rosado JA (2009). TRPC channels and store-operated Ca²⁺ entry. *Biochim Biophys Acta* 1793(2):223-30.

Sanes JR, Schachner M, Covault J (1986). Expression of several adhesive macromolecules (N-CAM, L1, J1, NILE, uvomorulin, laminin, fibronectin, and a heparan sulfate proteoglycan) in embryonic, adult, and denervated adult skeletal muscle. *J Cell Biol* 102(2):420-31.

Sanchez-Heras E, Howell FV, Williams G, Doherty P (2006). The fibroblast growth factor receptor acid box is essential for interactions with N-cadherin and all of the major isoforms of neural cell adhesion molecule. *J Biol Chem* 281(46):35208-16.

Literature

- Santuccione A, Sytnyk V, Leshchyns'ka I, Schachner M (2005). Prion protein recruits its neuronal receptor NCAM to lipid rafts to activate p59fyn and to enhance neurite outgrowth. *J Cell Biol* 25;169(2):341-54.
- Sasaki H, Yoshida K, Ikeda E, Asou H, Inaba M, Otani M, Kawase T (1998). Expression of the neural cell adhesion molecule in astrocytic tumors: an inverse correlation with malignancy. *Cancer* 15;82(10):1921-31.
- Schachner M (1997). Neural recognition molecules and synaptic plasticity. *Curr Opin Cell Biol*. 1997 Oct;9(5):627-34.
- Schaefer M, Plant TD, Obukhov AG, Hofmann T, Gudermann T, Schultz G. (2000). Receptor-mediated regulation of the nonselective cation channels TRPC4 and TRPC5. *J Biol Chem*. 2000 Jun 9;275(23):17517-26.
- Schlosshauer B (1989). Purification of neuronal cell surface proteins and generation of epitope-specific monoclonal antibodies against cell adhesion molecules. *J Neurochem* 52(1):82-92.
- Schmid RS, Graff RD, Schaller MD, Chen S, Schachner M, Hemperly JJ, Maness PF (1999). NCAM stimulates the Ras-MAPK pathway and CREB phosphorylation in neuronal cells. *J Neurobiol* 38(4):542-58.
- Schmitt-Ulms G, Legname G, Baldwin MA, Ball HL, Bradon N, Bosque PJ, Crossin KL, Edelman GM, DeArmond SJ, Cohen FE, Prusiner SB (2001). Binding of neural cell adhesion molecules (N-CAMs) to the cellular prion protein. *J Mol Biol* 14;314(5):1209-25.
- Schuch U, Lohse MJ, Schachner M (1989). Neural cell adhesion molecules influence second messenger systems. *Neuron* 3(1):13-20.
- Schuster T, Krug M, Stalder M, Hackel N, Gerardy-Schahn R, Schachner M (2001). Immunoelectron microscopic localization of the neural recognition molecules L1, NCAM, and its isoform NCAM180, the NCAM-associated polysialic acid, beta1 integrin and the extracellular matrix molecule tenascin-R in synapses of the adult rat hippocampus. *J Neurobiol* 49(2):142-58.
- Schwarz G, Droogmans G, Nilius B. (1994). Multiple effects of SK&F 96365 on ionic currents and intracellular calcium in human endothelial cells. *Cell Calcium*. 15(1):45-54.
- Seidenfaden R, Krauter A, Hildebrandt H (2006). The neural cell adhesion molecule NCAM regulates neuritogenesis by multiple mechanisms of interaction. *Neurochem Int* 49(1):1-11.
- Seki T, Arai Y (1991). Expression of highly polysialylated NCAM in the neocortex and piriform cortex of the developing and the adult rat. *Anat Embryol (Berl)* 184(4):395-401.
- Selvaraj S, Sun Y, Singh BB (2010). TRPC channels and their implication in neurological diseases. *CNS Neurol Disord Drug Targets* 9(1):94-104.
- Shim S, Goh EL, Ge S, Sailor K, Yuan JP, Roderick HL, Bootman MD, Worley PF, Song H, Ming GL (2005). XTRPC1-dependent chemotropic guidance of neuronal growth cones. *Nat Neurosci* 8(6):730-5.

Literature

- Singh BB, Liu X, Tang J, Zhu MX, Ambudkar IS (2002). Calmodulin regulates Ca(2+)-dependent feedback inhibition of store-operated Ca(2+) influx by interaction with a site in the C terminus of TrpC1. *Mol Cell* 9(4):739-50.
- Sorkin BC, Hoffman S, Edelman GM, Cunningham BA (1984). Sulfation and phosphorylation of the neural cell adhesion molecule, N-CAM. *Science* 225(4669):1476-8.
- Spizz G, Blackshear PJ (2001). Overexpression of the myristoylated alanine-rich C-kinase substrate inhibits cell adhesion to extracellular matrix components. *J Biol Chem* 276(34):32264-73.
- Stork O, Welzl H, Wolfer D, Schuster T, Mantei N, Stork S, Hoyer D, Lipp H, Obata K, Schachner M (2000). Recovery of emotional behaviour in neural cell adhesion molecule (NCAM) null mutant mice through transgenic expression of NCAM180. *Eur J Neurosci* 12(9):3291-306.
- Stork O, Welzl H, Cremer H, Schachner M (1997). Increased intermale aggression and neuroendocrine response in mice deficient for the neural cell adhesion molecule (NCAM). *Eur J Neurosci* 9(6):1117-25.
- Stork O, Welzl H, Wotjak CT, Hoyer D, Delling M, Cremer H, Schachner M (1999). Anxiety and increased 5-HT1A receptor response in NCAM null mutant mice. *J Neurobiol.* 40(3):343-55.
- Strekalova H, Buhmann C, Kleene R, Eggers C, Saffell J, Hemperly J, Weiller C, Müller-Thomsen T, Schachner M (2006). Elevated levels of neural recognition molecule L1 in the cerebrospinal fluid of patients with Alzheimer disease and other dementia syndromes. *Neurobiol Aging* 27(1):1-9.
- Strübing C, Krapivinsky G, Krapivinsky L, Clapham DE (2003). Formation of novel TRPC channels by complex subunit interactions in embryonic brain. *J Biol Chem* 278(40):39014-9.
- Strübing C, Krapivinsky G, Krapivinsky L, Clapham DE (2001). TRPC1 and TRPC5 form a novel cation channel in mammalian brain. *Neuron* 29(3):645-55.
- Stumpo DJ, Bock CB, Tuttle JS, Blackshear PJ (1995). MARCKS deficiency in mice leads to abnormal brain development and perinatal death. *Proc Natl Acad Sci U S A* 92(4):944-8.
- Swierczynski SL, Blackshear PJ (1995). Membrane association of the myristoylated alanine-rich C kinase substrate (MARCKS) protein. Mutational analysis provides evidence for complex interactions. *J Biol Chem* 270(22):13436-45.
- Tahiliani M, Koh KP, Shen Y, Pastor WA, Bandukwala H, Brudno Y, Agarwal S, Iyer LM, Liu DR, Aravind L, Rao A (2009). Conversion of 5-methylcytosine to 5-hydroxymethylcytosine in mammalian DNA by MLL partner TET1. *Science* 324(5929):930-5.
- Tai C, Hines DJ, Choi HB, MacVicar BA (2011). Plasma membrane insertion of TRPC5 channels contributes to the cholinergic plateau potential in hippocampal CA1 pyramidal neurons. *Hippocampus* 21(9):958-67.

Literature

Takai Y, Sugawara R, Ohinata H, Takai A (2004). Two types of non-selective cation channel opened by muscarinic stimulation with carbachol in bovine ciliary muscle cells. *J Physiol* 559(Pt 3):899-922.

Takizawa T, Nakashima K, Namihira M, Ochiai W, Uemura A, Yanagisawa M, Fujita N, Nakao M, Taga T (2001). DNA methylation is a critical cell-intrinsic determinant of astrocyte differentiation in the fetal brain. *Dev Cell* 1(6):749-58.

Tang J, Lin Y, Zhang Z, Tikunova S, Birnbaumer L, Zhu MX (2001). Identification of common binding sites for calmodulin and inositol 1,4,5-trisphosphate receptors on the carboxyl termini of trp channels. *J Biol Chem* 276(24):21303-10.

Tereshchenko Y, Morellini F, Dityatev A, Schachner M, Irintchev A (2011). Neural cell adhesion molecule ablation in mice causes hippocampal dysplasia and loss of septal cholinergic neurons. *J Comp Neurol* 519(12):2475-92.

Theis T, Mishra B, von der Ohe M, Loers G, Prondzynski M, Pless O, Blackshear PJ, Schachner M, Kleene R (2013). Functional Role of the Interaction between Polysialic Acid and Myristoylated Alanine-rich C Kinase Substrate at the Plasma Membrane. *J Biol Chem* 288(9):6726-42.

Theodosius DT, Bonhomme R, Vitiello S, Rougon G, Poulain DA (1999). Cell surface expression of polysialic acid on NCAM is a prerequisite for activity-dependent morphological neuronal and glial plasticity. *J Neurosci* 19(23):10228-36.

Theodosius DT, Bonfanti L, Olive S, Rougon G, Poulain DA (1994). Adhesion molecules and structural plasticity of the adult hypothalamo-neurohypophysial system. *Psychoneuroendocrinology* 19(5-7):455-62.

Todaro L, Christiansen S, Varela M, Campodónico P, Pallotta MG, Lastiri J, Sacerdote de Lustig E, Bal de Kier Joffé E, Puricelli L (2007). Alteration of serum and tumoral neural cell adhesion molecule (NCAM) isoforms in patients with brain tumors. *J Neurooncol* 83(2):135-44.

Todaro L, Puricelli L, Gioseffi H, Guadalupe Pallotta M, Lastiri J, Bal de Kier Joffé E, Varela M, Sacerdote de Lustig E (2004). Neural cell adhesion molecule in human serum. Increased levels in dementia of the Alzheimer type. *Neurobiol Dis* 15(2):387-93.

Trost C, Bergs C, Himmerkus N, Flockerzi V (2001). The transient receptor potential, TRP4, cation channel is a novel member of the family of calmodulin binding proteins. *Biochem J* 355(Pt 3):663-70.

Varea E, Náchter J, Blasco-Ibáñez JM, Gómez-Climent MA, Castillo-Gómez E, Crespo C, Martínez-Guijarro FJ (2005). PSA-NCAM expression in the rat medial prefrontal cortex. *Neuroscience* 136(2):435-43.

Vawter MP (2000). Dysregulation of the neural cell adhesion molecule and neuropsychiatric disorders. *Eur J Pharmacol* 29;405(1-3):385-95.

Vazquez G, Wedel BJ, Aziz O, Trebak M, Putney JW Jr (2004). The mammalian TRPC cation channels. *Biochim Biophys Acta* 6;1742(1-3):21-36.

Literature

- Victor K, Jacob J, Cafiso DS (1999). Interactions controlling the membrane binding of basic protein domains: phenylalanine and the attachment of the myristoylated alanine-rich C-kinase substrate protein to interfaces. *Biochemistry* 38(39):12527-36.
- von der Ohe M, Wheeler SF, Wuhrer M, Harvey DJ, Liedtke S, Mühlenhoff M, Gerardy-Schahn R, Geyer H, Dwek RA, Geyer R, Wing DR, Schachner M (2002). Localization and characterization of polysialic acid-containing N-linked glycans from bovine NCAM. *Glycobiology* 12(1):47-63.
- Walsh FS, Parekh RB, Moore SE, Dickson G, Barton CH, Gower HJ, Dwek RA, Rademacher TW (1989). Tissue specific O-linked glycosylation of the neural cell adhesion molecule (N-CAM). *Development* 105(4):803-11.
- Wang M, Bianchi R, Chuang SC, Zhao W, Wong RK (2007). Group I metabotropic glutamate receptor-dependent TRPC channel trafficking in hippocampal neurons. *J Neurochem* 101(2):411-21.
- Wang GX, Poo MM (2005). Requirement of TRPC channels in netrin-1-induced chemotropic turning of nerve growth cones. *Nature* 434(7035):898-904.
- Weinreb PH, Zhen W, Poon AW, Conway KA, Lansbury PT Jr (1996). NACP, a protein implicated in Alzheimer's disease and learning, is natively unfolded. *Biochemistry* 35(43):13709-15.
- Wessel D, Flügge UI (1984). A method for the quantitative recovery of protein in dilute solution in the presence of detergents and lipids. *Analytical Biochemistry* 138; 141-143.
- Williams EJ, Mittal B, Walsh FS, Doherty P (1995). A Ca²⁺/calmodulin kinase inhibitor, KN-62, inhibits neurite outgrowth stimulated by CAMs and FGF. *Mol Cell Neurosci* 6(1):69-79.
- Williams EJ, Walsh FS, Doherty P (1994). The production of arachidonic acid can account for calcium channel activation in the second messenger pathway underlying neurite outgrowth stimulated by NCAM, N-cadherin, and L1. *J Neurochem* 62(3):1231-4.
- Wu D, Zhang Y, Bo X, Huang W, Xiao F, Zhang X, Miao T, Magoulas C, Subang MC, Richardson PM (2007). Actions of neurotrophic cytokines and cyclic AMP in regenerative conditioning of rat primary sensory neurons. *Exp Neurol* 204(1):66-76.
- Wu D, Huang W, Richardson PM, Priestley JV, Liu M (2008). TRPC4 in rat dorsal root ganglion neurons is increased after nerve injury and is necessary for neurite outgrowth. *J Biol Chem* 283(1):416-26.
- Wu WC, Walaas SI, Nairn AC, Greengard P (1982). Calcium/phospholipid regulates phosphorylation of a Mr "87k" substrate protein in brain synaptosomes. *Proc Natl Acad Sci U S A* 79(17):5249-53.
- Wu X, Zagranichnaya TK, Gurda GT, Eves EM, Villereal ML (2004). A TRPC1/TRPC3-mediated increase in store-operated calcium entry is required for differentiation of H19-7 hippocampal neuronal cells. *J Biol Chem* 279(42):43392-402.

Literature

- Wuhrer M, Geyer H, von der Ohe M, Gerardy-Schahn R, Schachner M, Geyer R (2003). Localization of defined carbohydrate epitopes in bovine polysialylated NCAM. *Biochimie* 85(1-2):207-18.
- Xiao MF, Xu JC, Tereshchenko Y, Novak D, Schachner M, Kleene R (2009). Neural cell adhesion molecule modulates dopaminergic signaling and behavior by regulating dopamine D2 receptor internalization. *J Neurosci* 29(47):14752-63.
- Xu SZ, Zeng F, Lei M, Li J, Gao B, Xiong C, Sivaprasadarao A, Beech DJ (2005). Generation of functional ion-channel tools by E3 targeting. *Nat Biotechnol* 23(10):1289-93.
- Yabe U, Sato C, Matsuda T, Kitajima K (2003). Polysialic acid in human milk. CD36 is a new member of mammalian polysialic acid-containing glycoprotein. *J Biol Chem* 278(16):13875-80.
- Zabel C, Sagi D, Kaindl AM, Steireif N, Kläre Y, Mao L, Peters H, Wacker MA, Kleene R, Klose J (2006). Comparative proteomics in neurodegenerative and non-neurodegenerative diseases suggest nodal point proteins in regulatory networking. *J Proteome Res* 5(8):1948-58.
- Zhang Z, Reboreda A, Alonso A, Barker PA, Séguéla P (2011). TRPC channels underlie cholinergic plateau potentials and persistent activity in entorhinal cortex. *Hippocampus* (4):386-97.
- Zhang Z, Tang J, Tikunova S, Johnson JD, Chen Z, Qin N, Dietrich A, Stefani E, Birnbaumer L, Zhu MX (2001). Activation of Trp3 by inositol 1,4,5-trisphosphate receptors through displacement of inhibitory calmodulin from a common binding domain. *Proc Natl Acad Sci U S A* 98(6):3168-73.
- Zhu X, Chu PB, Peyton M, Birnbaumer L (1995). Molecular cloning of a widely expressed human homologue for the *Drosophila* trp gene. *FEBS Lett* 373(3):193-8.
- Zuber C, Lackie PM, Catterall WA, Roth J (1992). Polysialic acid is associated with sodium channels and the neural cell adhesion molecule N-CAM in adult rat brain. *J Biol Chem* 267(14):9965-71.

8. Abbreviations

ANK	Ankyrin repeats
APS	Ammonium persulfate
BCA	Bicinchoninic acid
BDNF	Brain-derived neurotrophic factor
bFGF	Basic fibroblast growth factor
BSA	<i>Bovine serum albumin</i>
CAM	Cell adhesion molecule
CaM	Calmodulin
CC-C	C- terminal coiled-coil region
CC-N	N- terminal coiled-coil region
CD56	Cluster of differentiation 56 (neural cell adhesion molecule)
CD36	Cluster of differentiation 36 (scavenger receptor)
CHL1	Close homolog of L1
CHO	Chinese hamster ovary
ChS	Chondroitin sulfate
CIRB	Calmodulin and IP ₃ -receptor binding site
Cy2/3/5	Cyanine dyes 2/3/5
D2R	Dopamine receptor D2
DAG	Diacylglycerol
DMEM	Dulbecco modified Eagle's medium
DNA	Deoxyribonucleic acid
ECD	Extracellular domain
ECM	Extracellular matrix
ED	Effector domain

Abbreviations

EGF	Epidermal growth factor
EDTA	Ethylenediaminetetraacetic acid
EndoN	Endosialidase
ERK1/2	Extracellular signal regulated kinase 1/2
Fc	Fragment, crystallizable
FCS	Foetal calf serum
FGF	Fibroblast growth factor
FGFR	Fibroblast growth factor receptor
Fn3	Fibronectin type 3
FRET	Fluorescence resonance energy transfer
GAP43	Growth associated protein 43
GDNF	Glial cell line-derived neurotrophic factor
GFP	Green fluorescent protein
GPI	Glycosylphosphatidylinositol
GST	Glutathione S-transferase
HBD	Heparin binding domain
HBS	HEPES-buffered saline
HBSS	Hanks's balanced salt solution
HEK293	Human embryonic kidney 293
His	Histidine
HNK-1	Human natural killer cell glycan
HRP	Horseradish peroxidase
ICD	Intracellular domain
Ig	Immunoglobuline
IF	Immunofluorescence
I	Inhibition

Abbreviations

IP	Immunoprecipitation
IP ₃	Inositol 1,4,5 trisphosphate
ITPG	Isopropyl-D-thiogalactopyranoside
KDan	5-deamino-3,5-dideoxyneuraminic acid
L1	Cell adhesion molecule L1
LB	Lysogeny broth
MARCKS	Myristolated alanine-rich C-kinase substrate
N2a	Neuro 2a
NCAM	Neural cell adhesion molecule
NCAM (-/-)	NCAM-deficient
Neu5Ac	5-N-acetylneuraminic acid
Neu5Gc	5-N-glycolylneuraminic acid
NGF	Nerve growth factor
NK	Natural killer
NSCC	Non-selective cation channels
OD	Optical density
PBS	Phosphate buffered saline
PD	Pull-down
PDZ-B	PDZ binding domain
PI-PLC	Phosphatidylinositol-specific phospholipase C
PKA	Protein kinase A
PKC	Protein kinase C
PIP ₂	Phosphatidylinositol (4,5) biphosphate
PLC	Phospholipase C
PLC β	Phospholipase C β
PLL	Poly-L-lysine

Abbreviations

POPC	1-palmitoyl-2-oleoyl- <i>sn</i> -glycero-3-phosphocholine
POPE	1-palmitoyl-2-oleoyl- <i>sn</i> -glycero-3-phosphoethanolamine
PrP	Prion protein
PSA	Polysialic acid
PST	Polysialyltransferases ST8Sia IV
PFA	Paraformaldehyde
RIPA	Radio immunoprecipitation assay
RPTP α	Receptor protein tyrosine phosphatase α
scFv	Single chain variable fragment
SDS	Sodium dodecyl sulphate
SDS-PAGE	Sodium dodecyl sulfate polyacrylamide gel electrophoresis
SOCE	Store operated calcium entry
St	Stimulation
STX	Polysialyltransferases ST8Sia II
TAE	Tris-acetate-EDTA
TACE	Tumor necrosis factor- α -converting enzyme
TEMED	Tetramethylethylenediamine
TiO ₂	Titanium dioxide
TRP	Transient receptor potential
TRPC	Transient receptor potential canonical
WB	Western blot

9. Publications

Results of this thesis are also included in following publications:

Kleene R, Cassens C, Bähring R, Theis T, Xiao MF, Dityatev A, Schafer-Nielsen C, Döring F, Wischmeyer E, Schachner M (2010a). Functional consequences of the interactions among the neural cell adhesion molecule NCAM, the receptor tyrosine kinase TrkB, and the inwardly rectifying K⁺ channel KIR3.3. *J Biol Chem* 10;285(37):28968-79.

Theis T, Mishra B, von der Ohe M, Loers G, Prondzynski M, Pless O, Blackshear PJ, Schachner M, Kleene R (2013). Functional Role of the Interaction between Polysialic Acid and Myristoylated Alanine-rich C Kinase Substrate at the Plasma Membrane. *J Biol Chem* 288(9):6726-42.

10. Acknowledgements

I wish to express my sincere gratitude to Prof. Dr. Melitta Schachner for giving me the opportunity to work in her esteemed group, with great scientists and for the chance of being able to be part of such an amazing project. Her fruitful discussions, support and guidance throughout these years have helped to develop my knowledge and skills in the field of molecular neurosciences. I feel deeply honoured to work for a great pioneer, who established the first professorship of molecular neuroscience in Germany. With her wide expertise in neuroscience and open mindedness I received all imaginable support for my professional development and education.

A special thanks goes to Prof. Dr. Matthias Kneussel for his spontaneous help of assessing my doctoral dissertation. Without his help I would probably still be looking for a perfect day for my disputation.

I want to express my heartiest acknowledgements to Dr. Gabriele Loers and Dr. Ralf Kleene for their extraordinary supervision, the inspiring discussions and their endless support for my thesis. They gave me the opportunity and freedom of contributing with my own ideas in the projects. Without their sincere efforts, it would have been much more difficult for me to get to the end of this road.

I would also like to thank Dr. Kent Duncan for his willingness as a english native speaker to check my thesis, to make sure that the final product qualifies as proper English.

I place on record, my sincere gratitude to all collaborators of this thesis. I want to thank Prof. Dr. Rita Gerardy-Schahn for sending us the PSA antibody 735 and the endosialidase, Prof. Dr. Yao Xiaoqiang for providing us the TRPC1 inhibitory antibody, Dr. Markus Delling for sending us TRPC constructs and Prof. Dr. Perry J. Blackshear for his support with the MARCKS antibody (rb) and different MARCKS-GFP constructs.

Acknowledgements

I want to thank my friend and colleague David Lutz, for sharing his valuable time and for his support to writing my thesis in English. A big thanks goes to all my colleagues, who shared with me the lab and provided a nice and productive working atmosphere.

Last but never the least I want to thank my dearest wife and best friend Ana-Maria for being on stand by for me, all this time when I needed support, encouragement, strength and love, which she has given me in uncountable ways and times. Lastly I cannot forget to thank the rest for my family to being there for me too.